Non-equilibrium Thermodynamics and Entropy Regulation in Living Systems

by

Nicolas Brodeur

A thesis submitted to the University of Ottawa in fulfillment of the requirements for the Doctorate of Philosophy in Physics

Ottawa-Carleton Institute for Physics
Department of Physics
Faculty of Science
University of Ottawa
August 2025

Declaration of Authorship

I, Nicolas Brodeur, hereby certify that this thesis is entirely my own original work except where otherwise indicated. I am aware of the University of Ottawa regulations concerning plagiarism, including those regarding consequent disciplinary actions. Any use of the works of any other author, in any form, is properly acknowledged at their point of use.

Abstract

This thesis explores the fundamental role of entropy production and entropy export as constructive properties of complex living systems, thus arguing for a paradigm shift in how we view biological systems through the lens of the Second Law of Thermodynamics. Our investigation is driven by the hypothesis that non-equilibrium thermodynamics can provide insights in understanding the physiological adaptability and resilience of the human body. The rationale is that complex living systems, such as humans, are characterized by self-organized and dissipative behaviors, necessitating the continuous internal production of entropy and its subsequent export to the environment.

Addressing directly the lack of empirical work in the application of entropy principles to humans, we first build the methodological foundation by introducing an experimental approach for the continuous measurement of entropy production and export in humans exercising under heat stress. We develop a two-compartment entropy flow model and, leveraging existing calorimetric data in humans, detail the use of direct and indirect calorimetry to quantify internal metabolic heat production (related to entropy production) and external heat dissipation (related to entropy export). Most importantly, we provide a thorough discussion on the challenges associated with the measurement of entropy rates in humans, both from a technical and conceptual perspective.

Building upon our validated methodology, we explore the biophysical, physiological and clinical relevance of entropy flow regulation in humans exercising under heat stress. By analyzing retrospective calorimetry data on heat fluxes and body temperature, we investigate how the rates of entropy production, export and overall accumulation are affected by key physiological factors such as age, fitness-level and the presence of a chronic disease (type-2 diabetes). We uncover significant impairments in entropy export, leading to increased entropy accumulation, in association with increased age, decreased fitness level, and the presence of a chronic disease (type-2 diabetes). Our findings suggest that the balance of entropy production and export is a critical factor in maintaining physiological stability and can serve as a potential indicator of health status, while potentially allowing the development of the novel therapeutic approaches in clinical settings.

Finally, we explore the underlying mechanisms of entropy dynamics by introducing a new stochastic model of entropy regulation in humans. Our model, which posits that the entropy export rate is dynamically adjusted in the body in response to the rate of internal entropy accumulation, is represented by a stochastic differential equation that coincidently

has the form of a Ornstein-Uhlenbeck process for humans in a resting state, and a time-driven Ornstein-Uhlenbeck process in the regime of alternating periods of exercise and recovery. By fitting our model to the experimental data for young, middle-aged and older participants, we quantify the state-dependent adaptation coefficients (i.e. the ability to respond quickly to a perturbation) and the stochasticity (i.e. noise strength) in the entropy export responses. Our approach thus provides a mechanistic framework for interpreting the dynamic interplay between entropy production and export.

This thesis provides crucial experimental and modeling steps towards a rigorous integration of non-equilibrium thermodynamics into human physiology and health. By establishing experimental feasibility, providing compelling empirical support for the physiological and clinical relevance of entropy balance, and proposing a quantitative modeling framework for entropy regulation, this work contributes to bridging the long-standing gap between fundamental physics and practical applications in human health.

Résumé

Cette thèse s'engage dans une exploration rigoureuse du rôle de la thermodynamique hors équilibre au sein des systèmes vivants complexes, en se focalisant spécifiquement sur la physiologie humaine. La prémisse centrale soutient que la production et l'exportation d'entropie constituent des propriétés fondamentales et constructives nécessaires au maintien de la stabilité physiologique, de la capacité d'adaptation et de la résilience du corps humain, plaidant ainsi en faveur d'un changement de paradigme dans notre perception des systèmes biologiques à travers le prisme de la Seconde Loi de la Thermodynamique. En effet, les organismes vivants, caractérisés par des comportements auto-organisés et dissipatifs, requièrent une continuelle production interne d'entropie et son exportation vers l'environnement.

Comme ce domaine de recherche est marqué par le manque de travaux empiriques, la première contribution majeure consiste au développement d'une approche expérimentale novatrice permettant la mesure en temps réel des taux de production et d'exportation d'entropie chez l'humain. Cette méthode s'appuie sur un modèle de flux d'entropie à deux compartiments tout en utilisant des données calorimétriques existantes. Nous détaillons ici l'utilisation de la calorimétrie indirecte et directe pour quantifier la production de chaleur métabolique (liée à la production interne d'entropie) et la dissipation externe de chaleur (liée à l'exportation d'entropie). Plus important encore, nous proposons une discussion honnête et rigoureuse des défis techniques et conceptuels inhérents à la mesure des taux d'entropie chez l'humain.

En nous appuyant sur notre nouvelle méthodologie, nous explorons ensuite la pertinence physiologique et clinique de la régulation des flux d'entropie par le corps humain durant des périodes d'exercice physique sous stress thermique. L'analyse rétrospective de données calorimétriques révèle des altérations significatives dans la capacité d'exportation d'entropie, entraînant ainsi une accumulation accrue d'entropie, en corrélation directe de l'âge, le niveau de forme physique et la présence d'une maladie chronique (diabète de type 2). Nos résultats suggèrent que l'équilibre entre la production et l'exportation d'entropie est un facteur déterminant pour le maintien de la stabilité physiologique et peut servir d'indicateur de l'état de santé, permettant également le développement potentiel de nouvelles approches thérapeutiques basées sur l'optimisation des flux d'entropie.

Enfin, nous explorons les mécanismes sous-jacents de la dynamique de l'entropie en introduisant un nouveau modèle stochastique de régulation de l'entropie du corps humain.

Notre modèle, qui postule que le taux d'exportation d'entropie est ajusté dynamiquement dans le corps en réponse au taux d'accumulation d'entropie interne, est représenté par une équation différentielle stochastique dont la forme coïncide avec celle d'un processus d'Ornstein-Uhlenbeck. En ajustant notre modèle aux données expérimentales pour des participants jeunes, d'âge moyen et plus âgés, nous quantifions les coefficients d'adaptation (reflétant la capacité à répondre rapidement à une perturbation) et la stochasticité (c'est-à-dire la force du bruit) dans les réponses d'exportation d'entropie. Nos résultats mettent en évidence un déclin significatif de ces coefficients d'adaptation lié avec l'âge, indiquant ainsi une capacité réduite des individus plus âgés à réguler efficacement leur exportation d'entropie face aux perturbations. Notre approche fournit un cadre explicatif pour interpréter la relation dynamique entre la production et l'exportation d'entropie.

Au final, notre travail établit une base solide vers l'intégration de la thermodynamique hors équilibre dans l'étude de la physiologie humaine. En démontrant la faisabilité expérimentale de la mesure des flux d'entropie dans le corps humain, en fournissant un soutien empirique convainquant quant à la pertinence clinique de l'entropie, puis en proposant un cadre de modélisation combinant l'auto-régulation du corps et les processus stochastiques, cette thèse contribue à combler le fossé entre la physique fondamentale et notre compréhension des êtres vivants.

Acknowledgements

I am sincerely grateful to my supervisors, Prof. André Longtin and Dr. Andrew J.E. Seely for accepting to embark with me on this wild adventure. You allowed me to shape this project based on my own curiosity and personal aspirations. This multidisciplinary effort truly is what I imagined and hoped my PhD project would be. I am also thankful for your patience and support regarding my family life and my passion for teaching.

I wish to thank Prof. Glen Kenny for his incredible help in understanding the experimental methods and patiently explaining to me the basic principles of human thermoregulation. Our fruitful collaboration was only made possible by your open-mindedness.

To all the lab members that helped me with your particular expertise when I was stuck on mathematical or modeling hurdles: Kamyar, Raphaël, Alexandre and Arthur.

To my family and friends that encouraged me over the years.

Finally, I am infinitely indebted to my love, Camille. You definitely shared the hard work. Thank you for believing in me.

Un merci tout spécial au petit Arthur qui me fait redécouvrir le monde. Et à toi, petit être qui s'auto-organise pendant l'écrire de cette thèse et qui est finalement né avant ma soutenance. Bienvenue parmi nous Hubert!

Nos kids qui regardent le monde, c'est encore plus beau que le monde tout seul.

- Émile Proulx-Cloutier

Table of Contents

List of Tables

List of Figures

Chapter 1

Introduction

Entropy.

This word has been the subject of many speculative and pseudo-scientific "theories", which could explain the aversion of many physicists when it is pronounced outside of a classical thermodynamics course. As a reader, you may have felt a sudden rise of skepticism upon reading the title of this thesis. Indeed, entropy has long suffered from an aura of mysticism and the misguidance of quacks that flooded the conversation with erroneous interpretations. But who's to blame? The lack of a completely satisfactory definition of entropy, despite its fundamental nature, combined with the evident polysemy [3] resulted in great confusion even among the scientific community.

Needless to say, entropy appears to be involved in the deepest inquiries we, homo sapiens, ever pursued: the seemingly irreversible directionality of time, the faith of our universe possibly destined to an equilibrium heat death and, most interestingly, the emergence of highly localized pockets of order and complexity called living systems. If the most exciting areas of research are those where roughly crafted questions abound, studying the connection between entropy and living systems surely is an intellectually seductive endeavour, but also a risky one. The main challenges here are first and foremost conceptual in nature as there exists currently no theoretical formalism able to accurately describe what

life is and how it operates. As a result, any attempt will inevitably be tainted with assumptions that may or may not be contextually adequate [4]. Nonetheless, it is possible to make great progress in our understanding of biological organisms through thermodynamic principles using reasonable assumptions [5].

The first challenge typically encountered in the study of life is the observation that physical systems generally evolve towards a state of equilibrium where matter remains, but the form and features are lost. This is, in essence, a manifestation of the Second Law of Thermodynamics and its associated principle of entropy maximization. However, the emergence and evolution of life forms on Earth shows the opposite trend; from the assembly of the first amino acids to the formation of the first bacterium, up to the first plants and mammals, it turns out that at each stage of development life is found to be more ordered and, thus, more unlikely. Then, how can life elude the Second Law? Put more bluntly, how can physics explain *any* biological process other than death and decomposition? And from a cosmic perspective, how can we reconciliate the paradoxical tendency of the universe to simultaneously increase both its disorder and apparent complexity?

The first step is recognizing that life emerges from the complex interplay of irreversible processes in which energy and matter are constantly exchanged and transformed. In other words, life is a term that we associate with the sustained dynamics of a network of processes rather than with a substance that inhabits matter [6]. The processes can maintain themselves within a highly coordinated state through autocatalysis [7] from which can emerge patterns on much larger scales, a property known as self-organization [8, 9]. But this is only possible in open systems that operate far from thermodynamic equilibrium where the Second Law holds a more nuanced authority.

Now, the transition - or evolution - from inanimate matter to living systems is certainly not obvious and there are multiple approaches to the study of the origin of life, each coming at a different angle or developmental stage. For example, one approach investigates the physico-chemical principles that could have led to the self-organization and evolution of chemical systems within the early Earth's geochemical environment [10]. Others in-

vestigate life as an information-processing unit where complexity can be quantified using information-theoretic principles [11, 12]. In some ways, these two competing perspectives can be reduced to the classic chicken and egg conundrum. Indeed, it remains unresolved which of the two important requirements of life, namely metabolism and genetic information, came first and provided the foundation for the other. Metabolism-first supporters emphasize the importance of energy capture and utilization as a driving force, thus arguing that a self-sustaining network of biochemical reactions predated and facilitated the development of the genetic machinery [6]. On the other hand, information-first proponents support the initial abiotic synthesis of RNA molecules (known as the RNA World Hypothesis [13]) given their self-replicating ability which can be seen as Darwinian evolution acting on the earliest forms of life. While this duality between metabolism and RNA will most likely be resolved by integrating insights from both scenarios [14], this debate highlights a very special characteristic of living systems, that of unclear boundaries and a highly non-intuitive mapping of causality between the underlying processes.

The genetic code is a wonderful example of such unclear boundaries. On one hand, it provides a set of instructions that directs the synthesis of proteins and regulates the cellular housekeeping operations. On the other hand, RNA and DNA act as the structural basis for information storage and processing. Put in computer terms, the genetic code embodies both the software (i.e. instructions) and the hardware (i.e. structure) in a way that is deeply interwoven, highlighting the ambiguous relationship between biological *structures* and *functions* [15]. Indeed, the functional role of a given constituent can be highly flexible and context-dependent [16]; meanwhile, a structure that evolved for a specific purpose can be co-opted to serve a different role [17, 18]. In the end, understanding living systems requires a framework that goes beyond the traditional reductionist approach because biological systems are non-fractionable [19], meaning that breaking them in smaller components only eliminates the interesting emergent properties acting on the higher levels of organization. This might well be the most applicable case of the *whole being greater than the sum of its parts* [4].

Life's complexity also entails that physical laws alone can hardly explain its emer-

gence [20]. Contrary to the Newtonian paradigm where the behavior of a system can be predicted from its initial conditions, living systems unfold from a much more creative science of chance, circumstances and unforeseeable possibilities [21]. In this context, we are left to identify new *principles* rather than *laws*. Then, the objective is to study the behavior of living systems by perturbing their dynamical steady-state and investigating the principles governing their response [22]. Currently, the most insightful framework is provided by thermodynamics and its extensions, which emphasize the role of energy flow, dissipation of energy gradients and the inherent drive of non-equilibrium systems towards the creation of order [17, 23, 24]. Within this framework, biological systems self-organize to resist the otherwise inevitable decay to thermodynamic equilibrium through a fine-tuning of the thermodynamic forces and flux that arise in the presence of sufficiently strong energy gradients [25].

In line with this perturbative framework, this thesis on human non-equilibrium thermodynamics and entropy balance takes as a starting point the well-established principle of energy conservation and then studies what, during the transformation of energy, is not conserved [26]. What is not conserved is the available energy to perform work. This idea is referred to as the degradation of energy quality (or usefulness) as energy is converted from one form to another and where, analogous to economic inflation, the remaining energy can no longer make things move or change like it used to [27]. One way to quantify this irreversibility in energy transformations is through the concept of entropy. It should be noted the entropy of interest here is not of the informational kind which relates to some abstract mathematical and statistical properties such as uncertainty and unpredictability [3].

Rather, we are interested in the energy transformation occurring in real macroscopic systems as a modern extension of the work of Carnot and Clausius on heat engines [28]. Then, the following questions naturally arise: how different are living systems compared to machines (such as steam engines) and can the same comprehensive framework be applied to both? After all, a bacterium swimming up a glucose gradient *appears to be acting* to get food with intrinsic agency, which contrasts with the machines' inability for self-directed actions (at least in the pre-AI era) [19, 29]. Certainly, the governing principles, whatever

they may be, confer to complex systems a convincing illusion of purpose.

William James Sidis noted that machines may be complicated systems, but their purpose (or teleology) comes from the living being that assembled them, whereas *living phenomena are essentially teleological* [30]. Similarly, Robert Rosen later argued that *a material system is an organism if, and only if, it is closed to efficient causation*, meaning that all the efficient causes within the system are produced by the system itself [31]. In other words, living systems possess, within themselves, both the reason and the finality of their existence. As we will see in the following chapters, this condition of existence is reminiscent of the role played by entropy production in the self-organization of what is called dissipative structures [32]. Indeed, a fundamental feature of dissipative structures, which are driven by the dissipation of energy gradients, is that the production of entropy acts both as a requirement (reason) and an inevitable consequence (finality) for their emergence and stability. This crucial statement embodies the overarching story of the present work, and much effort will be dedicated to dissecting its meaning and limitations.

Therefore, in an attempt to restore entropy's reputation as a useful conceptual tool in far from equilibrium situations, this thesis aims to contribute to a rigorous and intellectually honest conversation about the role of entropy production and entropy flow as constitutive properties of complex living systems. Here, as in standard textbooks on non-equilibrium thermodynamics [2], we define entropy production as the generation of entropy resulting from internal irreversible processes, and entropy flow (or export) as the entropy exchanged with the environment through the system's boundaries. Thus, the main objective of this thesis is to provide experimental and modeling support to the question of entropy regulation in complex living systems with a focus on the human body. More specifically, we seek to answer the following questions:

Question 1: How can we measure entropy production and entropy flow in humans?

Question 2: How is entropy involved in the thermodynamic stability (or homeostasis) of humans from a physiological and clinical perspective?

Question 3: How does the human body regulate its entropy production and entropy flow from a modeling perspective?

To explore these questions, we will first introduce in **Chapter 2** the essential concepts required to fully understand and appreciate our approach. We will present a brief history of the concept of entropy and its involvement in the description of thermodynamic systems ranging from the equilibrium to the non-linear non-equilibrium regime. We will introduce the important aspects of human thermoregulation along with the experimental details of the calorimetry instrumentation that allows the accurate measurement of heat production and dissipation in humans. Finally, we will cover the basic notions on stochastic differential equations and their application to stochastic thermodynamics.

Each of the three research questions above will be investigated individually and represent the main themes of the following chapters. Given the broad range of topics and research fields covered in this thesis, the distinct literatures will be properly introduced within their respective chapter.

Chapter 3 builds the methodological foundation of this thesis by introducing an experimental approach for the continuous measurement of entropy production and entropy flow in humans exercising under heat stress. Surprisingly, there exists very limited empirical work on the measurement of entropy rates in humans, with a significant contribution from Aoki [33,34] and a model of stress entropic load proposed by Bienertova-Vasku and her colleagues [35,36]. This is mainly due to the fact that it is experimentally incredibly challenging to accurately measure heat flows and temperature changes simultaneously in the body. However, owing to the outstanding work of our collaborator Prof. Glen P. Kenny [37] and his colleagues, we now have the ability to measure, in real-time, the thermodynamic quantities necessary to investigate the entropy dynamics in humans using a state-of-the-art calorimeter [38]. Therefore, this chapter details the experimental design, the development of a two-compartment entropy flow model, and the initial application of these methods to healthy middle-aged men that performed an alternating schedule of physical exercise and recovery. It uses existing calorimetric data, but further incorporates hitherto untapped,

concomitantly acquired skin and core temperature data and other calorimetry-derived temperature estimates. Most importantly, we provide a detailed discussion on the difficulties associated with the measurement of entropy rates in humans, both from a technical and conceptual perspective.

Building directly upon this validated methodology, **Chapter 4** extends the experimental analysis to explore the biophysical, physiological and clinical relevance of entropy flow regulation in humans exercising under heat stress. By analyzing retrospective calorimetry data on heat fluxes and body temperature, we investigate how the rates of entropy production, export and overall accumulation are affected by key physiological factors such as age, fitness-level and the presence of a chronic disease (type-2 diabetes). For these physiological conditions, we provide empirical evidence for the impairment of entropy export leading to a greater accumulation of entropy within the body, which can be interpreted as a thermodynamic measure of physiological stress. This chapter directly addresses the core **Question 2** of how entropy balance relates to biological integrity, health and illness, highlighting the potential of entropy-based metrics to differentiate between physiological states and identify potential risks. Furthermore, it initiates a discussion on the clinical implications of entropy regulation, for example by suggesting novel therapeutic approaches based on non-equilibrium thermodynamics principles, thereby bridging the gap between fundamental physics and practical applications in human health.

Building on this solid methodological groundwork (chapter 3) and evidence for the clinical importance of entropy (chapter 4), **Chapter 5** finally addresses **Question 3** by introducing a novel stochastic model of entropy regulation in humans. Our model posits that the human body regulates its rate of entropy export based on the current rate of total entropy change (or entropy accumulation). This relatively simple intuition was translated into a stochastic differential equation that coincidently has the form of a Ornstein-Uhlenbeck process in the resting state, and a time-driven Ornstein-Uhlenbeck process in the regime of alternating periods of exercise and rest. By fitting our model to the experimental data for young, middle-aged and older participants (from the aging study presented in the previous chapter), we quantified the state-dependent adaptation coefficients (i.e. the ability to re-

spond quickly to a perturbation) and the stochasticity (i.e. noise strength) in the entropy export responses. This approach provides a mechanistic framework for interpreting the dynamic interplay between entropy production and export. This combined deterministic and stochastic modeling contribution, involving a stochastic differential equation and further Fokker-Planck density analysis, is central to our objective of developing a physics-based understanding of physiological adaptability and resilience. By framing human thermoregulation and metabolic processes within the context of stochastic thermodynamics, this chapter offers new perspectives on the fundamental role of entropy in maintaining health and responding to physiological perturbations.

Publication notes

- **Chapter 3:** This chapter has been published in the journal *Entropy* and is titled *Continuous Monitoring of Entropy Production and Entropy Flow in Humans Exercising under Heat Stress* [39]. I am the main author of this manuscript, performed the data analysis, wrote the original draft. The experimental were provided by Dr. Notley. Comments and corrections were provided by Dr. Kenny, Dr. Longtin and Dr. Seely. It should be noted that the original text from the published manuscript has been modified in Chapter 3: the first paragraph of the manuscript was removed from Chapter 3 and used instead in the general Introduction of the thesis.

- **Chapter 4:** This chapter has been accepted for publication by the journal *Annals of the New York Academy of Science* and is titled *Real-time measurement of entropy production and export in humans: A step towards entropically-informed medicine* [40]. I am the main author of this manuscript, performed the data analysis, wrote the original draft. The experimental were provided by Dr. Kenny. Comments and corrections were provided by Dr. Kenny, Dr. Longtin and Dr. Seely. A new paragraph has been added in section 4.4 to discuss the sex-related differences in thermoregulation.

- **Chapter 5:** This chapter has been submitted to PRX Life [41]. I am the main author of this manuscript, performed the data analysis, and wrote the original draft. Dr. Longtin helped conceptualize the stochastic part of the model and Raphaël Lafond-Mercier helped with the Fokker-Planck analysis. The experimental data was provided by Dr. Kenny. Comments and corrections were provided by all co-authors.

Chapter 2

Background

2.1 Non-equilibrium Thermodynamics

This section serves as an overview of the theory of thermodynamics, first introducing the fundamental principles in equilibrium conditions (e.g. First and Second Law) and then moving towards their application in complex far-from-equilibrium systems such as the human body.

2.1.1 A Brief History of Thermodynamics

Thermodynamics was not formulated in the comfort of a laboratory with scientists and thinkers inquisitively contemplating the cosmos for new fundamental laws. It is not a story about napping under an apple tree or taking a bath with the golden crown of a king; its origin story comes from the smoky and clanking reality of the early 19th century industrial revolution. Ironically, this study of steam engines and other industrial machines will reveal dramatic consequences regarding the nature of our place in the universe, and the universe itself. But before we jump in the postulates and mathematical details of this theory, it is important to recognize that from these humble beginnings arose a science of a fascinating

and profound universality.

Thermodynamics began when engineers and physicists grappled with the seemingly simple yet profound problem of converting *heat* into *useful work* in the context of heat engines. Their main objective was to improve the efficiency of heat engines by minimizing, as much as possible, the heat wasted through friction and heat conduction. In their view, the irreversibility associated with heat loss was an engineering problem because nature was expected to be fundamentally reversible as prescribed by Newtonian dynamics. However, French engineer Sadi Carnot realized that even in the most idealized scenario, that of a reversible cycle operating between two temperature reservoirs (now called the Carnot cycle), there exists an unavoidable limit to how much heat could be converted into work. In other words, a certain amount of heat *must* be rejected to the cold reservoir, not as a result of engineering imperfections but as an indispensable theoretical condition to produce work [26].

Moreover, Carnot's analysis showed that this fundamental limit is independent of the machine and the manner in which work is obtained; it depends only on the temperatures that caused the flow of heat between the two reservoirs [2]. The efficiency η of an engine can be quantified as the ratio of the work done by the engine and the heat required to perform the work. This discovery led to Carnot's theorem, which states that for reversible engines that operate by absorbing an amount of heat Q_1 from a hot reservoir at temperature T_1 and discarding an amount of heat Q_2 to a cold reservoir at temperature T_2, the maximum efficiency is given by

$$\eta = \frac{W}{Q_1} = 1 - \frac{Q_2}{Q_1} = 1 - \frac{T_2}{T_1} \quad . \tag{2.1}$$

Therefore, the challenge of thermal efficiency of heat engines required a new conceptual framework, beyond classical mechanics, due to the involvement of the notions like heat and temperature. While the connection between heat and work was empirically known

from prehistoric times, where the friction generated by a rapidly rotating wood stick was used to create fire, their equivalence as a form of energy became clear only in the mid 19th century with the work of James Prescott Joule and Robert Julius Mayer. Building upon this newly established equivalence, Clausius (and many others simultaneously [42]) formulated the principle of energy conservation, also known as the First Law of Thermodynamics, where the total change in energy dU in a closed system in a time dt is given by

$$dU = dQ - dW \tag{2.2}$$

where dQ is the amount of heat exchanged ($dQ > 0$ if gained by the system) and dW is the mechanical energy (or work) performed by the system on its environment.

2.1.2 From the First to the Second Law

After formulating the First Law, Clausius kept building on Carnot's work of reversible cycle and made the interesting observation that equation (2.1) can be written as follows:

$$\frac{Q_1}{T_1} - \frac{Q_2}{T_2} = 0 \quad . \tag{2.3}$$

In doing so, Clausius identified a new quantity, $\mathrm{d}S = dQ/T$, that effectively acts as a state function since the sum of all the dS over a reversible cycle is zero. He coined the term entropy for this quantity. It was known that heat was not a state function (i.e. dQ is an inexact differential) because a certain amount of heat was discarded to the environment over a complete cycle, and similarly for the work dW. However, it turns out that, mathematically, $1/T$ happens to be the integrating factor that turns the inexact differential dQ into an exact differential dS [43].

Keeping in mind Carnot's perfectly reversible cycle, Coveney and Highfield highlighted that *by turning the crankshaft through one complete revolution, an engine may be returned to a position which the most able mechanic could not distinguish from its initial state. But the wasting of energy as heat will have ensured subtle changes that cannot be wiped out* [44]. Even if the conservation of energy remains valid (i.e. no energy was annihilated during that one cycle), the system as a whole (system plus environment) has changed irreversibly in its ability to produce useful work. The fundamental limitation associated with the conversion of heat into work provided one (of many) formulation of the Second Law of Thermodynamics [2]:

It is impossible to construct an engine which will work in complete cycle, and convert all the heat it absorbs from a reservoir into mechanical work.

Clausius then extended the analysis to arbitrary cyclic processes and, by removing the constraint of reversibility, realized that irreversibility simply makes the matter worst in terms of engine efficiency: the heat discarded to the cold reservoir will always be larger when irreversible processes are involved (i.e. $Q_2^{\text{irr}} > Q_2$). This led to Clausius's inequality $dS \geq dQ/T$, which implies that the entropy of isolated systems (i.e. systems that cannot interact with their environment) must always increase during an irreversible process.

In reality, the Second Law relies on the First Law by adding a necessary constraint that goes beyond the simple conservation of energy. While the First Law allows for the possibility of complete transformation between different forms of energy, the Second Law, as expressed by the inevitable increase of entropy in isolated systems, provides the framework to understand the directional nature of spontaneous processes [45]. As such, the First and Second Law embody vastly different interpretive frameworks, and only within their very distinct approaches of the constructive role of irreversible processes can the work presented in this thesis be fully appreciated.

A fundamental question remained unanswered: If heat is a legitimate form of energy, what kind of energy is it, and what is its materialistic support? For example, kinetic energy

can be well understood in terms of an object velocity, and work is related to moving an object by applying a force, all of which intuitively requires *energy*. However, heat is hardly controllable, as it diffuses all over, almost as an incoherent form of energy [27]. Initially, heat was thought to be an indestructible, massless substance or fluid, called *caloric*. This *heat fluid* could flow from hot bodies to cold bodies, causing the temperatures of both bodies to change until their caloric content (and temperatures) equalize. This theory was eventually abandoned, partly because of simple empirical evidence of principle violation (e.g., rubbing two ice cubes that subsequently melt demonstrates that caloric fluid cannot be a conserved quantity), but mostly with the establishment of the First Law. Consequently, the physical interpretation of heat remained a great mystery up until the development and acceptance of the atomic and molecular composition of matter, along with Boltzmann's theoretical advances in statistical mechanics.

Indeed, the work of Carnot and Clausius provided a story of the macroscopic world following the changes of macroscopically observable quantities, such as temperature and volume. Boltzmann, who was an early supporter of the atomic theory of matter, argued that heat and entropy were not physical substances, but rather emergent properties of systems made of a large number of atoms whose behavior could be understood from the laws of mechanics. Without going into detail, Boltzmann successfully expressed thermodynamics as a macroscopic consequence of a statistical averaging over the microscopic world. Most importantly, he correctly identified heat as the transfer of energy to the microscopic world through the hidden atomic modes of motion [43].

The insights shared by Clausius and Boltzmann refer to two levels of reality that collapse under a unified theory. Thermodynamics provides a rigorous mathematical framework in which the collective behavior of microscopic constituents can be simplified (or coarse-grained) into a reduced set of macroscopic variables. Equilibrium states, characterized by the absence of spontaneous macroscopic change, can be understood through the extremization of thermodynamic potentials. These potentials are analogous to those in classical mechanics, where the minima indicate stable equilibrium. We spent quite some time building a conceptual understanding of heat and entropy because the entropy state

function S plays a fundamental role in the definition of equilibrium states. Indeed, the Second Law states that for isolated systems, equilibrium is reached when the total entropy is maximized. Therefore, entropy can be seen as a thermodynamic potential that is maximized when the internal energy U and the volume V of the system are constant (i.e. isolated system). Instead of fixing the energy U, it is also possible to maintain the system at a constant temperature T by allowing the transfer of heat with a heat reservoir. This new set of constraints leads to a different stability criterion, that of the minimization of what is called the Helmholtz free energy F, defined as $F = U - TS$. Thus, the state of equilibrium corresponds to the most stable configuration defined by these extremum principles under the system's specific constraints. Identifying the principles governing the natural evolution of systems towards specific states will be our main interest in the following sections.

Before we move from the equilibrium framework to discuss the foundation of non-equilibrium thermodynamics, we should address a common misconception regarding the concept of entropy and its association with the idea of order and disorder. In his statistical approach to thermodynamics, Boltzmann related the entropy S of thermodynamic systems to the number of possible configurations of the atoms or particles through the equation

$$S = k_B \ln W \tag{2.4}$$

where S is the entropy, k_B is Boltzmann's constant and W is the number of microstates a system can be found in under specific conditions. Each configuration (or microstate) represents a single arrangement of particles within a volume. Boltzmann considered that each microstate has the same probability of occurring and that the system would simply transition from one static microstate to another in a way analogous to a movie tape made of still images. For example, figure 2.1 shows four different microstates (black squares) that are equiprobable according to Boltzmann. This reasoning led to a different interpretation of the Second Law's tendency of increasing entropy by Boltzmann, where the time evolution between the equiprobable microstates inevitably leads to macrostates characterized by

greater apparent disorder. However, this statistical illusion arises simply because there are an overwhelming number of microstates that are considered as "disordered" compared to the number of "ordered" microstates.

Our intuition and everyday experience certainly disagree that the disordered system on the left of figure 2.1 is equally probable as the human-like structure on the right, thus highlighting the improbability of the existence of living systems, as mentioned in the general introduction of this thesis. This paradox can be resolved by recognizing that living systems are open systems (i.e. red square of figure 2.1 and not isolated like the black squares) that maintain their low-entropy state (high order) by continuously importing free energy and exporting a larger amount of entropy to their surroundings.

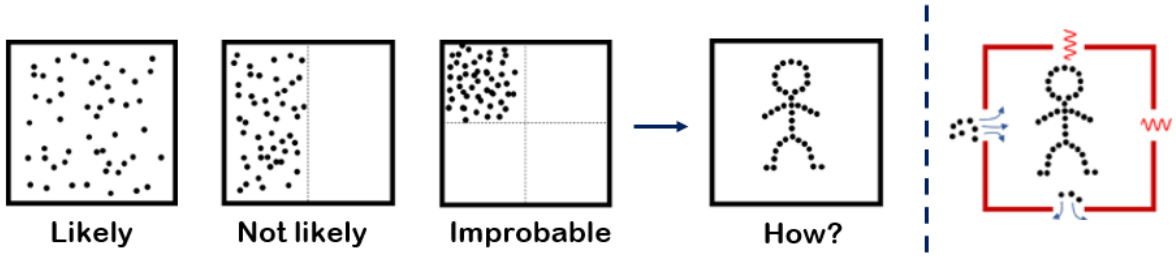

Figure 2.1: **Improbability of life in isolated systems.** The black squares represent an isolated system in four different (technically equiprobable) microstates with our intuitive probability of observing them individually (decreasing from left to right). It appears statistical improbable that the particles arrange themselves into a stable human being according to the Second Law of Thermodynamics. Although it is impossible in isolated systems, the red square on the right illustrates the possibility of such complex systems in different thermodynamic conditions, that is in open system maintained out of equilibrium.

Summary of the entropy change in equilibrium conditions

In its modern formulation, the entropy change of a system can be expressed as the sum of the following two parts:

$$dS = dS_i + dS_e \tag{2.5}$$

where dS_i is the change in entropy due to irreversible processes within the system and dS_e is the entropy change associated with the exchange of energy and matter. For a cyclic process that returns the system to its initial state, the net entropy change of the system dS must be zero

$$\oint dS = \oint dS_i + \oint dS_e = 0 \quad . \tag{2.6}$$

But, if the cycle involves irreversible processes such that entropy is generated (i.e. $dS_i/dt > 0$), then the entropy produced internally must be exported to the environment:

$$\oint dS_e = \oint \frac{dQ}{T} < 0 \quad . \tag{2.7}$$

For **isolated** systems (i.e. no exchange of energy or matter with the environment), the Second Law implies that

$$dS_e = 0 \quad \text{and} \quad dS_i \geq 0 \quad . \tag{2.8}$$

For **closed** systems (i.e. exchange of energy but no exchange of matter with the environment),

$$dS_e = (dS_e)_{\text{heat}} = \frac{dQ}{T} \quad \text{and} \quad dS_i \geq 0 \quad . \tag{2.9}$$

For **open** systems (i.e. exchange of energy and matter with the environment),

$$dS_e = \frac{dQ}{T} + (dS_e)_{\text{matter}} \quad \text{and} \quad dS_i \geq 0 \quad . \tag{2.10}$$

where the term $(dS_e)_{\text{matter}}$ is the exchange of entropy due to matter flow. This term originates from a difference in the chemical potential, leading to an exchange of particles (i.e., matter flow). In the latter case, the First Law $dU = dQ - dW$ is incomplete because we must also include the internal and kinetic energy of the particles flowing through the system.

2.1.3 The Foundation of Non-equilibrium Thermodynamics

Classical thermodynamics provides a robust framework for analyzing systems in static states with uniform intensive properties (e.g. temperature or pressure) throughout the system [46]. However, this approach is fundamentally limited to equilibrium states and their quasi-static transitions by idealized reversible processes. But this is not the world of the living where phenomena must occur over finite periods of time and where systems must be continuously maintained away from equilibrium. Unfortunately, the extension to non-equilibrium conditions requires us to challenge some of the core principles that allowed great understanding of equilibrium states, such as the extremization of the thermodynamics potentials. This is indeed problematic when one realizes that most thermodynamic variables and potentials have been explicitly defined by equilibrium conditions [47–49]. For example, the concept of temperature is well-defined by the Zeroth Law, and similarly for the concept of entropy as a state function conjugate to the temperature as revealed by the analysis of Carnot cycles [2]. Therefore, the typical starting point is the equilibrium formulation to which extensions are applied in the form of small deviations or the simple assumption that equilibrium interpretations are approximately applicable [50]. Nonetheless, it is possible to make some progress, especially in the characterization of non-equilibrium steady states [51] with the two fundamental assumptions detailed below.

The first fundamental assumption is the hypothesis of local equilibrium [52, 53]. This assumption posits that even in a system that is not in global thermodynamic equilibrium,

sufficiently small subsystems can be considered to be in a state of local equilibrium. Within these elemental volumes, local thermodynamic variables (e.g. temperature or pressure) are well-defined and admit their equilibrium interpretation [54]. For this assumption to be valid, the size of these elemental volumes must be large enough such that microscopic fluctuations do not affect the stability of the equilibrium state, but small enough to capture the spatial variations of thermodynamic quantities on the larger scale [2]. Additionally, the timescale of non-equilibrium changes must be much larger than that required to attain local equilibrium [50].

The second fundamental assumption relates to the applicability of the Second Law within these elemental volumes and postulates the non-negativity of the local entropy production rates. It is known from equilibrium thermodynamics that the overall entropy production dS_i of the whole system, irrespective of its type (i.e. isolated, closed or open), must be equal to or greater than zero:

$$dS_i = dS_i^1 + dS_i^2 + \cdots \geq 0 \quad . \tag{2.11}$$

However, the assumption of non-negativity of the local entropy production rates provides a stronger constraint on the individual subsystems such that $dS_i^k \geq 0$ must be true for all k. This statement about the locality of the Second Law will have important implications for the elaboration of the two-compartment entropy flow model in humans presented later in Chapter 3.

We now wish to extend to concept of entropy to non-equilibrium states, which is recognized as a non-trivial task [49, 55, 56]. Following the derivations from Prigogine and Kondepudi [2], the first step is to express entropy in the form of a balance equation. If we consider continuous systems with time and spatial dependence, the local increase in entropy can be defined by using the entropy density $s(x,t)$. Then, the local entropy production is given by

$$\sigma(x,t) \equiv \frac{ds_i}{dt} \geq 0 \quad \text{with} \quad \frac{dS_i}{dt} = \int_V \sigma(x,t) dV \quad . \tag{2.12}$$

As noted by Prigogine and Kondepudi [2], identifying the explicit expression for the local entropy production σ in terms of the irreversible processes occurring within the system (e.g. heat diffusion, conduction or chemical reactions) is the starting point in the study of non-equilibrium thermodynamics. The formal entropy balance equation can be derived from equation (2.5) by adding a time-dependence [5] on the different terms of entropy change such that

$$\frac{ds}{dt} = \frac{ds_i}{dt} + \frac{ds_e}{dt} = \sigma - \nabla \cdot \mathbf{J}_s \tag{2.13}$$

where the second term on the right-hand side corresponds to the divergence of the entropy current (or flow) J_s, which is analogous to the entropy dS_e exchanged through the system's boundary. Given the similarity of equation (2.13) with the traditional continuity equations, we will refer to dS_e as the *entropy flow* or *entropy export*, interchangeably. It should be noted that unlike dS_i/dt which must always be greater or equal to zero, dS_e/dt can be negative or positive. For a system at temperature T which exchanges energy with its environment through an energy flow J_u and matter through a diffusion current J_k of chemical species k (with chemical potential μ_k and partial molar energy u_k), the entropy flow J_s can be written as

$$\mathbf{J}_s = \left(\frac{\mathbf{J}_u}{T} - \sum_k \frac{\mu_k \mathbf{J}_k}{T} \right) = \left(\frac{\mathbf{J}_q}{T} + \sum_k \frac{u_k - \mu_k}{T} \mathbf{J}_k \right) \tag{2.14}$$

where the heat flow J_q is related to the energy flow J_u through the relation $J_u = J_q + \sum_k u_k J_k$. If the system is in a steady state, meaning that its temperature T is constant and the net rate of entropy change is zero (i.e. $ds/dt = 0$), then equation (2.13) implies

that the divergence of the entropy flow does not necessarily vanish [5]. Instead, we obtain

$$\nabla \cdot J_s = \sigma \quad . \tag{2.15}$$

This condition for a steady state (or stationarity state) leads to only two possibilities where both sides of equation (2.15) are:

- **non-zero**, in which case the entropy produced within the system (σ) must be removed by a flow of entropy to the environment. This situation characterizes a non-equilibrium steady state.

- **zero**, in which case the absence of entropy production ($\sigma = 0$) implies that the flow of entropy vanishes together with all other flows. This situation characterizes thermodynamic equilibrium.

As mentioned earlier, entropy flow can be positive (inflow of entropy) or negative (outflow of entropy). However, it follows from the requirements of a steady state (i.e. $dS/dt = 0$) and the non-negativity of entropy production that

$$\frac{dS_e}{dt} = -\frac{dS_i}{dt} \leq 0 \quad . \tag{2.16}$$

Equation (2.16) emphasizes that, to maintain a non-equilibrium steady state, it is necessary to continuously pump a negative flow of entropy of magnitude equal to the value of entropy production [5]. This mathematical statement can be interpreted as a modern formulation of Schrödinger's intuition, presented in his book *What is Life?*, about biological systems feeding off *negentropy*, relating this requirement of negative entropy flow to their ordered (low-entropy) state [57].

One of the most important results derived from the entropy balance equation in conjunction with the Gibbs relation $Tds = du - \sum \mu_k \, dn_k$ is that the entropy production σ can be isolated and expressed as follows [2, 5]:

$$\sigma = \mathbf{J}_u \cdot \nabla \frac{1}{T} - \sum_k \mathbf{J}_k \cdot \nabla \left(\frac{\mu_k}{T} \right) + \frac{\mathbf{I} \cdot (-\nabla \psi)}{T} + \sum_j \frac{\tilde{\mathbf{A}}_j \mathbf{y}_j}{T} \quad . \tag{2.17}$$

By inspecting equation (2.17), we can identify a structure within the different terms such that equation (2.17) can be reduced to a simpler (bilinear) form given by

$$\sigma = \sum_\alpha F_\alpha J_\alpha \tag{2.18}$$

where the entropy production can be expressed as the sum of the thermodynamic flows J_α multiplied by their conjugate thermodynamic force F_α. For example, a temperature gradient (or more specifically a gradient of $1/T$) causes the flow of heat. The different relations between the forces and their corresponding flows are identified in table 2.1. Equation (2.18) sets the foundation of non-equilibrium thermodynamics by providing a framework that explains how the existence of a thermodynamic force gives rise to a thermodynamic flow. It should be noted that thermodynamic forces are not forces in the mechanical sense but typically the gradient of thermodynamic quantities [58].

The importance of equation (2.18) cannot be understated in our conceptual understanding; thermodynamic flows arise from the existence of gradients (i.e. forces) and, acting as the emissaries of the Second Law, tend to eliminate these gradients unless external constraints prevent them otherwise. This is exactly what we refer to when we wrote in the Introduction that energy gradients are dissipated as a result of the Second Law. Nature certainly appears committed to the dissipation of energy gradients and, as we will see, can be quite creative in the ways in which it undertakes this mission.

Physical process	**Thermodynamic Force** F_α	**Thermodynamic Flow** J_α
Heat and matter flow	$F_\alpha = \nabla \frac{1}{T}$	Internal energy flow J_u
Diffusion	$F_\alpha = -\nabla \frac{\mu_k}{T}$	Diffusion current J_k
Electrical conduction	$F_\alpha = -\frac{\nabla \psi}{T} = \frac{E}{T}$	Ion current densities I_k
Chemical reactions	$F_\alpha = \frac{A_j}{T}$	Velocity of reaction $v_j = \frac{1}{V}\frac{d\xi_j}{dt}$

Table 2.1: **Table of thermodynamic forces and flows**. In the case of chemical reactions, the thermodynamic force depends on the affinity A_j of a reaction j, which characterizes the imbalance of chemical potentials ($A_j = 0$ at equilibrium), and the reaction velocity $d\xi/dt$.

2.1.4 Non-equilibrium thermodynamics: the linear regime

We summarized a general framework to describe the behavior of non-equilibrium systems in terms of the entropy production σ expressed as a linear relationship between thermodynamic forces F_α and flows J_α in the form of equation (2.18). Now, you may have noticed that explicit expressions for the forces F_α naturally appeared in the derivation of the entropy production (see table 2.1, but no expression have been derived for the flows J_α. Although the flows arise in the presence of forces, they are not entirely determined by them and potentially rely on other factors [2]. For example, the presence of a catalyst in a chemical reaction can increase the rate of the chemical reaction.

Therefore, further progress required an additional assumption about the functional relation between the flows and forces; for a system that is slightly perturbed from the equilibrium state, a Taylor expansion of the flows can be performed around their equilibrium values [59]. Noting that the equilibrium state implies both $J_\alpha^{eq} = 0$ and $F_\alpha^{eq} = 0$, and neglecting the second-order and subsequent terms of the expansion, the flows are expected to be linear functions of the forces such that

$$J_k = \sum_j L_{kj} F_j \tag{2.19}$$

where the coefficients L_{kj} are constants known as phenomenological coefficients. Interestingly, equation (2.19) is in fact a generalization of well-established empirical laws, some of which were derived more than a century earlier, characterizing transport phenomena involving a flow driven by a gradient (force). For example, Fourier's law for heat conduction states that a heat flow J_q is proportional to the temperature gradient ∇T, with the heat conductivity κ playing the role of the phenomenological coefficient:

$$J_q = -\kappa \nabla T(x) = [\kappa] \cdot [-\nabla T(x)] = L_{qq} \cdot F_q \quad . \tag{2.20}$$

Similarly, Fick's law describes the diffusion process where the mass flow J_k is proportional to the concentration gradient ∇n_k, with the diffusion coefficient $D_k \equiv L_{kk}$:

$$J_k = -D_k \nabla n_k(x) = [D_k] \cdot [-\nabla n_k(x)] = L_{kk} \cdot F_k \quad . \tag{2.21}$$

Therefore, equation (2.19) provides a unified thermodynamic formalism that encompasses and generalizes empirically discovered linear laws. Moreover, it reveals that not only can a force drive its associated flow (e.g., the thermal gradient driving the flow of heat), but it can also drive other flows through a coupling of the phenomenological coefficients. For example, the Seebeck thermoelectric effect occurs when a thermal gradient drives not only the flow of heat but also an electrical current; the reverse occurs when an electric current drives a heat flow in the opposite direction, known as the Peltier effect (see figure 2.2). The couplings between the different flows and forces, coined as *cross-effects*, were observed before theoretical developments were made (e.g., by Lord Kelvin) and have been further validated experimentally [1].

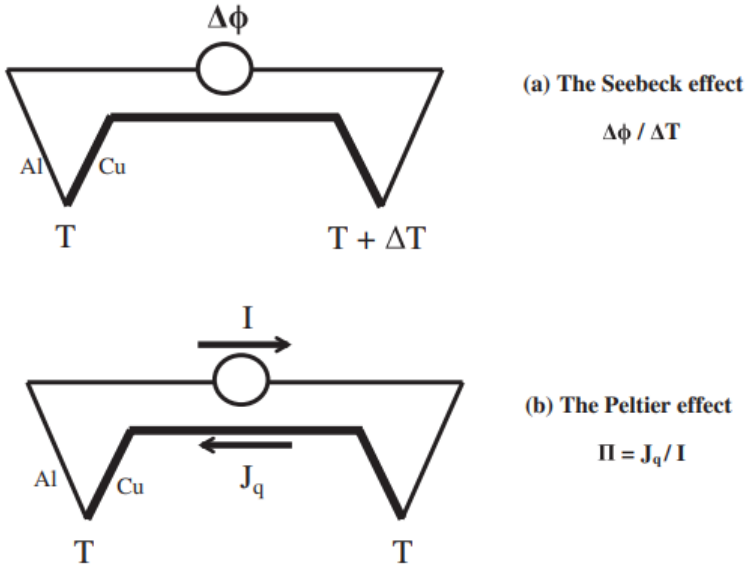

Figure 2.2: The thermoelectric effect is a *cross-effect* relating thermodynamic forces and flows. (a) In the Seebeck effect, two dissimilar metal wires are joined and the junctions are maintained at different temperatures. As a result an EMF is generated. The EMF generated is generally of the order of 10^{-5} V K^{-1} of temperature difference and it may vary from sample to sample. (b) In the Peltier effect, the two junctions are maintained at the same temperature and an electric current is passed through the system. The electric current drives a heat flow J_q from one junction to the other. The Peltier heat current is generally of the order of 10^{-5} J s^{-1} per amp [1]. Reproduced with permission from [2].

More specifically, if we explicitly write the equations that describe the thermoelectric cross-coupling, in the form of equation (2.19), for the Seebeck (J_q) and Peltier effect ($J_e \equiv I$), we find

$$J_q = L_{qq}\nabla\left(\frac{1}{T}\right) + L_{qe}\frac{E}{T} \qquad \text{and} \qquad J_e = L_{ee}\frac{E}{T} + L_{eq}\nabla\left(\frac{1}{T}\right) \quad . \tag{2.22}$$

We notice in equation (2.22) that the cross-coupling terms involve the phenomenological coefficients L_{qe} and L_{eq} respectively. Lord Kelvin and others had noticed experimentally

that these coefficients exhibited a general symmetry where $L_{ij} = L_{ji}$. Later, Lars Onsager provided the theoretical explanation for these symmetry relations, which are now known as the Onsager's reciprocal relations [60]. Onsager's proof of the reciprocal relationship is based on a statistical analysis of equilibrium fluctuations and involves the principle of detailed balance (i.e., microscopic reversibility). A key assumption in Onsager's derivation is the *regression hypothesis*, which asserts that *the average regression of fluctuations (in equilibrium) will obey the same laws as the corresponding macroscopic irreversible processes* [61]. In other words, because a system cannot distinguish whether the perturbation that pushes it out of equilibrium originates from an equilibrium fluctuation or is produced by an external cause, its response to the perturbation must be the same. Therefore, Onsager's intuition was to approach the problem from the perspective of a microscopic fluctuation analysis, which should yield a quantitatively similar behavior in a system's response as would the sudden change of a macroscopic variable [62].

Onsager's reciprocal relations are not just sophisticated derivations, they are a foundational aspect of linear irreversible thermodynamics because they allow the formulation of the first applicable general extremum principle in non-equilibrium systems [2]:

In the linear regime, the total entropy production in a system subject to flow of energy and matter, $dS_i/dt = \int \sigma \, dV$, reaches a minimum value at the non-equilibrium stationary state.

This principle, known as the Minimum Entropy Production (MinEP) Principle, was first derived by Ilya Prigogine [63]. As noted by Prigogine, in the linear range of irreversible processes, the entropy production assumes a role analogous to the thermodynamic potentials in equilibrium conditions; the MinEP principle states that near-equilibrium steady states are characterized by a minimum of the entropy production. While equilibrium states are characterized by zero entropy production, systems subjected to constraints that prevent them from reaching the equilibrium state evolve towards a non-equilibrium steady state where entropy production adopts the smallest finite value possible (see figure 2.4).

In this thesis, we are interested in studying the conditions under which complex

living systems can self-organize and sustain metabolic functions. Thus, it is natural to ask whether near-equilibrium systems are compatible with the level of organization observed in complex living systems. Prigogine argued that if a non-equilibrium state is perturbed, by virtue of the MinEP principle, the system will decay back to this initial reference state. In the words of Nicolis & Prigogine, the reference state is asymptotically stable, which implies that *in a system obeying linear laws, the spontaneous emergence of order in the form of spatial or temporal patterns differing qualitatively from equilibrium-like behavior is ruled out* [8].

In summary, systems in the linear regime tend to evolve towards stationary states (i.e. steady states), where entropy production attains its minimum value compatible with the constraints acting on the system. Under such conditions, complex spatial or temporal patterns cannot emerge, certainly not at the level required for biological organisms to exist. Therefore, the emergence of complexity must be connected to far-from-equilibrium conditions, where the linear relationship between the forces and flows breaks down. Only non-linear interactions between the forces and flows can amplify instabilities (or fluctuations) that are then stabilized by a continuous flow of energy through the system. Before continuing the exploration of non-equilibrium systems in the non-linear regime, let us first examine an example of a non-equilibrium stationary state which will be highly relevant to the work presented in Chapter 3.

Example of non-equilibrium stationary state: thermal gradient

To obtain a better understanding of entropy production and entropy flow in non-equilibrium stationary states, we will provide next the example of a system driven by a thermal gradient. This example is particularly useful for appreciating the development of the two-compartment entropy flow model presented in Chapter 3. Let us consider a system of length L in contact with a hot thermal reservoir at a temperature T_h at one end and a cold thermal reservoir at temperature T_c at the other (see figure 2.3). In this example, we assume that heat conduction is the irreversible process at play. Then, using the associated heat flow J_q and force (i.e. thermal gradient) from table 2.1, the entropy production per

unit volume σ is given by:

$$\sigma = \mathbf{J_q} \cdot \nabla \frac{1}{T} \quad . \tag{2.23}$$

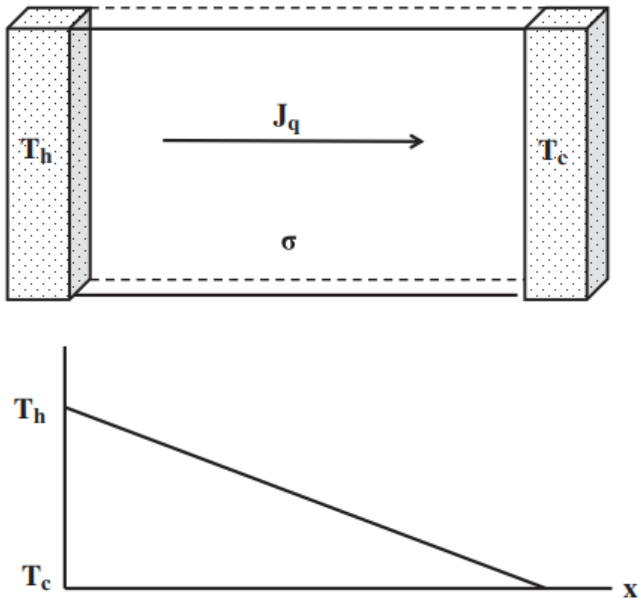

Figure 2.3: A simple thermal gradient maintained by a constant flow of heat. In the stationary state, the entropy current $J_{s,out} = dS_i/dt + J_{s,in}$. The stationary state can be obtained either as a solution of the Fourier equation for heat conduction or by using the theorem of minimum entropy production. Both lead to a temperature $T(x)$ that is a linear function of the position x. Reproduced with permission from [2].

If we restrict the problem to a 1-dimensional system for which the temperature gradient is only in the x-direction, σ per unit length is given by

$$\sigma(x) = J_{qx} \left(\frac{\partial}{\partial x} \frac{1}{T(x)} \right) = -J_{qx} \left(\frac{1}{T^2} \frac{\partial T(x)}{\partial x} \right) \quad . \tag{2.24}$$

The total entropy production within the system is obtained by integrating σ (see equation (2.12))

$$\frac{\mathrm{d}S_i}{\mathrm{d}t} = \int_0^L \sigma(x)\,\mathrm{d}x = \int_0^L J_{qx}\left(\frac{\partial}{\partial x}\frac{1}{T}\right)\mathrm{d}x \quad . \tag{2.25}$$

A stationary state requires that the temperature distribution does not vary in time (i.e. $T(x)$ is also stationary), implying that a uniform heat flow $J_q \neq J_q(x)$ is passing through the system; it would result otherwise in the accumulation or depletion of heat, thus leading to temperature variation with time. In fact, it is possible to show that $T(x)$ is a linear function of x in a stationary state (see bottom panel of figure 2.3) using Fourier's law and the conservation of energy in the case of heat flow. Moreover, a stationary state also implies the total entropy change of the system is zero

$$\frac{\mathrm{d}S}{\mathrm{d}t} = \frac{\mathrm{d}S_i}{\mathrm{d}t} + \frac{\mathrm{d}S_e}{\mathrm{d}t} = 0 \quad . \tag{2.26}$$

In other words, the total entropy can be constant only if the total entropy produced with the system (dS_i/dt) is compensated by an equal entropy flow (dS_e/dt)leaving the system. Given that J_q is constant as argued above, we can explicitly evaluate equation (2.25)

$$\frac{\mathrm{d}S_i}{\mathrm{d}t} = \int_0^L J_q\left(\frac{\partial}{\partial x}\frac{1}{T}\right)\mathrm{d}x = \frac{J_q}{T}\bigg|_0^L = \frac{J_q}{T_c} - \frac{J_q}{T_h} > 0 \tag{2.27}$$

where the term $J_{\mathrm{s,in}} = J_q/T_h$ corresponds to the entropy exchanged from the hot reservoir to the system and $J_{\mathrm{s,out}} = J_q/T_c$ corresponds to the entropy exchanged from the system to the cold reservoir. The entropy exchanged with the exterior (i.e. the reservoirs) corresponds to what we call the entropy flow dS_e/dt and is given by $dS_e/dt = [J_q/T_h - J_q/T_c]$ such that

$$\frac{\mathrm{d}S}{\mathrm{d}t} = \frac{\mathrm{d}S_i}{\mathrm{d}t} + \frac{\mathrm{d}S_e}{\mathrm{d}t} = \left[\frac{J_q}{T_c} - \frac{J_q}{T_h}\right] + \left[\frac{J_q}{T_h} - \frac{J_q}{T_c}\right] = 0 \quad . \tag{2.28}$$

We notice that the positivity of the entropy production dS_i/dt is satisfied by equation (2.27). In summary, this relatively simple example highlights the fact that a non-equilibrium system can be maintained in a stationary state where the entropy balance requires that entropy production within the system must be compensated by an outflow of entropy ($dS_e/dt < 0$) to the environment. The linearity of the flow-force relationship was used to determine the entropy production dS_i/dt in equation (2.27).

The derivation of this near-equilibrium system will be useful in Chapter 3 for the development of the entropy flow model in humans, which shares a similar entropy balance equation and method for quantifying entropy rates based on measurable heat flows at their respective temperatures. The key difference, however, is the assumption of stationarity, which cannot hold for humans that alternate between physical exercise and resting periods. Thus, given the expected imbalance between heat production within the body and heat dissipation to the environment, we will need to introduce an explicit time dependence of both the heat flows and compartment temperatures (i.e. numerators and denominators of equation (2.28).

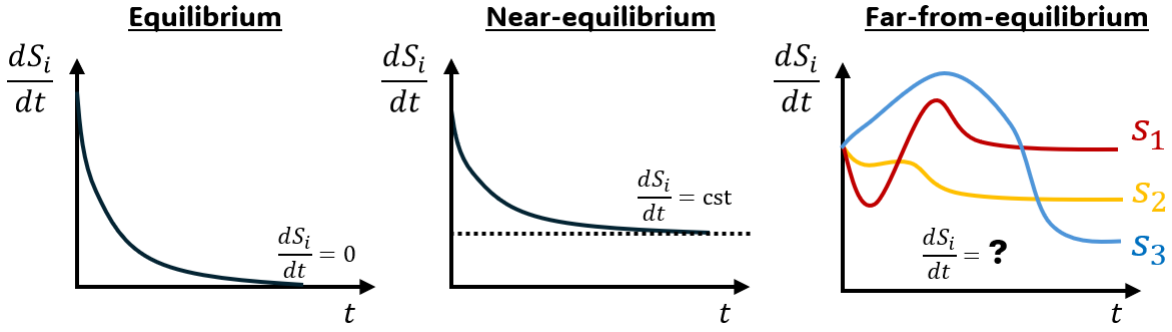

Figure 2.4: Time variation of the entropy production dS_i/dt in equilibrium (left), near-equilibrium (middle) and far-from-equilibrium conditions.

2.1.5 Non-Equilibrium Thermodynamics: The Non-Linear Regime

Predicting and understanding the behaviour of systems far from thermodynamic equilibrium presents significant scientific challenges, partly due to the complexity of the underlying (non-linear) dynamics and the potential for multiple stationary states. In contrast to the unique stable states predicted for equilibrium and near-equilibrium regimes, in the non-linear from-equilibrium regime, there is no single universally accepted general principle that predicts the state to which the system will evolve (see figure 2.4). This apparent unpredictability and the multiplicity of states are fundamental aspects of this regime. In fact, these two characteristics are not surprising considering the richness stemming from standard nonlinear dynamics.

This wealth of behavior gives rise to a class of phenomena, called dissipative structures, that arise spontaneously in the presence of sufficiently strong energy gradients. Many systems have been found to exhibit self-organization and pattern formation as a result of complex internal dynamics [19]: Bénard cells (spatially organized convection cells), chemical clocks (temporal oscillations), and reaction-diffusion systems, leading to spatial patterns (such as Turing patterns). The transition to such organized states often occurs when a control parameter driving the system further from equilibrium (such as a temperature gradient) crosses a critical threshold, similar to a phase transition. This suggests that pattern formation is intrinsically linked to a system's capacity to extract energy from the external gradient to maintain the organization of newly formed internal structures.

The term *dissipative* structures stems from the fact that their existence and maintenance depend on the continuous dissipation of free energy through irreversible processes, which inevitably generates entropy. The key point here is that far from equilibrium, the processes that produce entropy become the drivers of self-organization; order emerges *because* of entropy production, not *despite* entropy production. As mentioned in the introduction, this distinction provides the basis for establishing entropy production and entropy export as constitutive properties of complex systems. In this realm, dissipative structures can arguably be considered as a new state of matter.

All the systems mentioned above are consistently described as requiring conditions far from equilibrium where non-linear dynamics rule. Thus, the analysis of non-linear thermodynamic systems involves a similar set of tools used in the general literature of non-linear dynamics, e.g. Lyapunovs's stability theory and linear stability analysis [2] combined with stochastic methods (e.g. fluctuation-dissipation theorems [64]).

However, non-linear thermodynamics has an additional considerable difficulty related to the problematic definition of thermodynamic variables [58]. This problem of standard thermodynamic concepts, such as temperature and entropy, not being univocally defined, was highlighted earlier in the transition from equilibrium to near-equilibrium conditions. And the problem gets worse the further we are from equilibrium, even more so when the state variables can fluctuate, and when the *state* itself can be difficult to identify. This makes applying entropy-based stability criteria or deriving thermodynamic relationships far more complex than in systems where local equilibrium can be assumed and classical variables are relatively well-defined. Non-equilibrium thermodynamics is mostly interested in microscopic systems where we can hope for analytical results and a explanatory understanding; but for macroscopic systems, we rather seek an descriptive understanding based on postulated principles that must be verified experimentally.

The Maximum Entropy Production Principle (MEPP or MaxEP) has been widely proposed and explored as a potential organizing principle for far-from-equilibrium systems [62, 65, 66], particularly for selecting among multiple stationary states [67]. As implied by its name, the MEPP proposes that complex non-equilibrium systems, driven by external forces and possessing sufficient degrees of freedom, tend to evolve towards and maintain stationary states where the rate of entropy production is maximized given the constraints acting on them [68]. Therefore, the MEPP suggests that irreversible processes occur not only with positive entropy production (as required by the Second Law) but at the *fastest possible rate* given the external constraints.

This principle has been applied to various phenomena, including atmospheric and oceanic circulation [69], fluid turbulence [22], and biological systems [70–72], with variable

degrees of satisfaction [4, 73, 74]. The physical intuition behind MEPP is that dissipative structures can maintain a lower entropy state (i.e., locally more ordered) because, from the perspective of the Second Law, they contribute to a greater increase in the total entropy of the larger system in which they are embedded (i.e., the universe itself). Consequently, the MEPP suggests that the emergence of dissipative structures simply is the most efficient way for the universe to dissipate the energy gradients and ultimately achieve the equilibrium state. For example, life on Earth contributes to dissipate the low-entropy energy emitted by the Sun by radiating back into space higher entropy energy at a faster pace than if life were absent. Although the energy balance of Earth is approximately in a steady state (i.e., solar radiation inflow approximately equals infrared radiation outflow from Earth), the transformation process of energy allows the emergence of life.

A primary challenge for the MEPP is the lack of a universally accepted theoretical foundation, although it is sometimes associated with Jayne's principle of Maximum Entropy (MaxEnt) [75]. Moreover, the applicability and predictive power of the MEPP are highly conditional on the correct and complete identification of the constraints acting on the system, which is a non-trivial and ambiguous task [76]. Therefore, the success of matching the MEPP with observations is a good indicator that the relevant constraints may have been identified, but it fails to prove the validity of the principle itself. And given the richness of the emerging phenomenon in question, it may, in fact, be impossible to provide definite proof of a universal principle. Nonetheless, it is reasonable to assume that a system's capacity for self-organization is directly linked to its ability to produce entropy internally and export entropy externally.

Summary of the selection principles in thermodynamics

In thermodynamics, the selection principles governing the state of a system vary fundamentally with its distance from equilibrium and, ultimately, can be connected to the behavior of entropy production. For systems in a **state of equilibrium**, the governing selection principle is derived directly from the Second Law of Thermodynamics: isolated systems evolve towards a state of maximum entropy, representing the most probable macroscopic

configuration with the largest number of accessible microstates, which is a unique, stable state characterized by zero entropy production. For systems constrained by their environment (e.g., in contact with a reservoir at a constant temperature or pressure), equilibrium is characterized by the minimization of appropriate thermodynamic potentials, such as the Gibbs free energy or Helmholtz energy.

In states **near equilibrium**, typically characterized by linear relationships between thermodynamic forces and fluxes, the system cannot achieve zero entropy production due to imposed constraints (e.g. thermal gradient), but it evolves towards a unique, stable non-equilibrium stationary state. This state is governed by Prigogine's Minimum Entropy Production (MinEP) principle, which posits that the steady state minimizes the rate of entropy production relative to any other (transient) state in the linear regime.

For systems operating **far from equilibrium**, which can exhibit non-linear relationships and potentially multiple stable or metastable stationary states, there is no universally accepted general principle that dictates the specific state the system will select. Nonetheless, the Maximum Entropy Production Principle (MEPP) has been widely proposed as a selection criterion and suggests that from a broad range of possible stationary states consistent with the boundary constraints, the system selects the one with the highest rate of entropy production. However, its general formulation and applicability (especially to living systems) remain a subject of ongoing research and debate.

2.2 Human Thermoregulation and Calorimetry

This section bridges the theoretical concepts of non-equilibrium thermodynamics introduced in the previous section with more concrete physiological processes occurring within the human body. The main objective is to explain how energy and heat flows are managed by the body and how they are measured experimentally. Together with temperature measurements, they form the basis for calculating the real-time entropy rates in humans, which will be discussed in Chapters 3 and 4, and allow the modeling of entropy regulation

in Chapter 5.

2.2.1 The Human Body as a Thermodynamic System

In the previous section, much emphasis was placed on the role of external energy gradients in driving the internal dynamics of non-equilibrium systems. Living systems that are continuously maintained in non-equilibrium states by a chemical energy gradient are no exception to this rule. However, there is a universal characteristic of complex living systems (e.g., animals) that separates them from non-living dissipative structures. The chemical energy gradient that fuels their internal dynamics (i.e., glucose and fat storage) has been internalized over the course of evolution, possibly to free the organisms from the imperative and immediate need for constant external energy input. This contrasts with Bénard convection cells, for example, which break down as soon as the thermal gradient is reduced below the critical threshold value. As a result, living systems are less reliant on external conditions and more on their ability to maintain their self-organization despite changing environmental conditions. Not being constantly at the mercy of circumstances requires an active network of physiological responses that enable proper thermoregulation of the body.

Thermodynamics was first developed to study the efficiency of heat engines in which thermal energy is used to produce useful work accompanied by inevitable heat loss. Given the similarities, it is reasonable to ask ourselves if the human body is simply a complicated heat engine that requires the constant production of heat to perform work such as walking or lifting a box. If this were the case, the maximal efficiency of the human body, with an internal temperature of $T_1 = 310$ K (37 °C) and ambient temperature around $T_2 = 300$ K, would be approximately 3% according to equation (2.1). Fortunately, the efficiency of the human body is higher than that of the heat engine, with a maximum of approximately 20-25% depending on the physical task performed [37]. Moreover, biological systems must be able to operate and dissipate heat to a certain degree at ambient temperatures exceeding body temperature, which would violate the Second Law in the case of heat engines. Therefore, the analogy between the human body and a heat engine does not hold because unlike

heat engines, the body does not have the ability to obtain work from heat energy [77]. As mentioned earlier, the body can only obtain work from the chemical binding energy of the molecules we ingest as food.

2.2.2 Principles of Human Thermoregulation

Meticulous regulation of core body temperature is central to maintaining this far-from-equilibrium state, a process known as thermoregulation. Humans, like all endotherms, require constant metabolic activity as a source of heat and achieve homeostasis through a feedback control system [78]. The primary objective is to maintain the deep body temperature within a remarkably narrow physiological range (36-38 °C), despite significant internal perturbations, such as exercise-induced heat stress [79] or exposure to hostile environmental conditions [80]. This precise temperature control is vital for ensuring optimal biochemical reaction rates and protein stability within an organism [81]. For example, when the deep-body temperature exceeds 40 °C, the likelihood of experiencing heat-related injuries and heat stroke increases [82].

To achieve a stationary state in which the body temperature does not change, the internal production of heat must be compensated by external heat dissipation. If heat is not eliminated, body temperature quickly rises to dangerous temperatures; for example, during physical exercise at moderate intensity, body temperature rises by approximately 3°C per hour, causing a complete collapse by the end of the second hour of exercise [77]. Consequently, the body devised cleaver and efficient heat loss mechanisms to ensure temperature stability.

2.2.3 Bioenergetics of the Metabolism

Although Carnot's theorem does not apply to the human body, it is still restricted by the principle of the conservation of energy dictated by the First Law of Thermodynamics. In the context of the human body, the energy balance equation includes terms related to thermal energy (i.e., heat content) and mechanical work, as well as chemical energy in the

form of carbohydrates, fat, and proteins (i.e., food substrates). The rate at which chemical energy is liberated within the body through metabolic processes, predominantly from the catabolism of these food substrates, is referred to as the metabolic energy expenditure $\dot{M}$ [37]. This liberated energy is subsequently transformed either into mechanical work $\dot{W}$ performed by the body (e.g., cycling against a resistance and lifting weight) and, to a significantly larger extent (80-100%), transformed into heat within the body. The heat generated internally from metabolic activity is referred to as **metabolic heat production** $\dot{Q}_{int}$. Then, the energy balance for the chemical energy conversion is given by

$$\dot{M} = \dot{Q}_{int} + \dot{W} \tag{2.29}$$

Metabolic heat production is constrained to positive values (i.e. $\dot{Q}_{int} > 0$) because the body must continuously metabolize to maintain homeostasis, a situation analogous to a non-equilibrium steady state being maintained by the constant application of an external gradient. During physical activity, metabolic energy expenditure can increase substantially, reflecting the higher energy demands of muscle contraction and associated processes [79,83]. For example, depending on the activity performed, the metabolic rate can increase by a factor of three when walking slowly and by a factor of up to nine when running at 12 km/h when compared to the resting metabolic rate [84].

To understand how heat is produced through various metabolic pathways, we must first understand the oxidation processes of carbohydrates (primarily glucose) and fats [83]. The complete oxidation of glucose, called cellular respiration, involves a series of intermediate steps (i.e., glycolysis, Krebs cycle, and electron transport chain) with the ultimate goal of converting glucose into energy in the form of ATP molecules. By omitting all the intermediate steps, glucose oxidation can be summarized as follows:

$$C_6H_{12}O_6 + 6\,O_2 \rightarrow 6\,CO_2 + 6\,H_2O + \text{energy} \tag{2.30}$$

where the output energy consists of heat and ATP molecules (1 mol of glucose makes 30-32 mol of ATP by using 6 mol of oxygen). A useful metric for characterizing carbohydrate oxidation is the *caloric equivalent*, defined as the energy produced per liter of oxygen consumed, which is $e_c = 21.13$ kJ/L [37].

Next, the liberation of chemical energy from fat molecules is often exemplified by the oxidation of palmitic acid:

$$CH_3(CH_2)_{14}COOH + 23\,O_2 \rightarrow 16\,CO_2 + 16\,H_2O + \text{energy} \tag{2.31}$$

where 1 mol of palmitic acid leads to the formation of 106 mol of ATP, requiring 23 mol of oxygen. The *caloric equivalent* for the oxidation of fat, that is, the energy produced by the full oxidation of fat, is $e_f = 19.63$ kJ per liter of O_2 consumed [37].

It is well known that the body simultaneously uses both the oxidation of carbohydrates and fats, and the proportion of substrate utilization can change, for example, during physical exercise depending on intensity. However, a careful analysis of the stochiometric coefficients in equations (2.30) and (2.31) shows an imbalance between O_2 consumption and CO_2 production: for glucose oxidation, 6 O_2 consumed leads to 6 CO_2 produced (i.e., 1:1 ratio), whereas for fat oxidation, 23 O_2 consumed leads to 16 CO_2 produced (i.e. 1:0.7 ratio). The proportion of energy liberated from each oxidation process can be obtained from the *Respiratory Exchange Ratio* R (sometimes called the respiratory quotient), which is defined as the ratio of CO_2 produced to O_2 consumed: $R = \dot{V}CO_2/\dot{V}O_2$. R values near 1 indicate that carbohydrates are the predominant fuel source, while R near 0.7 reflects the use of fats [37]. Any value of R in between indicates a mix of both carbohydrate and fat metabolism. Therefore, the total energy liberated by metabolic activity, that is, the metabolic energy expenditure (see equation (2.29)), is given (in Watts) by [85].

$$\dot{M} = \frac{\left(\dot{V}O_2 \cdot \left[\frac{R-0.7}{0.3} e_c + \frac{1-R}{0.3} e_f\right]\right)}{60} \tag{2.32}$$

where $\dot{V}O_2$ corresponds to the oxygen consumption rate (in $\mathrm{L{\cdot}min^{-1}}$). We see that if R is closer to one, the second term becomes small and the first term dominate, the latter corresponding to glucose oxidation. Conversely, if R is closer to 0.7, then the first term becomes small, and only the second term contributes, leading to predominant fat metabolism. Because the body dynamically regulates the utilization of these substrates based on energy demands, availability, and environmental conditions [79], R is typically time-dependent. Equation (2.32) is highly relevant to the work presented in this thesis because the measurement of metabolic heat production $\dot{Q}_{int}$ is closely related to the measurement of metabolic energy expenditure through equation (2.29).

In summary, although both carbohydrates and fats are vital energy substrates, they exhibit distinct characteristics regarding their energy yield per unit mass and oxygen requirements. More specifically, fats are more energy-dense but require more oxygen to be metabolized (as reflected by the lower caloric equivalent values, $e_f < e_c$) compared to carbohydrates. Moreover, a key difference between the two substrates is that carbohydrates provide quicker energy access and can be partially metabolized anaerobically (i.e., without oxygen). Indeed, during high-intensity or prolonged exercise, limitations in oxygen supply result in the use of a different metabolic pathway to produce ATP: *glycolysis* (also known as the Embden-Meyerhof pathway). In this anaerobic process, glucose is converted into pyruvic acid, which, under low-oxygen conditions, is later converted into lactic acid, which is known to contribute to muscle fatigue [79]. Although anaerobic metabolism is less efficient for energy conversion (i.e. ATP yield per glucose molecule) than aerobic metabolism, it provides useful energetic resources when oxygen requirements exceed the capacity of the cardiorespiratory system [83].

2.2.4 Calorimetry Techniques for Measuring Heat Flows

Calorimetry is, by definition, the measurement of heat, and a calorimeter is a device that measures the heat emitted or absorbed by a mass [37]. Calorimetry has been traditionally used in the study of physiology and thermoregulation, with the famous work of Lavoisier and Laplace involving an animal calorimeter (made of ice and snow) dating back to the 18th century [86]. In their pioneering work, they demonstrated that heat production in animals is a product of the combustion of carbon fuel. In modern times, calorimetry studies human thermoregulatory responses under various environmental conditions (e.g., heat acclimation in vulnerable populations in the context of global warming [80], firefighters' heat tolerance in extreme temperatures [87]) or in relation to intrinsic factors such as age, sex, life habits, and certain chronic health conditions (e.g., diabetes) [78, 79].

It should be noted that the calorimetry data analyzed in the following chapters of this thesis was collected previously by Prof. Kenny's research group and was originally intended to study the thermal response in humans in association with age [88], fitness level [89] and diabetes [90]. All of these studies were approved by the University of Ottawa Ethics Board and volunteers provided written informed consent before their participation. Further details on the experiment protocols and participants' characteristics are given in section 4.2.1.

In our context of interest, the datasets mentioned above (and further described in Chapter 4) also provide the basis for a new interpretation in terms of entropy production and entropy export rates in humans, which was not previously possible given the significant technical challenges of such measurements as evidenced by the overall lack of experimental data in the literature. Therefore, an important contribution of the work presented in this thesis (mostly in Chapter 3) consists of establishing a methodological framework capable of measuring the thermodynamic quantities necessary for the real-time assessment of entropy rates. Given that the human body operates primarily based on principles of thermoregulation, the measurement of entropy rates, which correspond to heat transfer divided by temperature (see section 2.1), largely depends on the accuracy of the measurement of heat

flows and internal temperatures.

In what follows, we describe the experimental methods used in our calorimetry datasets to measure metabolic heat production by indirect calorimetry and the total heat dissipated from the body by direct calorimetry.

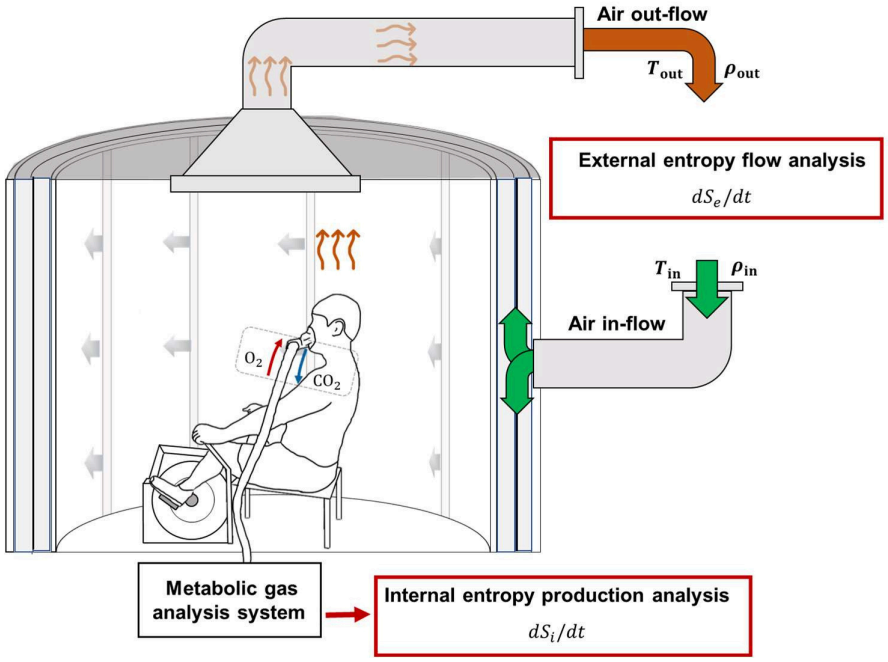

Figure 2.5: **Calorimetry chamber and experimental design.** The participants exercised on an upright cycle ergometer within the calorimetry chamber, which essentially acts as a thermal heat bath that maintains a fixed ambient temperature T_{in} and absolute humidity ρ_{in}. Internal entropy production is measured using indirect calorimetry; expired gases enter an automated metabolic gas analysis system that measures oxygen uptake and carbon dioxide production to continuously yield the rate of metabolic energy expenditure and metabolic heat production $\dot{Q}_{int}$, and subsequently the entropy production rate dS_i/dt. External entropy export rate, dS_e/dt, is measured using direct calorimetry; changes in temperature and absolute humidity between the air outflow (T_{out} and ρ_{out}) and inflow (T_{in} and ρ_{in}) allow for the measurement of heat dissipation rate $\dot{Q}_{out}$ and subsequently the entropy export rate from the body.

Direct calorimetry is based on a fundamental thermodynamic principle: the conservation of energy (i.e. First Law) within an isolated system. A calorimeter is a sealed

and highly insulated system that prevents any exchange of energy with the exterior. While there are many types of calorimeters [86], in the present thesis, we focus on the modified Snellen air calorimeter currently located at the University of Ottawa and operated by Prof. Glen Kenny's research group [38]. Direct calorimetry is considered the gold standard for measuring the total heat loss [91, 92]. Figure 2.5 shows a cross-sectional view of the calorimetry chamber, in which the participants were seated on an upright cycle ergometer. This state-of-the-art calorimeter functions by precisely controlling the temperature and humidity of the air inflow through the sealed chamber. Subsequently, by measuring the differences in air temperature ΔT_{air} and humidity $\Delta \rho_v$ between the inflow and outflow, the rates of dry and evaporative heat loss can be calculated. From a thermodynamic perspective, the continuous inflow of air within the chamber is analogous to a reservoir maintained at a constant temperature and humidity, and the objective is to measure the heat exchanged between the participant and the reservoir (see figure 3.1).

Quantitatively, dry heat loss $\dot{Q}_{dry}$ corresponds to heat dissipated from the body due to heat conduction, convection and radiation at the skin surface, and is given by

$$\dot{Q}_{dry} = c_{air} \times \dot{m}_{air} \times \Delta T_{air} \tag{2.33}$$

where c_{air} =1.005 J·(kg· °C)$^{-1}$ is the specific heat of air, $\dot{m}_{air}$ is the mass flow of air (kg air/s) out of the calorimetry chamber, and $\Delta T_{air} = T_{out} - T_{in}$ is the difference in temperature between the outflow and inflow of air from the calorimetry chamber. It should be noted that the radiative heat emitted by the participant is not directly measured; however, the interior of the calorimetry chamber is made of reflective walls that reflect any radiant heat emitted, which is ultimately transferred to the circulating air and accounted for in the measured temperature difference ΔT_{air} [37]. The evaporative heat loss $\dot{Q}_{evap}$ corresponds to the heat transferred to the air through the evaporation of sweat on the skin surface, which leads to a change in the absolute humidity between inflow and outflow. Evaporative heat loss is given by

$$\dot{Q}_{evap} = L_{vap} \times \dot{m}_{air} \times \Delta\rho_v \tag{2.34}$$

where L_{vap}=2.426 J per gram of sweat and is the latent heat of the vaporization of sweat, and $\Delta\rho_v = \rho_{out} - \rho_{in}$ is the difference in absolute humidity (g of water/kg air) between the outflow and inflow of air from the calorimetry chamber.

Indirect calorimetry is the method traditionally used to estimate metabolic energy expenditure in the body from substrate utilization [37]. It operates on the principle that energy liberated from metabolic activity predominantly arises from the oxidation of carbohydrates and fats, and to a lesser extent, proteins. Measuring the consumption rate of oxygen $\dot{V}_{O_2}$ and emitted carbon dioxide $\dot{V}_{CO_2}$ from the expired gases and quantifying the respiratory exchange ratio $R = \dot{V}_{CO_2}/\dot{V}_{O_2}$ allows the estimation of the metabolic energy expenditure $\dot{M}$ from equation (2.32).

As shown in figure 2.5, during the experimental studies, participants breathed through a mouthpiece (with a nose clip), and expired gases were directed into an automated metabolic gas analysis system. This system continuously determines the concentrations of expired O_2 and CO_2 using a calibrated electrochemical gas analyzer [88]. When used concurrently with direct calorimetry (e.g., in the modified Snellen calorimeter), the expired air is vented back into the chamber after going through the analysis system to ensure that respiratory heat loss from temperature and humidity changes in respiratory gases is accounted for in the total heat loss measurement.

In all the experimental studies presented in this thesis, participants performed physical exercise by pedaling on a cycle ergometer (see figure 2.5). However, the ergometer itself was located outside the calorimeter chamber and mechanically linked to the pedals inside the chamber. This configuration ensured that the heat generated from the resistance unit (i.e. magnetic resistance from the generation of eddy currents) did not contribute to the difference in heat content of the air measured by ΔT_{air} [38]. This specifically designed

ergometer allows for the generation of a variable and measured resistive force against which the participants pedal.

As shown by equation (2.29), the work rate is related to the metabolic energy expenditure $\dot{M}$ and the metabolic heat production $\dot{Q}_{int}$. Most experimental protocols require to impose a specific and identical metabolic heat production rate to participants during the exercise bouts, such that the internal heat stress across participants is standardized. This is achieved by continuously measuring in real-time the metabolic energy expenditure $\dot{M}$ (using equation (2.29)) and simultaneously adjusting the cycling resistance (and thus the work rate $\dot{W}$) accordingly such that $\dot{Q}_{int} = \dot{M} - \dot{W}$ remains constant.

2.2.5 Temperature Measurements

In the previous section, we detailed the methodology employed for measuring the heat flows (i.e. metabolic heat production and total heat loss). However, the quantification of entropy changes (i.e. $\Delta S = \Delta Q/T$) also requires the assessment of core and skin temperature in the two-compartment model presented in Chapter 3. In fact, temperature measurements in the body are quite challenging and a great source of debate [93, 94], mainly due to the heterogenous distribution of temperature across the body. There are two main approaches, namely thermometry and calorimetry, that offer distinct but complementary temperature estimates in the body [37].

The **thermometry approach** involves the direct measurement of tissue temperature (i.e. local measurement) using thermal probes. For example, deep body temperature, which often represents the core temperature, can be estimated by inserting a probe inside the rectal cavity. Rectal temperature is often used in thermoregulation studies because the participants can tolerate the presence of the probe for extended periods of time. However, rectal probes are known to react slowly to changes in core temperature due to the low heat conductivity of the air within the rectal cavity [95]. Nonetheless, rectal temperature is still viewed as a reliable measurement of body temperature for field assessment and monitoring of heat-related injuries [96]. For such experiments, esophageal temperature

probes are typically preferred given their faster response to changes in temperature [93]. Esophageal probes are inserted through the nostril down to the eight thoracic vertebrae, causing discomfort in participants over prolonged periods [79]. There exist other deep body probes, although less frequently used, such as ingestible temperature capsules to measure gastrointestinal temperature and, for more specific studies, intra-muscle and subcutaneous probes can be used [95].

Finally, skin temperature is also typically measured using thermometry (i.e. probes). Given the heterogeneity of temperature distribution across the skin surface, obtaining a single representative value requires measurements at multiple sites. Mean skin temperature is then calculated as a weighted average of the temperatures measured at these designated sites. For example, in the experimental data presented in Chapter 3, mean skin temperature was calculated using four temperatures weighted to the following proportions: upper back (30%), chest (30%), quadriceps (20%) and back calf (20%). The chosen probe sites can vary between studies depending on the experiment design and desired accuracy, and their relative weight in the average temperature calculation typically reflects their relative proportion of body surface area [93]. Representative time series of skin temperature measurements are shown in figure 2.6 for the aging, fitness level and type 2 diabetes studies [88–90].

The conventional approach to estimating mean body temperature $\bar{T}_b$ from thermometry employs a two-compartment model and weighting the contributions of core and skin temperatures following the equation

$$\bar{T}_b = \alpha\, T_C + (1 - \alpha)\, T_s \tag{2.35}$$

where T_c is core temperature, T_s is skin temperature, and α is a weighting coefficient representing the relative contribution of core and skin temperatures for the calculations of $\bar{T}_b$ [37]. The value of α depends on the experiment design; for example, a typical value

of $\alpha = 0.90$ (i.e. 90% core, 10% skin contribution to $\bar{T}_b$) in normal conditions, whereas $\alpha = 0.80$ in hot environments and $\alpha = 0.66$ in moderate/cold environments [93].

In contrast to directly measuring body temperature using probes (i.e. thermometry), the **calorimetry approach** combines the use of direct and indirect calorimetry measurements to estimate the change in body heat content [37]. Indeed, any imbalance between the metabolic heat production rate $\dot{Q}_{int}$ (measured by indirect calorimetry) and the rate of total heat loss $\dot{Q}_{out}$ (measured by direct calorimetry) leads to either accumulation or depletion of heat within the body. The rate of heat storage is defined as $\dot{Q}_{st} = \dot{Q}_{int} - \dot{Q}_{out}$. It is important to note that calorimetry cannot provide a direct temperature measurement, but only changes in body temperature ΔT_b following the imbalance between the inflow and outflow of heat. Then, using basic thermodynamic principles, the change in body temperature during a time interval Δt is given by

$$\Delta T_b = \frac{\dot{Q}_{st} \cdot \Delta t}{m \cdot c_p} \tag{2.36}$$

where m is the participant's mass and c_p is the average specific heat capacity of living tissues [37]. In experimental studies, particularly those involving exercise, a common approach is to use thermometry to establish a baseline body temperature during an initial resting period when conditions are stable, and temperature probes are considered accurate. Subsequently, during exercise and recovery periods, when temperatures are changing dynamically, the relative changes in body temperature are instead estimated using calorimetry by calculating the rate of heat storage from the balance of heat flows. Representative time series of body temperature measurements are shown in figure 2.7 for the aging, fitness level and type 2 diabetes studies [88–90].

Although calorimetry does not provide a spatial temperature distribution, it is the most accurate method for estimating the total amount of heat stored internally based on the fundamental principle of energy balance [37]. Chapter 3 presents an insightful comparison

between thermometry and calorimetry for the quantification of entropy changes in the body. Moreover, further limitations of both methods are discussed in great detail in section 3.4.4 of Chapter 3.

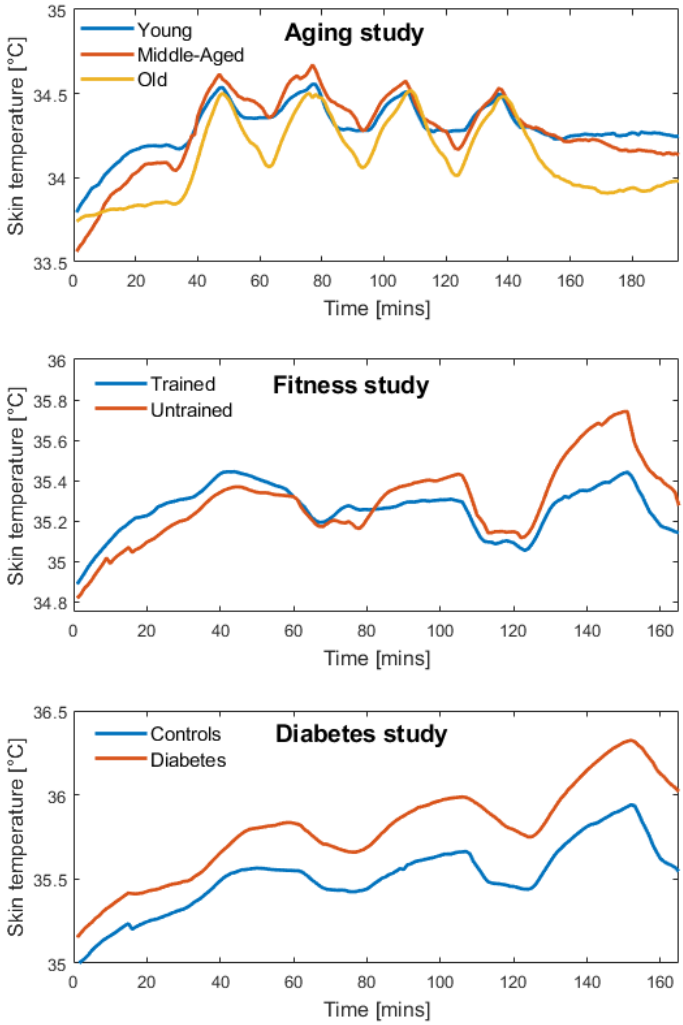

Figure 2.6: **Skin temperature** Skin temperature measurements (T_s) as a function of time for the aging study (top panel), fitness study (middle panel) and diabetes study (bottom panel). The associated experiment protocols are given in table 4.1. The colored curves represent the average skin temperature for each group. For a single participant, mean skin temperature was calculated from a weighted average of four skin temperature probes located on the biceps (30%), chest (30%), quadriceps (20%) and front or back calf (20%).

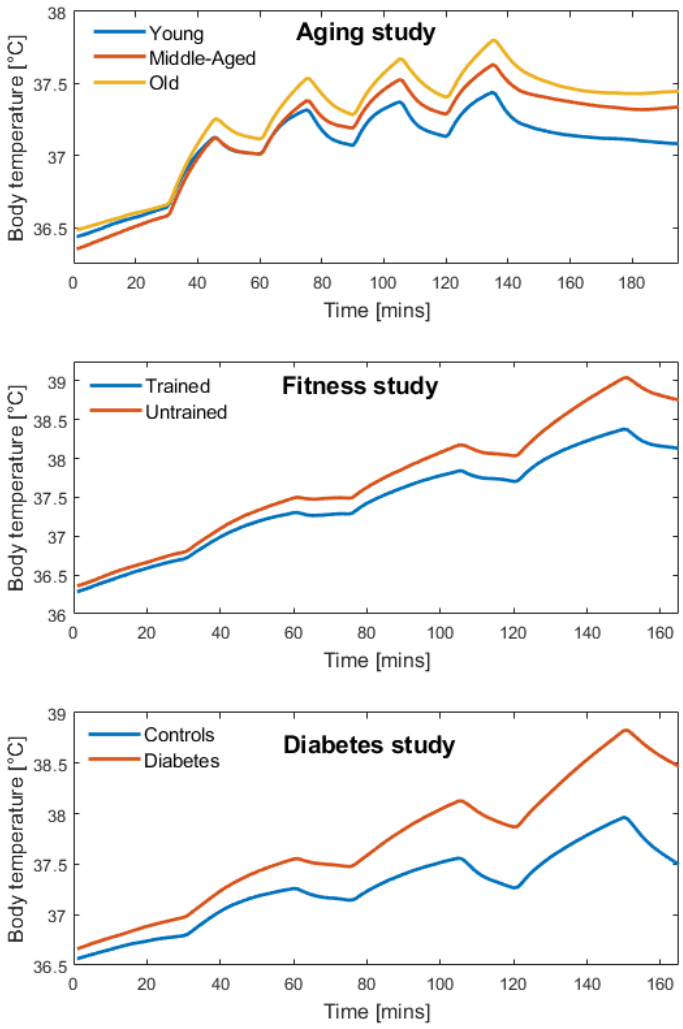

Figure 2.7: **Body temperature.** Body temperature measurements (T_b) as a function of time for the aging study (top panel), fitness study (middle panel) and diabetes study (bottom panel). The associated experiment protocols are given in table 4.1. The colored curves represent the average body temperature for each group. The body temperature at $t = 0$ was measured by thermometry using a weighted average between a rectal probe (90%) and mean skin temperature (10%). Then, changes in body temperature were estimated by calorimetry using the rate of heat storage (i.e., from the balance of heat flow)

2.2.6 Thermoregulation from an entropy perspective

Conceptualizing thermoregulation in animals through the lens of entropy generation has been a subject of interest in the past [97–99]. A common approach in this field is to model entropy generation based on the enthalpy changes associated with the chemical reactions fueling the metabolic processes [35]. In essence, such models quantify the entropy generated from the oxidation of nutrients and effectively calculate the entropy change *before* the resulting energy is fully transformed into heat within the body (i.e. not measuring heat directly). This approach is particularly useful to study entropy generation when the body is maintained close to a steady-state, for example to investigate the effect of diet on lifespan entropy change [100–103]. In contrast, the calorimetry approach, used previously by Aoki [33,98] and the one detailed in this thesis, measures the rates of entropy production and export based on the direct measurement of heat, thus *after* heat has been generated by the metabolic processes. As such, our approach allows to study entropy production and export in real-time when the body is perturbed away from a steady-state (e.g. through physical exercise).

Over the last few decades, thermoregulation models of animals (including humans) have progressed significantly [104,105]. An important stepping stone was the development of two-compartment models (or two-node models) which simplify the body into a "core" and a "skin" shell to simulate heat generation and transfer from basic physiological responses like sweating. To provide a more detailed analysis of the physical and physiological phenomena at play, more sophisticated models divided the body into multiple segments (e.g., head, trunk and limbs), each composed of multiple tissue layers with different properties (e.g. heat conductivity and capacity) [106]. These multi-node and multi-segment models, such as the Stolwijk's model [105, 107], can better capture the dynamics of the vascular and central nervous system responses to heat stress by accounting for realistic anatomical and thermal properties of the body. These advanced models, which allow a more personalized modeling in terms of body composition, gender and age, could provide valuable insights into the entropy dynamics of animals as they accurately predict heat transfers, localized temperatures and sweat rates of individual body parts [108, 109].

2.3 Stochastic Processes

Stochastic Differential Equations (SDEs) are ordinary differential equations that describe the time evolution of a system of variables that are subjected to both deterministic and random forces. These fluctuations can arise from various natural sources and can be modeled as noise through a stochastic process. In physics, SDEs provide a framework to study the probabilistic behaviour of physical systems driven by noise, and originate in Einstein's theory of Brownian motion in 1905 followed by Langevin's analysis (1908) of a massive particle under the influence of a rapidly fluctuating random force and a frictional force from the surrounding fluid. It has also been applied to a broad range of systems in science, engineering and medicine, such as the brain activity [110] and the opening/closing dynamics of ion channels [111].

SDEs usually involve a deterministic part that can be described using standard ordinary differential equations, and a stochastic part that adds randomness and therefore a degree of unpredictability to the system's time evolution. The stochastic part implies that if one could perform repeated observations of a stochastic process starting from an identical initial condition, the specific sequence of values of the process (known as a realization) would be different. In systems exhibiting nonlinearity, the stochastic part can lead to new most probable stable states that differ from the deterministic equilibria, or trigger continual transitions between coexisting deterministic states (i.e. noise-induced transitions) [112]. The latter case can be exemplified by the trajectory of a particle subjected to a double-well potential where the particle's position alternates randomly between the two deterministic state that are minima of the associated potential function; this potential is simply the negative gradient of the deterministic "drift" part in 1D (see figure 2.8).

A typical example consists of the motion of a Brownian particle subject to both deterministic forces (like friction or an external potential) and random forces due to collisions with the surrounding fluid molecules [50]. However, unlike deterministic variables, the future values of a stochastic process cannot be predicted with certainty. Consequently, the treatment of SDEs requires special care because stochastic processes are typically not dif-

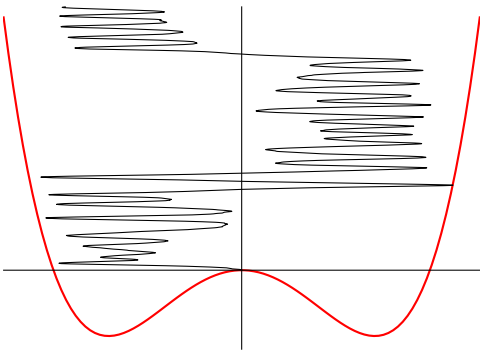

Figure 2.8: **Double well and Langevin equation** The red curve shows the double well potential. The black curve shows the trajectory of a particle subjected to Gaussian white noise and friction, immersed in the double well potential (time progresses from bottom to top). The trajectory corresponds to the numerical integration of the associated Langevin equation (similar to equation (2.40)). (Image credit: HeMath, CC BY-SA 4.0, via Wikimedia Commons)

ferentiable and thus the standard calculus approach (Riemann integrals) cannot be applied directly. There are specialized rules to evaluate the integral of a SDE (i.e. solving the SDE) which lead to different interpretations (Îto and Stratonovich) and different contextual use cases [113].

The simplest model where a dynamical variable $y(t)$ depends on noise can be written as

$$\frac{dy}{dt} = f(y,t) + \xi(t) \tag{2.37}$$

where $f(y)$ is an arbitrary function that depends on y and $\xi(t)$ represents the fluctuations. In this specific case, the noise is said to be ''additive" because the noise term is simply added to the deterministic component. Some stochastic processes are better modeled with

multiplicative noise where the coefficient of the noise also depends on the value of the state variable. In such case, the SDE takes the form (in 1D):

$$\frac{dy}{dt} = f(y,t) + g(y,t)\,\xi(t) \quad . \tag{2.38}$$

In this thesis, we will limit the stochastic analysis to additive noise as given by equation (2.37). Obviously, the type of noise $\xi(t)$ will influence the dynamics of $y(t)$. The most used type of noise is the Gaussian white noise which is characterized by two key properties: its amplitude at any point in time follows a Gaussian distribution, and its values at different times are uncorrelated (i.e. correlation time is zero). This lack of correlation is often represented mathematically by a delta function for the noise's autocorrelation:

$$\langle \xi(t)\xi(t') \rangle = 2D\delta(t-t') \tag{2.39}$$

where D is the noise amplitude. Gaussian white noise is often a simplifying assumption used in many models due the central limit theorem which states that the sum of many independent random variables tends towards a Gaussian distribution. Moreover, the resulting Gaussian distribution is quite practical because it is mathematically tractable, meaning that it allows a proper mathematical treatment which will be appreciated later when dealing with Fokker-Planck equations.

The dynamics of many physical systems can be expressed in the form of equation equation (2.37), and more specifically a subset called Langevin equations that have the form

$$\frac{dy}{dt} = -\alpha y + \xi(t) \quad . \tag{2.40}$$

Langevin equations consist of a deterministic part, typically representing a force driving the system to an equilibrium point (notice the minus sign), and a stochastic part, representing random forces or noise arising from the environment (e.g., thermal fluctuations) [114]. The most famous example is the Brownian motion of a particle in a fluid, where the deterministic part describes the friction force, and the stochastic part describes random molecular collisions. In this specific case, the Langevin equation describing the velocity of a particle undergoing Brownian motion is given by

$$m\frac{dv}{dt} = -\lambda v + \xi(t) \quad . \tag{2.41}$$

A stochastic model that is expressed in the form of a Langevin equation where the noise term $\xi(t)$ corresponds to Gaussian white noise is referred to as an Ornstein-Uhlenbeck process. This particular process is of great interest to this thesis as the stochastic model of entropy regulation developed in Chapter 5 builds on this theory. Interestingly, the Ornstein-Uhlenbeck process is considered to have "colored" noise because, although it is driven by Gaussian white noise (which is "uncolored"), the resulting stochastic process itself exhibits time-correlated fluctuations, characterized by an exponentially decaying autocorrelation function [115]. For greater details on the derivation of the autocovariance for the Ornstein-Uhlenbeck process in our specific use case, the reader is referred to Appendix 5.6.

We mentioned earlier that repeated observation of the same stochastic process yields different trajectories due to the random contributions from noise. Therefore, instead of looking at the individual realizations, it is sometimes useful to adopt the complementary perspective of the probability density of the possible outcomes. For example, if you set up an experiment where a large number of Brownian particles starts exactly at the origin (i.e. initial density is a delta-function at the origin) and you let the system evolve in time, the distribution of the positions at a time t will have a Gaussian form that spreads over time (more specifically with a variance that increases linearly with time) [116]. This

idea of describing the time-evolution of the probability density by propagating the initial conditions under the action of the SDE is known as the Fokker-Planck approach [115]. The main advantage of such approach is that a stochastic differential equation can be recast into a deterministic partial differential equation for the density $\rho(y,t)$, known as the Fokker-Planck equation (in 1D):

$$\frac{\partial \rho}{\partial t} = \frac{1}{2}\frac{\partial^2}{\partial y^2}\left[g^2(y)\,\rho\right] - \frac{\partial}{\partial x}\left[f(y)\,\rho\right] \tag{2.42}$$

where the functions $f(y,t)$ and $g(y,t)$ are the same as those of equation (2.38). The asymptotic regime can be obtained by setting the left hand side of equation (2.42) to zero, which yields (if it exists) the stationary density $\rho_s = \rho(y,\infty)$.

Now equipped with this theoretical formalism, it should be noted that SDEs must ultimately be solve numerically using integrating methods that adequately incorporate their stochastic nature. The simplest approach is called the Euler-Maruyama method in which the SDE can be rewritten as

$$dy = f(y,t)dt + g(y,t)\cdot\xi(t)dt \tag{2.43}$$

where $\xi(t)dt \equiv dW$ is a Gaussian random variable with zero mean and variance equal to dt [112]. Put in a numerically integrable form with small fixed time increments Δt, we obtain

$$y(t+\Delta t) = y(t) + f(y,t)\cdot\Delta t + \sqrt{\Delta t}\cdot dW_n \tag{2.44}$$

where the variables dW_n are independent random variables sampled for a Gaussian distribution with mean zero and unit variance.

Chapter 3

How to measure entropy rates in humans

Abstract

Complex living systems, such as the human organism, are characterized by their self-organized and dissipative behaviors, where irreversible processes continuously produce entropy internally and export it to the environment; however, a means by which to measure human entropy production and entropy flow over time is not well-studied. In this article, we leverage prior experimental data to introduce an experimental approach for the continuous measurement of external entropy flow (released to the environment) and internal entropy production (within the body), using direct and indirect calorimetry, respectively, for humans exercising under heat stress. Direct calorimetry, performed with a whole-body modified Snellen calorimeter, was used to measure the external heat dissipation from the change in temperature and relative humidity between the air outflow and inflow, from which was derived the rates of entropy flow of the body. Indirect calorimetry, which measures oxygen consumption and carbon dioxide production from inspired and expired gases,

was used to monitor internal entropy production. A two-compartment entropy flow model was used to calculate the rates of internal entropy production and external entropy flow for 11 middle-aged men during a schedule of alternating exercise and resting bouts at a fixed metabolic heat production rate. We measured a resting internal entropy production rate of (0.18 ± 0.01) W/(K·m^2) during heat stress only, which is in agreement with published measurements. This research introduces an approach for the real-time monitoring of entropy production and entropy flow in humans, and aims for an improved understanding of human health and illness based on non-equilibrium thermodynamics.

3.1 Introduction

Non-equilibrium systems, like cells, organs, and organisms, actively exchange matter and energy with their environment. Far from a state of equilibrium, new structures and functions can emerge from the complex interplay of irreversible processes that continuously produce entropy as energy gradients are dissipated. These systems, referred to as dissipative structures, are characterized by self-organized behavior in the presence of sufficiently strong energy gradients. In such cases, complex systems can spontaneously form to feed upon these energy gradients, adopting highly ordered configurations that are impossible under equilibrium conditions. Complex living systems, such as the human body, can be regarded as open thermodynamical machines that inherently transform energy sources, mostly into heat, in order to produce a relatively small portion of useful work. Here, we develop an experimental–theoretical framework to understand heat and entropy flows in healthy humans who alternate work and rest periods.

The rate of entropy change in a system can be expressed as the sum of the rates of entropy produced within the system and the entropy exchanged with its surroundings. Mathematically put, the entropy balance equation can be written as

$$\frac{dS}{dt} = \frac{dS_i}{dt} + \frac{dS_e}{dt} \tag{3.1}$$

where dS/dt corresponds to the rate of entropy change of the system, dS_i/dt is the internal entropy production, and dS_e/dt is the entropy exchange (or entropy flow) with the environment through the system's boundaries. We note that this entropy balance equation for a system is compatible with the increase in entropy in the universe when irreversible processes take place. Irrespective of the absolute value and sign of dS/dt, the rate of entropy change of the universe will always be positive. It is well known from Prigogine's work that for near-equilibrium steady states, for which linear relationships between the thermodynamic forces and fluxes are assumed, entropy production is minimal [32]. Intuitively, if some set of constraints prevents a system from achieving an equilibrium state where entropy production is zero, then the closest state to equilibrium becomes the single steady state where entropy production is minimal. This principle generally applies to linear systems that exhibit only a few degrees of freedom [69].

The application of non-equilibrium thermodynamics to biophysical systems has a long-standing history [5]; however, it has been traditionally restricted to microscopic considerations down to the level of chemical reactions. On a larger scale, Zakharov and Sadovsky developed a theoretical model for the thermal regulation of animals based on the entropy production principle [97], but their analysis focuses on passive heat exchange with the environment (i.e., heat conduction and diffusion), which is not the main mechanism through which humans dissipate heat during exercise (i.e., skin cooling from the evaporation of sweat). On the experimental side, Aoki studied the entropy flows and entropy production of the human body under basal conditions at different ambient temperatures using the calorimetry measurements of Hardy and Du Bois [33, 117]. His calculations included contributions from the entropy flow of energy exchange (i.e., heat and radiation) and mass exchange associated with the respiration process, although the latter was found to be negligeable compared to the former. Others have studied the entropy generation of humans during their lifespan [101], while a general interest is growing to link thermodynamics and entropy considerations with health and disease [35, 71]. Overall, there exist a very limited number of studies that provide experimental investigations of the production and exchange of entropy in complex living systems and none, to our knowledge, that can

monitor entropy production in real-time.

Entropy, unlike energy, is not a conserved quantity; rather, entropy is preserved in that, once created, it cannot be destroyed [118]. It can, however, be dissipated externally from the system that created it to prevent entropy accumulation within. In this sense, entropy production refers to the irreversible transformation of energy within a system (e.g., metabolic activities), while entropy flow refers to the rate of transfer of entropy across a boundary (e.g., from the skin to the ambient room).

Stationary states resemble equilibrium states in that their thermodynamic properties, like temperature and entropy, do not vary over time. However, unlike in equilibrium, heat and entropy flows can occur in a stationary state, while maintaining a constant temperature, provided that the thermodynamic flows that enter the system or are created within it are exactly matched by their outflowing counterparts. In the case of living systems, stationarity is obtained when the net rate of entropy change in the body is zero; in that case, the internal entropy produced by metabolic irreversible processes is exactly balanced by the entropy dissipated to the environment. However, the human body does not have an infinitely fast reaction time, such that any increase in internal entropy production will be immediately matched by an equal increase in entropy flow to the environment. In other words, there will be a transient period, for example after the onset of exercise, when the body is not in a stationary state, which leads to an increase in body temperature and the accumulation of entropy. Although the body can be considered to be approximately at a steady state for the timescale of a day [33], participants are not expected to be in a steady state for the duration of an experiment where heat stress and exercise are involved [86].

In the present paper, we introduce a two-compartment entropy flow model for the continuous monitoring of entropy production in humans evaluated during physical exercise under heat stress. The thermodynamical definition of entropy will be applied to this experiment, as opposed to the informational definition of entropy derived from information theory. The system under study here, namely the human body, is considered a classical system, not a quantum one, since it cannot be properly described in terms of quantized

microstates. Although it remains debated whether the entropy of the human body can be measured, entropy rates and their imbalances are quantifiable and measurable.

3.2 Material and Methods

3.2.1 Human Subjects and Experimental Design

The results of this experiment are based on prior published data which studied the impact of heat and exercise stress on humans. The experimental design of the study has been previously and thoroughly described [88]. Briefly, heat transfers were measured during exercise and resting periods under heat stress for 11 healthy and habitually active middle-aged males (43 $\pm$ 2 years). In the study, participants entered the calorimetry chamber and initially rested for 30 min. Then, they performed four 15 min exercise bouts of cycling on an upright, seated cycle ergometer, at a constant rate of metabolic heat production equal to 400 W. Each bout was separated by a 15 min resting period with a final recovery period of 60 min. Physiologic properties, such as body temperature and heart rate, as well as thermodynamic properties, such as heat and entropy flows, were continuously monitored and reported as averages over 1 min intervals. The temperature inside the calorimetry chamber was set to 35 °C with a relative humidity of 20%. The calorimetry chamber thus essentially acts as a heat bath at a constant temperature and relative humidity by imposing fixed boundary conditions on the participants.

3.2.2 Internal Heat Production Measured with Indirect Calorimetry

The modified Snellen calorimeter, shown in figure 2.5, is a state-of-the-art whole-body air calorimeter that allows the study of human heat exchange in different ambient conditions [38]. It provides a very precise, continuous measure of the heat dissipated (dry $\pm$ evaporative heat exchange) by the human body during rest and exercise [37]. When combined with the rate of internal heat production, or metabolic heat production (indirect calorimetry), body heat storage can be quantified.

Internal heat production is derived from the metabolism. The chemical energy stored within the body and liberated through metabolic processes is transformed into external work (e.g., cycling) and metabolic heat (see figure 3.1b). Written in the form of the First Law of Thermodynamics, the metabolic energy expenditure, $\dot{M}$ (i.e., chemical energy liberated), is transformed into metabolic heat production $\dot{Q}_{int}$ and external work $\dot{W}$ performed by the participants on the cycle ergometer:

$$\dot{M} = \dot{Q}_{int} + \dot{W} \quad . \tag{3.2}$$

We assume that the internal work performed by the organs to generate internal flows (e.g., the heart pumping blood) is ultimately transformed into heat through friction and dissipation, which is accounted for in the measurement of metabolic heat production, because chemical energy is needed to provide this work. The metabolic energy expenditure, $\dot{M}$, can be measured using indirect calorimetry and the external work rate, $\dot{W}$, is known; the metabolic heat production, $\dot{Q}_{int}$, can then be readily obtained from equation (3.2)

$$\dot{Q}_{int} = \dot{M} - \dot{W} \quad . \tag{3.3}$$

The rate of metabolic energy expenditure, $\dot{M}$, was estimated spirometrically from the respiratory exchange ratio, R, between the rate of carbon dioxide production,$\dot{V}_{CO_2}$, and the rate of oxygen consumption, $\dot{V}_{O_2}$ [37], both measured at L·min^{-1}, using the following equation

$$\dot{M} = \frac{\left(\dot{V}_{O_2} \cdot \left[\frac{R-0.7}{0.3} e_c + \frac{1-R}{0.3} e_f\right]\right)}{60} \tag{3.4}$$

where e_c is the caloric equivalent per liter of oxygen for the oxidation of carbohydrates

(e_c=21,130 J), and e_f is the caloric equivalent per liter of oxygen for the oxidation of fat (e_f=19,630 J). The value for R is measured in real-time throughout the experiment to calculate (and regulate) heat production. An R value near 0.7 indicates that fat is the predominant fuel source, a value of 1.0 is indicative of carbohydrates being the predominant fuel source, and a value between 0.7 and 1.0 suggests a mix of both fat and carbohydrates. The expired air was directed into a mixing box where $\dot{V}_{O_2}$ was measured and then vented back into the calorimetry chamber, so that temperature and humidity differences between the chamber and respiration gases could be accounted for. The external work rate, $\dot{W}$, was continuously adjusted by changing the cycling resistance during the exercise periods to ensure the targeted metabolic heat production, $\dot{Q}_{int}$, of 400 W remained constant over time. The typical values for the work rates were in the range of 70 W (not part of the 400 W target for $\dot{Q}_{int}$), which represents moderate-to-high intensity exercise. Historically, indirect calorimetry has been regarded as the gold standard and still is the reference standard and clinically recommended mean for the accurate measurement of energy expenditure [91,92]; alternative methods can approximate $\dot{M}$ and $\dot{Q}_{int}$ from the heart rate, subjective sensations, or empirical tables [37].

3.2.3 External Heat Dissipation Measured with Direct Calorimetry

The rate of external heat transfer from the body to the surroundings, denoted by $\dot{Q}_{int}$, corresponds to the sum of dry heat loss, $\dot{Q}_{dry}$, evaporative heat loss, $\dot{Q}_{evap}$, and heat loss through respiration, $\dot{Q}_{resp}$, such that

$$\dot{Q}_{out} = \dot{Q}_{dry} + \dot{Q}_{evap} + \dot{Q}_{resp} \quad . \tag{3.5}$$

Dry heat loss ($\dot{Q}_{dry}$) results from heat exchange with the environment via conduction,

convection, and radiation at the skin surface, and is given by

$$\dot{Q}_{dry} = c_{air} \times \dot{m}_{air} \times \Delta T_{air} \tag{3.6}$$

where c_{air} =1.005 J·(kg· °C)$^{-1}$ is the specific heat of air, $\dot{m}_{air}$ is the mass flow of air (kg air/s) out of the calorimetry chamber, and ΔT_{air} is the difference in temperature between the outflow and inflow of air from the calorimetry chamber. The evaporative heat loss, $\dot{Q}_{evap}$, consists of the heat dissipated from the skin resulting from the evaporation of sweat, and is calculated from the change in absolute humidity inside the calorimeter

$$\dot{Q}_{evap} = L_{vap} \times \dot{m}_{air} \times \Delta \rho_v \tag{3.7}$$

where L_{vap}=2.426 J per gram of sweat and is the latent heat of the vaporization of sweat, and $\Delta \rho_v$ is the difference in absolute humidity (g of water/kg air) between the outflow and inflow of air from the calorimetry chamber. The modified Snellen whole-body air calorimeter has an accuracy of ±2.3 W for the measurement of total body heat loss, $\dot{Q}_{out}$, representing a measurement error that is smaller than 1% [38]. Lastly, the heat loss through respiration, $\dot{Q}_{resp}$, results from the dry and evaporative heat transfer between respired gases and the body. In the current experimental setup, the respired gases were vented back into the calorimetry chamber and thus were mixed with the air outflow, from which were measured $\dot{Q}_{dry}$ and $\dot{Q}_{evap}$ [88]. Although it only had a negligeable contribution to the total heat loss because the ambient temperature was very close to body temperature at 35 °C, $\dot{Q}_{resp}$ was indirectly accounted for through the measurement of $\dot{Q}_{dry}$ and $\dot{Q}_{evap}$.

3.2.4 Rate of Heat Storage in the Body

The heat produced internally (i.e., metabolic heat production, $\dot{Q}_{int}$) is partly dissipated to the environment as $\dot{Q}_{out}$, and partly stored within the body; the balance between the rate of metabolic heat production and the rate of heat dissipation corresponds to the rate of

heat storage:

$$\dot{Q}_{st} = \dot{Q}_{int} - \dot{Q}_{out} \quad . \tag{3.8}$$

Heat stored within the body leads to increase in body temperature, and thus the rate of heat storage can serve to calculate variations in body temperature, as described in the following section. Additionally, note that energy can also be stored within the body through the formation of energy-rich compounds. However, as the experiment of Larose et al. shows, energy storage can be neglected as the participants had a light meal in the morning and no subsequent food intake throughout the duration of the experiment [88].

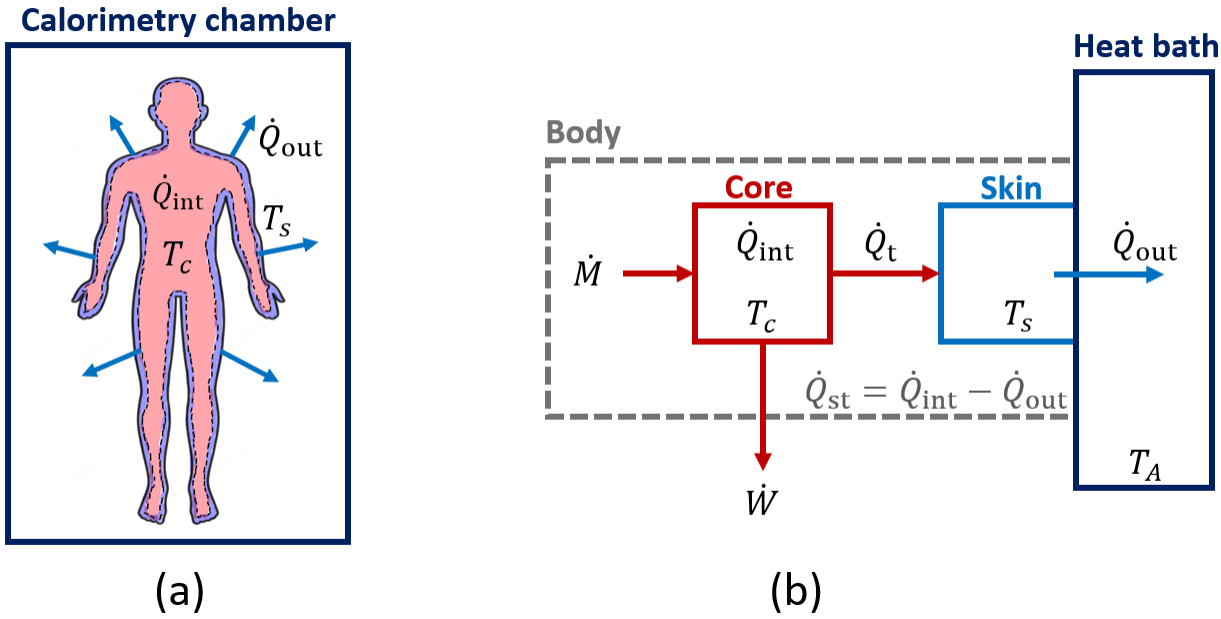

Figure 3.1: Two-compartment model of entropy flow in humans composed of the core and skin compartments. Entropy is produced throughout the body through irreversible metabolic processes and dissipated to the external environment through the skin. Panel **(a)** shows the physiological viewpoint of heat production and dissipation, while panel **(b)** shows the corresponding thermodynamic diagram. The temperature, T_A of the heat bath refers to the ambient temperature inside the calorimetry chamber. The design of the experiment allows for the computation of entropy flows from the heat flows.

3.2.5 Temperature Measurements Using Thermometry and Calorimetry

Thermometry was used to measure the core and skin temperatures. The core temperature was measured by inserting a rectal temperature probe a minimum of 12 cm past the anal sphincter. The skin temperature was calculated using a weighted average of four skin temperature probes located on the upper back (30%), chest (30%), quadriceps (20%), and back calf (20%). Then, the whole-body temperature was estimated via a weighted average of the core temperature (90%, measured with the rectal probe) and skin temperature (10%,

measured by the weighted average of the four different skin probes).

While thermometry provides accurate temperature measurements under resting conditions, it tends to underestimate temperature variations during exercise [93]. Hence, the baseline values for the core temperature were determined using thermometry during the initial resting period. During the subsequent exercise and recovery periods, the relative changes in body temperature, ΔT_b , during a time interval, Δt, were determined using calorimetry through the balance of heat flows, and are given by

$$\Delta T_b = \frac{\dot{Q}_{st} \cdot \Delta t}{m \cdot c_p} \tag{3.9}$$

where $\dot{Q}_{st}$ corresponds to the rate of heat storage in the body, defined using the heat balance given by equation (3.8). The numerator of equation (3.9) corresponds to the change in body heat content during the time interval, Δt, m is the total body mass of the participant (in kg), and c_p is the specific heat capacity of living tissues (in $\mathrm{J{\cdot}kg^{-1}{\cdot}K^{-1}}$).

3.2.6 Two-Compartment Non-Stationary Model of Entropy Production

In a multicompartment model, the rate of entropy change of an open system is given by the sum of the rates of entropy change within each subsystem, k (based on equation (3.1), see figure 3.1 for the thermodynamic diagram of the flows). Using a two-compartment core–skin model, the rate of entropy change of the body is given by

$$\left(\frac{dS}{dt}\right)_{body} = \sum_{k=1}^{n} \left(\frac{dS}{dt}\right)_{k} = \left(\frac{dS}{dt}\right)_{core} + \left(\frac{dS}{dt}\right)_{skin} \tag{3.10}$$

where the local rate of entropy change within subsystem k, written in the for of equation

(2.13), is given by

$$\left(\frac{dS}{dt}\right)_k = -\frac{1}{T_k}\vec{\nabla}\cdot\vec{J}_k + \sigma_k \quad . \tag{3.11}$$

The first term on the right-hand side of equation (3.11) corresponds to the divergence of the total heat flow, $\vec{J}_k$, through the boundary of subsystem k, and the second term, σ_k, corresponds to the entropy production due to irreversible processes occurring within subsystem k, which must be greater or equal to zero according to the Second Law of Thermodynamics ($\sigma_k \geq 0$). We determined that the temperature variations between two consecutive data recordings a minute apart were very small; therefore, we could neglect any term containing time derivatives of temperature. We restricted the entropy-rate contributions to real-time heat production and dissipation because the human body is physiologically inefficient at converting chemical energy into mechanical work (e.g., lifting a box, cycling, etc.). Depending on the task performed, between 80% and 100% of the energy is converted into heat along the metabolic pathways [37]. Further, Aoki showed that the entropy flow associated with the mass–flow of respiratory gases can be neglected [33].

The internal entropy production within the core is driven mainly by heat production from metabolic activities, i.e., $\sigma_c = \dot{Q}_{int}/T_c$. It is important to note that indirect calorimetry, used to estimate the metabolic heat production through gas exchange, cannot determine the oxygen consumption in each compartment because it is a whole-body measurement. Therefore, the measurement of metabolic heat production also includes the heat generated by the skin. Since entropy production from heat generation within the skin is thus already accounted for, we can assume that $\sigma_s = 0$. Equation (3.10) then becomes:

$$\left(\frac{dS}{dt}\right) = \frac{\dot{Q}_{int}}{T_c} + \dot{Q}_t\left(\frac{1}{T_s} - \frac{1}{T_c}\right) - \frac{\dot{Q}_{out}}{T_s} \tag{3.12}$$

where $\dot{Q}_t$ is the heat flow transferred from the core to the skin, T_c and T_s are, respectively, the core and skin temperatures, $\dot{Q}_{int}$ is the rate of metabolic heat production in the body, $\dot{Q}_{out}$ is the rate of heat dissipation from the skin to the environment. Note the similarities between equations (3.12) and (2.28), where the latter was derived for a non-equilibrium stationary state involving a thermal gradient. These two equations become equivalent if the heat flow Q_i are constant through the body (as are the J_q in equation (2.28)). Equation (3.12) can be derived similarly from the multi-box model used by Ozawa et al. in the context of entropy production in the planetary atmosphere [119].

The second term of equation (3.12) corresponds to the entropy change associated with the transfer of heat from two compartments at different temperatures (i.e., core and skin). If the core and skin temperatures were equal, this term would vanish as expected. Most importantly, equation (3.12) is valid for both stationary and non-stationary states. In stationary states, body heat content and temperatures are time-independent, implying that all heat flows are equal, which consequently leads to $dS/dt = 0$.

The heat flow transferred from the core to the skin, $\dot{Q}_t$, cannot be evaluated with the present experimental setup. If we define $\Delta T = T_c - T_s$ as the difference between core and skin temperatures, we find that

$$\left(\frac{1}{T_s} - \frac{1}{T_c}\right) \approx \frac{\Delta T}{T_s^2} \tag{3.13}$$

provided that ΔT is small. Indeed, the relative difference between the core and skin temperature is close to 1% when expressed in Kelvin units. This justifies the following approximation

$$\left(\frac{dS}{dt}\right)_{body} = \frac{dS_i}{dt} + \frac{dS_e}{dt} \approx \frac{\dot{Q}_{int}}{T_c} - \frac{\dot{Q}_{out}}{T_s} \quad . \tag{3.14}$$

It can be seen from equation (3.14) that the rate of entropy production is given by $dS_i/dt = \dot{Q}_{int}/T_c$, and the rate of entropy flow is given by $dS_e/dt = -\dot{Q}_{out}/T_s$. It is important to note that even though we use the standard notation for time derivatives, expressed in J/K per second, the heat and temperature measurements are reported as averages over 1 min intervals. Hence, entropy rates in units of ($\mathrm{J{\cdot}K^{-1}{\cdot}s^{-1}}$) are obtained by converting heat measurements from 1 min intervals (i.e., per minute) into per second intervals. The current experimental setup does not have a time resolution down to the second, but it has an incredible accuracy for heat measurements on the order of one minute [38].

Finally, the cumulative entropy change in the body, $\Delta S(t)$, which can be interpreted as a measure of thermodynamic irreversibility or stress, is calculated as

$$\Delta S(t) = \int_{t_0}^{t} \left(\frac{dS}{dt'} \right) dt' \approx \sum_{i=0}^{t} \langle \frac{dS}{dt} \rangle_i \cdot \Delta t \tag{3.15}$$

where the rates of entropy change are averaged over 1 min intervals.

3.2.7 Data and Statistical Analysis

The data analysis was performed using an in-house program written in MATLAB R2023a (The MathWorks, Natick, MA, USA). When any normalization was applied to the time-series curves, the values were normalized for each individual prior to calculating the group averages. Unless stated otherwise, all the entropy rates and changes presented below were normalized using unit body mass using the participants' weight.

3.3 Results

3.3.1 Resting Entropy Production during Heat Stress

The resting rates of entropy production during heat stress, shown in table 3.1, were calculated by averaging the entropy production rates during the initial resting period inside the calorimetry chamber and normalized using body-surface area (BSA) or mass. The BSA was estimated from the measures of standing height and body mass following the standard method of Du Bois and Du Bois [120]. The BSA-normalized value for the resting entropy production rate is in good agreement with that of Aoki [33], while our mass-normalized value is approximately 25% higher. This discrepancy can be easily understood by considering the differences in the experimental design. In Aoki's study, the data were recorded for a single individual who was 54 years old, 179 cm in height, 74.7 kg in weight, and had an estimated BSA of 1.54 m^2 . Aoki also showed that the production of entropy under basal conditions is nearly constant for calorimeter temperatures in the range of 26–32 °C, with an average basal rate of specific entropy production (i.e., per unit body area) of 0.172 ± 0.003 W/(K·m^2). In contrast, our study involved 11 participants with an average age of 43 ± 2 years, weight of 84 ± 6 kg, and an estimated BSA of 2.0 ± 0.1 m^2. Moreover, the ambient calorimeter temperature in our study was set to 35 °C, which is outside the range investigated by Aoki. We could not identify other independent measurements of human entropy production to which we could compare our results.

3.3.2 Entropy Rate Curves

The rates for internal entropy production, external entropy flow and their difference, and whole-body entropy change are shown in figure 3.2. Each entropy rate curve was normalized using the individuals' weights prior to calculating the group averages. Figure 3.2a shows the group-averaged internal entropy production rate, dS_i/dt (in blue), and the absolute values of entropy flow, dS_e/dt (in red), with their respective shaded regions representing plus/minus one standard deviation. The entropy production rates for the first 30 min represent the resting entropy production rates. The initial rest period was followed by

Study	**Resting dS_i/dt BSA-normalized** $[W/K/m^2]$	**Resting dS_i/dt Mass-normalized** $[W/K/kg]$
This study	0.18 ± 0.01	4.3 ± 0.4
Aoki [33]†	0.172 ± 0.003	3.47

Table 3.1: Resting entropy production rate (mean ± SD) normalized by the participants' body surface area (BSA) on the left and mass on the right. Resting dS_i/dt are obtained by averaging the entropy production rates during the first 30 minutes when participants are resting inside the calorimetry chamber. Then, our values shown above were obtained by averaging the entropy production rate of 11 middle-aged men at a single ambient temperature of 35 °C. The uncertainty attached reflects the standard deviation over this average. † Aoki's study measured the basal entropy production of a single middle-aged male. Aoki's values reported above correspond to the average of multiple measurements conducted at different ambient temperatures.

four periods of exercise, during which the production of metabolic heat was fixed and maintained at a constant level by the experimental design. The entropy flows initially rose at the start of exercise, although at a slower rate than the entropy production rates; they also declined faster than their initial rise at the start of the resting periods. The entropy flows did not recover their initial resting values over the course of the experiment, as seen in the higher plateaus during the inter-exercise resting periods. An additional cooldown time at the end of the experiment would have expectedly restored the entropy flows to their resting values. Moreover, the maximal entropy flows for the first exercise bout consistently reached a smaller value than those for the remaining three exercise bouts.

The rate of internal entropy change in the body is shown in figure 3.2b; that is, the difference between the rate of entropy production and entropy flow plotted in figure 3.2a. It should be noted that dS/dt is not restricted to positive values like the entropy production rate is; it can take positive or negative values, depending on the magnitude of both contributions and the sign of the entropy flows. In the first few minutes of exercise, the entropy production rate increases abruptly while the entropy flow increases almost linearly at a much lower rate. The difference between both terms thus takes a positive

value. In contrast, at the onset of a resting period following an exercise bout, the entropy production rate decreases abruptly while the entropy flow is still elevated, which leads to a negative rate of entropy change. Entropy production and entropy flow are independent variables that originate from different mechanisms. While entropy production is most often activated consciously in living systems in response to an external stimulus (e.g., the cue to start exercising), entropy flow is an involuntary physiological response to the variation in internal entropy production or a notable change in ambient conditions.

Finally, figure 3.2c shows the accumulation of entropy within the body, which corresponds to the time integration of the rate of entropy change from figure 3.2b. The initial rise in entropy accumulation is due to the lack of entropy balance when the participants entered the calorimetry chamber. Indeed, it typically takes multiple hours for participants to achieve heat balance when resting under such conditions [37, 121]. Each exercise bout is associated with a significant increase in accumulated entropy, followed by a smaller decrease during the resting periods. We noticed that the entropy accumulated over the experiment did not completely dissipate despite the recovery period of 60 min at the end. Instead, a new stationary state was found to exist, where entropy production and entropy flow were approximately balanced. The net rate of entropy change vanished, and thus the entropy was no longer accumulating, but instead steady around an asymptotic value that reflects the net change in body entropy following the recovery period.

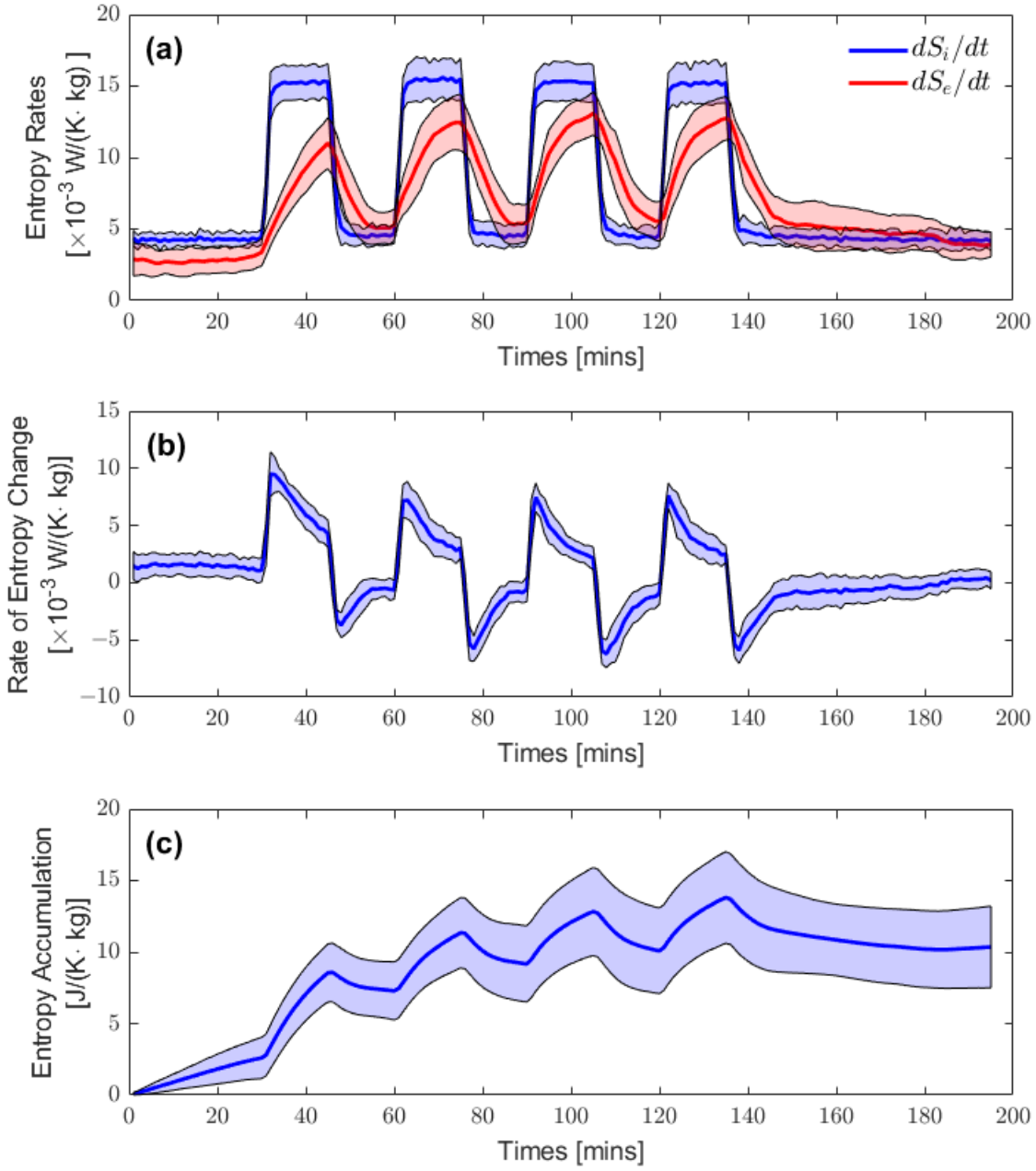

Figure 3.2: Panel **(a)** shows the average entropy production rate (dS_i/dt) in blue and the absolute values of entropy flow ($|dS_e/dt|$) in red, as a function of time, calculated using the following equations, $dS_i/dt = \dot{Q}_{int}/T_c$ and $dS_e/dt = \dot{Q}_{out}/T_s$, from equation (3.14). Solid lines indicate the average values and the shaded areas indicate the standard deviation among the participants. Panel **(b)** shows the rate of entropy change (dS/dt) that corresponds to the sum of the entropy production and dissipate rates. Panel **(c)** shows the entropy accumulation that corresponds to the cumulative entropy change over time calculated from equation (3.15). All the curves presented here are normalized using the participants' weights prior to computing the shown group averages.

3.3.3 Quasi-Static Entropy Change Model

The variation in body temperature over a short period of time (e.g., 1 min) is relatively small; in fact, it is sufficiently small that the slow rate of change in body temperature could be considered as the result of an internal quasi-static process. Fundamental in classical thermodynamics, a quasi-static process is an idealized process in which a system undergoes incremental and slow changes such that it is, at every instant, at equilibrium [43]. Time series can thus be viewed as a succession of equilibrium states that are infinitely close to one another. In our experiment, heat storage within the body increased incrementally in a similar manner during the exercise periods. Using the well-known formalism of classical thermodynamics, the infinitesimal entropy change associated with the transfer of heat, dQ, is given by $dS = dQ/T$. The heat transfer, dQ, can be expressed as a temperature variation, dT, through $dQ = mc \cdot dT$, with m being the mass of the participant, and c being the average specific heat of the body. Therefore, the entropy change within the body over a single interval is given by

$$\Delta S_i = \int_{T_i}^{T_{i+1}} \frac{dQ}{T} = mc \times \ln\left(\frac{T_{i+1}}{T_i}\right) \tag{3.16}$$

where T_i and T_{i+1} are, respectively, the initial and final temperatures over a 1 min interval. These temperatures can be estimated using either thermometry (i.e., the use of temperature probes) or calorimetry (i.e., the balance of heat flows) [37]. Since quasi-static processes are akin to a succession of equilibrium states, no variations in time (or rates) are formally defined. In other words, all that can be analyzed is the entropy change during a single interval, and not the instantaneous rates that typically appear as time derivatives.

Figure 3.3 shows the entropy change in the body calculated from equation (3.16) using two distinct methods for core temperature measurement, namely, thermometry (in red) and calorimetry (in blue). Thermometry was found to provide a noisy time series for entropy change in the body. The higher variance for each data point compared to the calorimetry

time series originates from the inability of the rectal probes to adequately assess changes in core temperature. We have also found that thermometry appears to underestimate the entropy change at critical points, like the onset and offset of exercise periods, as observed in figure 3.3, while the calorimetry time series exhibits a larger amplitude between the extrema. This observation also suggests that thermometry has a delayed reaction compared to the calorimetric approach. This delayed reaction to increases in entropy changes in the body can be attributed to a slower response to in temperature changes, which in turn is due to the low heat conductivity of the air surrounding the rectal probe [37, 122]. Overall, the results suggest that thermometry is less-sensitive and -responsive compared to calorimetry for the continuous measurement of body entropy changes over short intervals.

It should be noted that there is a negligible difference in the resulting rate of entropy change if the core temperature is measured via thermometry or calorimetry when using equation (3.14). Nevertheless, the heat flows, $\dot{Q}_{int}$ and $\dot{Q}_{out}$, in the numerators of equation (3.14) must be measured using calorimetry (indirect and direct calorimetry, respectively). Therefore, calorimetry remains essential for the calculation of entropy rates. However, the results shown in figure 3.3 indicate a noticeable difference between both methods when using the quasi-static model when entropy change is not calculated from heat flows, but rather from temperature variations. In this case, calorimetry provides a much more reliable measurement than thermometry.

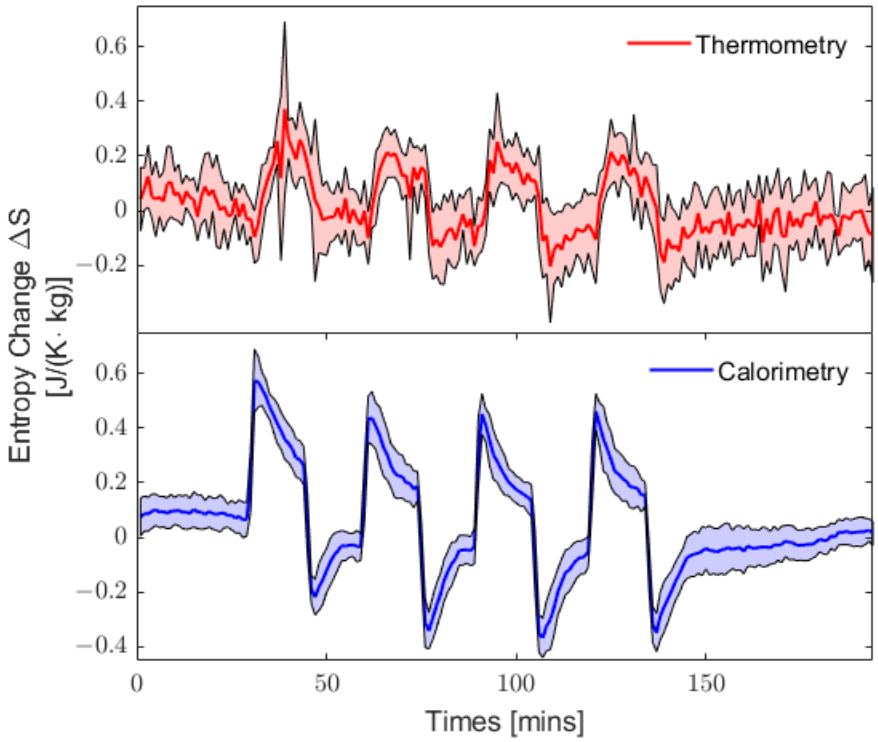

Figure 3.3: Comparison of the entropy change within the body calculated using Equation (3.14) with core temperatures estimated from thermometry (in red) and indirect calorimetry (in blue).

There is a striking similarity between the quasi-static approach that uses calorimetry to estimate temperatures and the two-compartment model that uses the balance of entropy flows (see the entropy change curve in figure 3.2b). In fact, considering that the temperature variation, $\Delta T_i = T_{i+1} - T_i$, during a single interval is relatively small, one can expand the logarithm in equation (3.16) into a first-order Taylor expansion, such that the

entropy change in the body can be expressed as

$$\Delta S_i = mc\left(\frac{\Delta T_i}{T_i} + \dots\right) \approx \frac{mc\,\Delta T_i}{T_i} = \frac{\dot{Q}_{st}}{T_i} = \frac{\dot{Q}_{int}}{T_i} - \frac{\dot{Q}_{out}}{T_i} \quad . \tag{3.17}$$

The resemblance between equations (3.14) and (3.17) is not surprising given that similar assumptions are made in their respective derivation. For example, small temperature variations, ΔT_i, are implied in the entropy flow model by neglecting terms of higher order when taking the time derivative of temperature. Although these models lead to similar results, there are nevertheless key conceptual differences that allow for alternative interpretations. The main difference between both models relates to their thermodynamic interpretation. The quasi-static approach implies that the body is always near the equilibrium state (infinitely close), which is invalid in the case of living systems where equilibrium conditions are only obtained after death. On the other hand, the two-compartment model recognizes the existence of non-equilibrium states during exercise and a slow return to a stationary state (far from equilibrium) during rest. Additionally, the quasi-static approach assumes the whole body to be in equilibrium and therefore considers the body as a single compartment at a homogeneous temperature; that is, there is no distinction between core and skin temperatures in equation (3.17), in contrast to equation (3.14).

3.4 Discussion

The present study demonstrates the feasibility of real-time entropy production monitoring in humans exercising under heat stress using a calorimetric approach. Our entropy flow model leads to a resting entropy production rate that is slightly higher (possibly due to the presence of heat stress), yet in good agreement with that of Aoki [33]. However, this value requires repeated and independent measurement without heat stress to be considered a reference standard for resting entropy production. No published results other than those of Aoki are available, which is remarkable given the central nature of entropy production to human life, as publicly recognized by Schrodinger in 1944 [57]. Furthermore, we have in-

vestigated the use of classical thermodynamics and the associated entropy change resulting from quasi-static processes. The latter approach highlights the superiority of calorimetry over thermometry to estimate body temperature time series.

3.4.1 On the Relevance of the Entropy Analysis

The entropy flow analysis presented here does not considerably differ from a heat flow approach since body temperature is highly constrained, which is a direct consequence of the narrow range of temperature stability in warm-blooded animals. However, our experimental paradigm offers the possibility of quantifying entropy flows in human bodies and their alteration in association with health, illness and aging, and of further evaluating the possible interpretations of these results and their limitations. In doing so, our entropy analysis allows a deeper explanation of regulatory behavior in novel contexts. For example, a similar entropy flow analysis could be applied to physical systems that do not operate mainly under thermal exchanges, as is the case for the human body, thus offering a unified principle to explain the regulatory behavior of larger classes of physical systems. For physical systems that do not operate under thermal exchanges, entropy flow analysis can still be applied and provide insights into their inner mechanisms; the analysis of these systems is not limited to the use of the first law of thermodynamics, but can be extended to the second law.

3.4.2 On the Necessity of Considering Non-Equilibrium States

In thermodynamics, the equilibrium state of a system is characterized by its temperature. However, if a participant is resting at a stable temperature and then starts exercising at a high intensity, their body temperature will increase. Once exercise is stopped, and after a sufficiently long cooldown period, the body temperature will eventually decrease to its original value. Since the initial and final temperatures are the same, we could say the body is in the same state, but the participant has depleted most of their energy resources and is exhausted. They would not be able to sustain the same high-intensity exercise; therefore, the initial and final states are different. The most remarkable insight from the theory of

thermodynamics is its ability to describe a system in terms of a reduced set of variables, like pressure and temperature. On the other hand, in the study of complex living systems, the human body cannot be similarly reduced to a set of simple thermodynamic variables and, thus, its state cannot be properly defined at all-times. Using quantized energy levels to describe the state of systems, namely through the formalism of statistical mechanics, is even less within reach. The definition of a state function implies path independence between two distinct states with different temperatures. For humans, body temperature does not characterize the state of the system because (1) irreversible processes in the body lead to path-dependent transitions and (2) the chemical composition of the body varies during exercise periods.

3.4.3 Non-Equilibrium Steady State: Temperature Gradient of Subcompartments

An alternative approach to estimating the entropy production rate in humans could be to assume that the body is always in a steady state, although a non-equilibrium one. The entropy flow rate could then be calculated from the direct calorimetry measurement of the heat dissipated into the environment divided by the skin temperature and, thus, eliminates the necessity to estimate the metabolic entropy production rate using indirect calorimetry. Given the steady-state approximation, the skin compartment receives and dissipates the same amount of heat from the core; otherwise, skin temperature would not be constant, and the steady-state assumption would not hold. This situation corresponds to a constant heat flow, $\dot{Q}_i$ in equation (3.12), being transferred across all compartments. Then, the entropy production rates of the core, $(dS_i/dt)_{core}$, and that associated with the transfer of heat between the core and the skin region, $(dS_i/dt)_t$, are given, respectively, by the first and second terms of equation (3.12). Interestingly, the interplay of the entropy production rates of the core and the skin systems leads to the following equation

$$\frac{(dS_i/dt)_t}{(dS_i/dt)_{core}} = \frac{T_c - T_s}{T_s} \quad , \tag{3.18}$$

which is mathematically equivalent to evaluating the relative temperature difference between the core and the skin. This relative difference, or more commonly the temperature gradient, between the skin and the core has been studied previously by Cuddy et al. [123]. They have shown that the temperature gradient between the core and the skin during exercise is more indicative of volitional fatigue (i.e., an inability to maintain exercise intensity) compared to the singular measure of core temperature. Although a greater temperature gradient could be seen as a sign of better regulation from a thermodynamics perspective, having a lower skin temperature may not necessarily be beneficial from a physiological perspective. For example, having a lower skin temperature could also mean (1) that you are unable to effectively increase blood flow to the skin, which leads to entropy accumulation within the core, or (2) that you are less efficient at cooling the skin since the rate of sweat evaporation increases with skin temperature [37].

3.4.4 Limitations

Indirect calorimetry estimates internal heat production rates through the expired gases by assuming that they are the product of the oxidation of carbohydrates and, thus, considers that only aerobic metabolism is involved. Anaerobic metabolism, based on glycolysis, is used mainly when the cardiorespiratory system is unable to provide enough oxygen, that is, for short bursts of activity (e.g., sprinting) at a very high intensity or during prolonged exercise when oxygen requirements are not met [83]. The anaerobic contribution to metabolic heat production was minimized here by keeping the exercise sessions no longer than 30 min (enough to see a difference in entropy rates), and the recovery periods long enough ($\geq$15 min) for the body to replenish its aerobic substrates before the start of the following exercise bout.

One might expect body temperature to be easily measured; however, it is difficult to adequately assess the temperature distribution across the body [93], especially during exercise, when heat is generated non-uniformly. There is in fact a notable increase in activated muscles where the temperature can reach up to 40 °C [37, 124, 125]. Each organ's temperature depends on the level of blood perfusion and proximity to heat-generating muscles.

Thus, reducing both of the two compartments (core and skin) to single temperature averages represents an obvious limitation. We relied on the work of physiologists and thermal engineers for the best estimation of body temperatures. In particular, modeling the flow between a core compartment and a skin compartment may need adjustments depending on where in the body those compartments are located, e.g., the trunk vs. the head, which entail different sets of tissue composition and thickness. Relatedly, improvements in measuring techniques, both for heat flows and temperature, could allow for the elaboration of a refined multicompartment model where the core (and possibly the skin) region would be further divided into subsystems (e.g., thorax, head, limbs, etc.). While being relatively easy to implement from a mathematical perspective, such an extension to our model would certainly present exceptional experimental challenges associated with measuring these extra variables within a calorimetry chamber in participants performing exercises. We note that similar challenges of modeling scale and tissue heterogeneity, from the mesomacroscopic level all the way down to the nano–meso level of molecular interfaces, arise in other contexts. For example, in biorheology one must choose the biophysical compartments and the linear versus extended Onsager formalism with which to model non-equilibrium thermodynamics [126]. Overall, although the calorimetry method does not provide any information about the temperature distribution, it remains the most accurate method with which to estimate the total amount of heat stored internally from the balance of heat flows. We have showed that thermometry, the alternative approach, leads to inaccurate entropy time series, likely because it provides a highly localized measurement due to the use of a limited number of local probes (typically rectal and/or esophageal) that do not reflect the whole-body temperature or any extrapolation thereof [94]. In the case of a rectal probe, it tends to react quite slowly to changes in core temperature, due to the low heat conductivity of the air that surrounds it in the rectal cavity [95, 96].

In our approach, the internal entropy production rates and external entropy flows were measured using different physical quantities based on indirect and direct calorimetry, respectively. We specifically chose direct calorimetry as the best method to measure the external heat production of the body, and indirect calorimetry to measure the internal

heat production, as they are best possible and available means to do so continuously over time. However, important limitations exist. While the statistical error, presented as the standard deviation in figures 3.2 and 3.3, reflects the biological variability of only 11 subjects, systematic errors may also be present. Systematic errors may be related to the apparatus and measurement techniques that could impact the magnitude and timeline of the computed entropy changes, which were calculated by simultaneously subtracting the rates of entropy production and the entropy flows continuously over time, as is shown in figure 3.2. However, years of research with different experimental configurations has led to an understanding and elimination of many of the systematic errors relating to the apparatus shown in figure 2.5. For example, this modified Snellen human calorimeter was specifically designed to measure rapid transients in heat loss from an exercising participant with its fast response time (particularly for evaporative heat loss), low thermal inertia, and an unparalleled accuracy of 2.3 W for the measurement of total heat loss [38,86]. Hence, we believe the systematic errors are small and similar across the duration of the experiment and, thus, do not impact our measurements to the extent that they would negate our conclusions about entropy accumulation as a measure of stress. Further experiments could improve the accuracy and reliability of indirect and direct calorimetry as measures of internal and external entropy production, particularly in non-stationary conditions.

3.4.5 Entropy Production in Living Systems

Living systems actively work to maintain the necessary non-equilibrium conditions for metabolic processes to keep running (e.g., chemical gradients for ATP and polymers, and ion gradient across cell membranes). These non-equilibrium conditions can be seen as constraints applied by the system on itself to preserve its structural and dynamical integrity [127]. Although the existence of these self-constraints maintains lower entropy states through a greater microscopic organization, it allows the system to be more efficient at performing work on a macroscopic scale, where thermodynamic entropy flows are possibly maximized. It should be noted that the maximization of entropy production does not imply a maximal generation of energy waste, so long as the energy consumed through metabolic processes enables the living system to achieve greater work output or

self-organization. Survival then depends on the ability to make use of an energy source efficiently [128, 129]. A system's capacity for internal order and sustained functions is constrained by its rate of entropy production and entropy flow. Similarly, health and fitness could be described as retaining the ability to maximally increase entropy production when needed. The accumulation of entropy over long periods of time (e.g., years or decades) could be the reason why biological systems lose in efficiency and eventually fail.

Entropy production is a necessary condition for self-organization (maintenance and healing), while entropy flow is required to prevent entropy accumulation within the body. In this regard, an impairment of entropy production or flow is indicative of a lack of adaptability and, possibly, bad clinical outcomes. On the other hand, it also implies that optimizing the resting and maximal entropy production rates could improve the health status of a patient and their clinical outcome. Therefore, if health is associated with entropy production, numerous additional therapeutic approaches that are not currently considered could be investigated. For example, interventions intended to augment basal or maximal entropy production, the monitoring of entropy production, therapeutic temperature modulation to stimulate entropy production, and the use of entropy production to identify perioperative risks for major surgery all represent separate novel therapeutic options. The accumulation of entropy within the body due to the impairment of entropy flow leads to the concept of entropy as a general measure of stress (e.g., stress entropic load [35]). Strategies to reduce entropy accumulation over prolonged periods of time could become a useful prevention tool to help long-term health and fitness. However, prior to the elaboration of any entropic-based clinical treatment, we first need to better understand how entropy production and entropy flow are affected by different medical conditions (e.g., diabetes) and, more generally, by the inevitable aging process.

3.5 Conclusions

In the present study, we introduced a two-compartment entropy flow model that allows for the real-time monitoring of entropy production in humans exercising under heat stress. Our

calorimetric approach provides the much-needed experimental data to further investigate human entropy production in non-equilibrium conditions. This opens new perspectives on the study of fundamental concepts such as health and illness, based on thermodynamic principles and entropy production impairment.

Chapter 4

Clinical applications of entropy measurements

Abstract

Biological organisms are open thermodynamic systems in which internal structure and function arise from a network of heat and entropy-producing processes, requiring external export of heat and entropy to the environment. System stability, including health and healing, is hypothesized to relate to the mass-normalized rate of entropy production and export, and the capacity to augment both when required. Using a novel methodological framework that allows the continuous measurement of heat fluxes and body temperature, we can estimate entropy production and export in humans during exercise under heat stress. We report the impairment of entropy export leading to entropy accumulation in association with increasing age, decreased fitness, and the presence of diabetes. In all conditions, impairment was also found to be negatively correlated with the $\dot{V}O_2{}^{\max}$ fitness measure. Our analyses make use of direct calorimetry to quantify rates of heat loss, and indirect calorimetry to measure metabolic heat production and core temperature in real-

time. Our results highlight the potential relevance of the entropy balance to the definition of health and open the possibility of designing novel therapeutic approaches based on nonequilibrium thermodynamics to improve patient care.

Graphical Abstract

Biological organisms maintain internal structure and function through heat and entropy-producing processes, which also require external export to the environment. Using calorimetry, we report the impairment of entropy export in humans exercising under heat stress, leading to entropy accumulation, in association with increasing age, decreased fitness, and the presence of diabetes. This study, based on a nonequilibrium thermodynamics framework, and emphasizes the relevance of entropy balance in health and has potential for clinical translation.

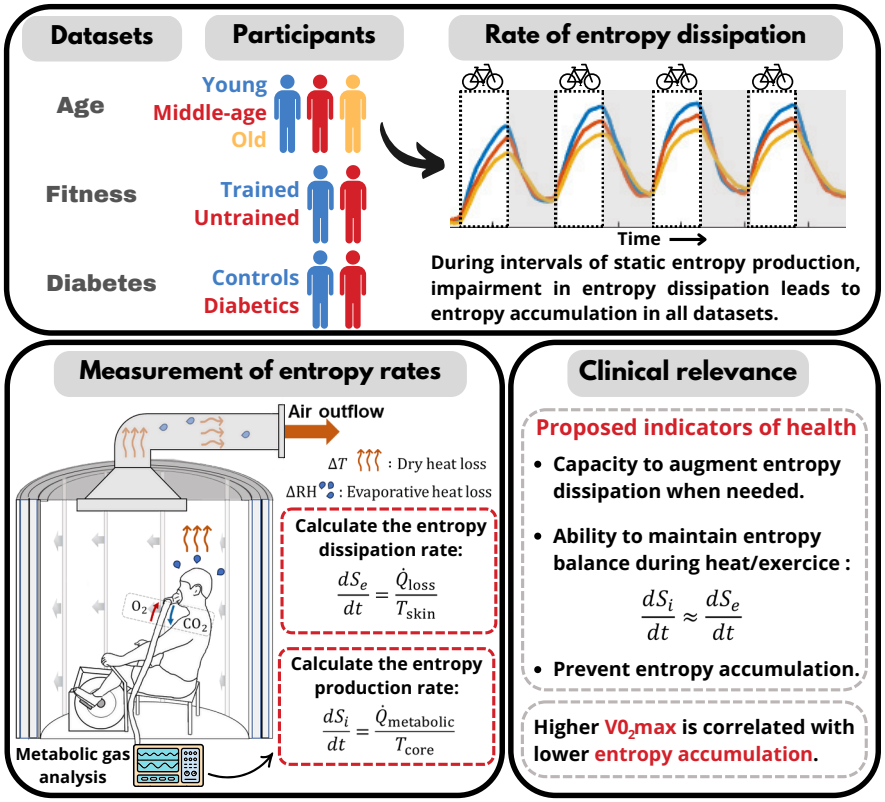

4.1 Introduction

Historically, medicine views the human body as a machine consisting of interacting organs, with a primary emphasis on the management of macroscopic variables such as body temperature, blood pressure, and glucose levels. However, although machines can be arbitrarily *complicated*, they do not exhibit the *complexity* observed in living systems. Biological organisms, and more specifically heterotrophs and homeothermic organisms, have long been recognized for their similarity to dissipative structures [32], that is, systems for which structures and functions arise from the complex interplay of internal processes (not external design), a property known as self-organization [9]. Self-organization, among other properties of dissipative structures, is responsible for the distinctive behavior of living systems, including their capacity for self-healing, maintaining or returning to stable homeostatic states in the face of perturbations [16, 130]. The formalism of dissipative structures involves a branch of thermodynamics describing systems that are far from equilibrium and are created and maintained through energy dissipation and entropy-generating processes [8]. Therefore, unlike machines for which entropy generation implies reduced maximal work output and thus efficiency, complex dissipative structures emerge from the very nature of the entropy-generating processes that compose them.

Living systems actively seek energy gradients to degrade, extracting free energy from their environment in the form of energy-dense (low entropy) food and oxygen. They also export to the environment higher entropy wastes (e.g., CO_2, stools) as well as heat, that is irreversibly produced internally when chemical energy is transformed through various metabolic pathways. The human body is known to be quite inefficient in its use of energy to produce useful work (e.g., walking, lifting an object), as more than 80% of the chemical energy is ultimately converted into heat [37], while heat transfer represents the largest contribution to entropy production and export [33]. However, unlike energy and matter, entropy is not conserved but rather preserved, in the sense that it can be created but not destroyed. Once entropy is produced, it must be exported externally to the body to prevent internal entropy accumulation and the associated rise in disorder (physical or informational).

Thus, to maintain internal order, living systems must pump out disorder. In other words, achieving and maintaining health stability require constant energy consumption, for which entropy production is the price to pay. But the stability of complex living systems further depends on their ability to export the entropy produced internally from metabolic activity such that the entropy balance remains close to zero throughout time [39]. The study of entropy production and export in clinical contexts is alluring, as it could allow us to understand the quantity and quality of energy transformations that occur within the human body and explore their implications in various physiological and pathological conditions [71]. Although the entropy analysis of biological organisms has been studied in the past [35, 36, 98, 100, 131], to our knowledge, a very limited number of studies demonstrated the capacity to accurately measure entropy rates in humans in clinically relevant settings (see Bienertova et al. (2016) and Zlamal et al. (2018) in a non-clinically setting).

Entropy changes come in various forms, such as thermal and chemical mixing. In this paper, we present a foundational technical contribution where heat fluxes and body temperature are concurrently measured over time, thus enabling entropy rate estimates, and discuss its potential for physiological and clinical advances. A pedagogical example, in the thermal context of interest here, sees an entropy change during some time increment equal to an amount of heat ΔQ entering or leaving a system, divided by the temperature of the system during that heat transfer. A positive ΔQ leaving body compartment X at temperature T_1 enters another compartment (or the environment) Y at lower temperature T_2: the total entropy change in the body is $\Delta S = \Delta Q/T_2 - \Delta Q/T_1$ which is a positive quantity. Thus, entropy increases in spite of the fact that energy is conserved, because the flow of heat from hot to cold is irreversible.

We experimentally illustrate the technique by showing that, for fixed entropy production rate, entropy export is impaired in humans exercising under heat stress in association with increased age, reduced fitness level, or with a chronic illness (individuals with type 2 diabetes). We also discuss insights into how thermodynamic entropy production, normalized by mass or surface area, could be used as an indicator of health and potentially

guide the development of therapeutic approaches to improve patient care. Our objective is to bridge multiple bodies of literature, ranging from non-equilibrium thermodynamics to thermal physiology and clinical research. Our work aims to extend the study of thermoregulation, which traditionally involves the use of the first law of thermodynamics (i.e., conservation of energy through heat balance analysis), to incorporate the fundamental concept of entropy from the perspective of the second law, where the irreversible processes driving metabolic activity inevitably generate entropy.

4.2 Material and Methods

4.2.1 Experimental Design

Our analysis was based on retrospective data collected by the research group of Prof. G. Kenny, who studied the effects of age [88], fitness-level [89], and type 2 diabetes [90] on thermal regulation of the body during exercise under heat stress. In a typical experimental design, participants entered the whole-body air calorimeter (device that provides a precise measurement of the heat dissipated by the human body) for an initial resting period of 30 min to ensure the stability of the ambient conditions within the chamber (temperature and relative humidity). The baseline temperatures and rates of heat production (assessed by indirect calorimetry) and dissipation of the participants were recorded continuously. The participants then followed an alternative schedule of exercise bouts (cycling on an upright seated cycle ergometer housed in the calorimeter) and recovery periods. During the exercise bouts, targets for metabolic heat production rate were fixed at specific rates by experimental design for all participants by adjusting the cycling resistance. The details of each study are listed below, and participant characteristics are summarized in table 4.2. For additional information on the methodology, including an extensive discussion of the limitations of calorimetry, the reader is directed to our previous work [39]. The protocols of alternating exercise and recovery periods for all studies are described and shown schematically in table 4.1.

Table 4.1: Summary of exercise/heat stress protocols

Study	Schedule	Schematic
Aging	Exercise: 15 minutes (x4) Recovery: 15 minutes T = 35 °C RH = 20%	
Fitness-level	Exercise: 30 minutes (x3) Recovery: 15 minutes T = 40 °C RH = 15%	
Type 2 diabetes	Exercise: 30 minutes (x3) Recovery: 15 minutes T = 40 °C RH = 15%	

Aging study: The experimental design of the study conducted by Larose et al. is thoroughly detailed elsewhere [88]. Briefly, heat transfer was measured during and following exercise in heat stress for healthy and physically active males of three different age groups: 11 young (26 ± 2 years), 11 middle-aged (43 ± 2 years), and 11 older males (63 ± 3 years), all having similar physical characteristics (table 4.2) except for percentage of body fat, which was positively correlated with age. The experimental design consisted of four 15-min exercise bouts of cycling on an upright seated cycle ergometer at a constant rate of metabolic heat production equal to 400 W, each followed by a 15-min inactive period with a final recovery period of 60 min. The temperature inside the calorimetry chamber was set to 35 °C with a relative humidity of 20%. Core temperature was measured by inserting a thermocouple probe into the rectal cavity. Skin temperature was calculated using a weighted average of four skin temperature probes located on the upper back (30%), chest (30%), quadriceps (20%) and back calf (20%).

Fitness study: The experimental design of the study by Stapleton et al. is thoroughly detailed in Stapleton et al. [89]. Briefly, 20 middle-aged male participants were

Study	Group	N	Age (years)	Height (cm)	Weight (kg)	BSA (m^2)	VO_2max ($ml \cdot kg^{-1} \cdot min^{-1}$)	Body fat (%)
Aging	Young	11	26 ± 2	181 ± 8	84.3 ± 6.2	2.0 ± 0.1	43.4 ± 6.7	16.9 ± 5.0
	Middle-aged	11	43 ± 2	178 ± 5	85.5 ± 7.4	2.0 ± 0.1	41.8 ± 6.1	23.3 ± 3.2
	Older	11	63 ± 3	178 ± 6	87.7 ± 10.2	2.1 ± 0.1	33.8 ± 5.7	28.3 ± 6.1
Fitness	Trained	10	49 ± 5	181 ± 5	82 ± 8	2.02 ± 0.11	51.0 ± 6.8	19.1 ± 4.3
	Untrained	10	48 ± 5	180 ± 8	85 ± 7	2.05 ± 0.13	37.3 ± 3.5	23.1 ± 6.3
Diabetes	Controls	17	61 ± 5	175 ± 5	83 ± 11	2.0 ± 0.1	36 ± 5	26.1 ± 7.3
	Diabetic	17	59 ± 6	175 ± 5	84 ± 13	2.0 ± 0.1	33 ± 7	26.9 ± 4.9

Table 4.2: Summary of the participants' characteristics for all three datasets.

recruited based on their fitness levels (10 trained and 10 untrained participants) (see table 4.2 for physical characteristics). All participants initially rested in the calorimetry chamber for 30 min and then performed three exercise bouts (cycling) of 30 min at increasing fixed rates of metabolic heat production (300 W, 400 W, and 500 W), each followed by a recovery period of 15 min. The air calorimeter was maintained at an ambient temperature of 40 °C and relative humidity of 15%. Core temperature was measured by inserting a thermocouple probe into the esophagus. The mean skin temperature was calculated as the weighted average of four skin temperature measurement [132] (30% biceps, 30% chest, 20% quadriceps, and 20% front calf).

Diabetes study: The experimental design has been thoroughly detailed in a previous study by Notley et al. [90]. Briefly, 34 participants were recruited, comprising 17 with controlled type 2 diabetes (59 ± 6 years) and 17 without type 2 diabetes (61 ± 5 years) (see table 4.2 for physical characteristics). Participants entered the calorimetry chamber for an initial 30 min of seated rest, during which basal metabolic rates were measured as reference values. Participants then completed three 30 minutes bouts of exercise on a semi-recumbent cycle at metabolic heat production rates (normalized by body surface area) of 150, 200 and 250 W/m^2, which corresponds approximately to 300 W (light), 400 W (moderate), and 500 W (vigorous) in absolute terms, each followed by a 30 min recovery. The temperature inside the calorimetry chamber was set to 40 °C with a relative

humidity of 15%. Core temperature was measured by inserting a thermocouple probe into the rectum. For some participants, core temperature was measured at the esophagus (n=3 for individuals without type diabetes; n=4 for individuals with type 2 diabetes). The mean skin temperature was calculated as the weighted average of four skin temperature measurement18 (30% biceps, 30% chest, 20% quadriceps, and 20% front calf).

4.2.2 Heat measurement using direct and indirect calorimetry

The internal heat production rate, or metabolic heat production rate $\dot{Q}_{int}$, was measured continuously using indirect calorimetry. The rate of chemical energy liberated from metabolic processes, referred to as metabolic energy expenditure $\dot{M}$ (in Watts), is transformed into external work rate (e.g., cycling) and metabolic heat rate. Metabolic energy expenditure rate was estimated spirometrically by directing the expired air from the participants into a metabolic gas analysis system (see figure 2.5) and measuring the respiratory exchange ratio between the rate of carbon dioxide production and the rate of oxygen consumption [37]. In these experiments, the external work rate $\dot{W}$ done on the cycle was continuously adjusted by changing the cycling resistance to ensure that the targeted values of metabolic heat production remained constant during the exercise periods. From energy conservation and accounting for the work done on the cycle, metabolic energy expenditure ($\dot{M}$) is equal to metabolic heat production ($\dot{Q}_{int}$) added to the work done during the exercise cycle. Indirect calorimetry is regarded as the gold standard, the reference standard and clinically recommended method for accurate measurement of energy expenditure ($\dot{M}$). By measuring $\dot{M}$, and subtracting work performed, one can calculate internal metabolic heat production [91, 92]

$$\dot{Q}_{int} = \dot{M} - \dot{W} \quad . \tag{4.1}$$

The external heat dissipation rate to the surroundings, denoted by $\dot{Q}_{out}$, was measured by direct calorimetry using a modified Snellen calorimeter [38], which is a state-of-the-art whole-body air calorimeter, as shown in figure 2.5. The two main contributions of

heat dissipation by the body are: (1) dry heat loss resulting from the heat exchange with the environment via conduction, convection, and radiation at the skin surface, calculated using the temperature difference between the outflow and inflow of air in the calorimeter, and (2) evaporative heat loss resulting from the evaporation of sweat on the skin, calculated from the change in absolute humidity within the calorimeter. The modified Snellen whole-body air calorimeter has an accuracy of ±2.3 W for the measurement of total body heat loss (i.e., dry ± evaporative heat loss), representing a measurement error smaller than 1% [38].

The heat produced internally (i.e., metabolic heat production) is partly dissipated to the environment through various physiological mechanisms (e.g., increase in blood flow to the skin), and in the case of insufficient heat dissipation, is partly stored within the body. Generally, the balance between the rate of metabolic heat production and the rate of heat dissipation corresponds to the rate of heat storage $\dot{Q}_{st}$, such that $\dot{Q}_{st} = \dot{Q}_{int} - \dot{Q}_{out}$.

4.2.3 Temperature measurements

The initial body temperature, measured during the initial resting period, was estimated using a weighted average between the core temperature (90%) and mean skin temperature (10%), both determined thermometrically, as detailed above. Thermometry-derived temperature measurements are accurate under resting conditions but tend to underestimate temperature variations during exercise [93]. Changes in whole-body temperature during exercise are best estimated by calorimetry using the rate of heat storage (i.e., the balance of heat flow) [37]. Therefore, thermometry was used to obtain the baseline body temperature (prior to exercise) and then temperature changes were calculated using calorimetry. Core and skin temperature measurements as a function of time are provided in supplementary material.

4.2.4 Entropy model

A two-compartment core-skin entropy flow model was used to derive an expression for the rate of entropy change dS/dt. For a detailed derivation of the entropy flow model, please refer to Brodeur & al [39]. In our model, we characterize the entropy balance following the framework established by Prigogine where entropy production (or generation) results from irreversible processes that occur [32]. Considering that the dominant contributions of entropy change correspond to heat generation and thermal exchange (i.e., neglecting the entropy change associated with the exchange of mass), we obtained the following equation for the rate of entropy change of the body:

$$\left(\frac{dS}{dt}\right)_{body} \approx \frac{\dot{Q}_{int}}{T_b} - \frac{\dot{Q}_{out}}{T_s} \tag{4.2}$$

where $\dot{Q}_{int}t$ is the metabolic heat production, $\dot{Q}_{out}$ is the external heat dissipation rate (the outflow is positive-definite), T_b is the calorimetry-derived whole-body temperature estimate and T_s is the thermometry-derived mean skin temperature. The negative sign on the right-hand side of equation (4.2) ensures that both entropy rates are positive-definite (negative-definite) if they flow inward (outward) through the system boundary by physical conventions. Comparing this equation to the standard entropy rate balance equation where dS/dt is given by the sum of dS_i/dt and dS_e/dt or, more intuitively, what is produced minus what is exported to the environment:

$$\frac{dS}{dt} = \frac{dS_i}{dt} + \frac{dS_e}{dt} \quad . \tag{4.3}$$

We obtain the following expressions for the entropy production rates and entropy export rate:

$$\frac{dS_i}{dt} = \frac{\dot{Q}_{int}}{T_b} \tag{4.4}$$

and

$$\frac{dS_e}{dt} = -\frac{\dot{Q}_{out}}{T_s} \tag{4.5}$$

According to the Second Law of Thermodynamics, the entropy production rate must always be greater than zero as metabolic activity continuously produce heat such that $\dot{Q}_{int} > 0$ (or equal to zero in case of death). Unlike the rate of entropy production, the rate of entropy change dS/dt is not limited to positive values and can have either positive or negative values, depending on the relative magnitudes of the contribution of dS_i/dt and dS_e/dt (see equation (4.3)). For instance, at the onset of exercise, the entropy production rate increases rapidly (by experimental design), while the entropy export rate increases gradually at a much slower rate: dS/dt is then positive. In contrast, at the onset of the recovery period, the entropy production rate decreases abruptly, whereas the entropy export rate remains elevated and negative, leading to a negative rate of entropy change. Therefore, dS/dt is typically positive during exercise periods (i.e., the body is accumulating entropy), and negative during recovery periods when the body actively exports the excess entropy accumulated during the previous exercise period. When the entropy export rate decreases and ultimately settles to the entropy production rate, the net rate of entropy change then becomes zero at some time after the last exercise bout, and the body eventually reaches a (stable) stationary state akin to homeostasis.

The cumulative entropy change, or entropy accumulation, in the body at any time t, $\Delta S(t)$, is obtained by integrating the rate of entropy change. Given that rates are reported as averages over 1-minute intervals, $\Delta S(t)$ is thus obtained by adding the entropy accumulated during every 1-minute interval Δt_i up to time t as follows

$$\Delta S(t) = \sum_{i=0}^{t} \langle \frac{dS}{dt} \rangle_i \cdot \Delta t_i \quad . \tag{4.6}$$

The cumulative entropy change can be interpreted as a measure of thermodynamic irreversibility [39] or stress [35]. To normalize for size, all entropy production rates were normalized by mass or body surface area. Following physical convention, entropy rates that are referred to as specific rates were normalized by the participants' mass and values were normalized prior to calculating group averages.

4.2.5 Statistical analysis

Data analysis was performed using an in-house program written in MATLAB (The MathWorks, Natick, MA, USA). ANOVA tests for same-size group comparison and post hoc p-values (two-tail t-test) were performed using the statistics and machine learning toolbox from MATLAB. All values are reported as mean ± standard deviation.

4.3 Results

4.3.1 Resting entropy production rates

Table 4.3 shows the resting entropy production rate dS_i/dt under heat stress, normalized by body surface area (BSA) (first column) and weight (second column), the latter being generally referred to as the specific entropy production rate. The resting rates of entropy production were calculated by averaging the entropy production rates during the initial resting period inside the calorimetry chamber (i.e., prior to any exercise). We found resting entropy production rates to be not statistically different across all age groups when normalized by body surface area; however, a statistically significant difference between young and older participants was observed for the specific entropy production rate ($p = 0.04$), which is normalized by weight. Standard deviations of calculated values were higher when using mass normalization due to a greater variance in the participants' weight compared

Table 4.3: Initial resting entropy production rate (dS_i/dt) under heat stress

Study	**Group**	**Resting** dS_i/dt ($W/K/m^2$)	**Specific resting** dS_i/dt ($x10^{-3}$ $W/K/kg$)
Aging	Young	0.18 ± 0.01	4.3 ± 0.4*
	Middle-aged	0.18 ± 0.01	4.3 ± 0.4
	Older	0.17 ± 0.02	3.9 ± 0.5*
Fitness	Trained	0.19 ± 0.02	4.8 ± 0.5
	Untrained	0.19 ± 0.02	4.6 ± 0.8
Diabetes	Controls	0.17 ± 0.02	4.1 ± 0.5
	Diabetics	0.17 ± 0.02	4.1 ± 0.5
Aoki	1 male	0.172 ± 0.002	$3.47^{\dagger}$

* Significant difference (p-value < 0.05) † Uncertainty was not provided in the original study.

to the variance in their body surface area.

4.3.2 Entropy rates and entropy accumulation

The specific rates of internal entropy production dS_i/dt, absolute entropy export rate dS_e/dt, entropy change dS/dt and the cumulative entropy change (or entropy accumulation) for age, fitness level, and diabetes status are shown in figure 4.1. The exercise/recovery protocols can be appreciated directly from the entropy production time-series (first row of figure 4.1), where the elevated plateaus refer to exercise periods, whereas the heights of these plateaus indicate the relative exercise intensity (e.g., constant exercise intensity for the aging data versus increasing difficulty for the fitness level and diabetes data). Because metabolic heat production was fixed at specific values by the experimental design for all participants during exercise intervals, the specific rates of entropy production also showed the same behavior; however, small differences that are not statistically significant can be observed between groups and are attributed to mass normalization. Moreover, it should be noted that metabolic heat production and hence the entropy production rate were not

fixed during the recovery periods, as participants reached their own resting state. Body and skin temperature time-series, which are measured in real-time and required to calculate the rates of entropy production and export through equations (4.4) and (4.5), are provided in Chapter 2 (see figures 2.7 and 2.6).

The specific entropy export rates, shown in the second row of figure 4.1, are reported as absolute values for visualization. The general behavior of entropy export rates is to increase initially at the onset of exercise periods with a comparably faster decay at the offset. Entropy export rates did not recover their initial resting values over the course of the experiments, with visibly higher plateaus during the inter-exercise resting periods.

Differences in entropy export were observed between the different groups for all datasets. However, entropy export rates cannot be compared directly because the entropy production rates exhibit small differences between groups (although not statistically significant ones). Nonetheless, it is interesting to note that the maximal entropy export rate for the first exercise bout was consistently lower than that of the remaining exercise bouts for all age groups (figure 4.1B), even though the entropy production rates remained approximately constant across all exercise bouts.

The third row of figure 4.1 shows the rate of specific entropy change at the end of the exercise periods. This is an interesting quantity as it measures the distance from the stationary state of entropy balance; the higher the rate of specific entropy change, the further the body is from a steady state (or homeostasis). Conversely, a smaller rate of entropy change implies that the body is accumulating entropy more slowly, and thus, is closer to a stable state. Figure 4.2 shows the average rate of specific entropy change over the last two minutes of each exercise period for all studies. We found that the rate of specific entropy change was a good predictor for clinical evaluation, as the calculated rates significantly and consistently increased in association with age, sedentary lifestyle, and the presence of diabetes. In the latter two studies, statistically significant differences were observed only at moderate- and high-intensity exercise levels (figure 4.2).

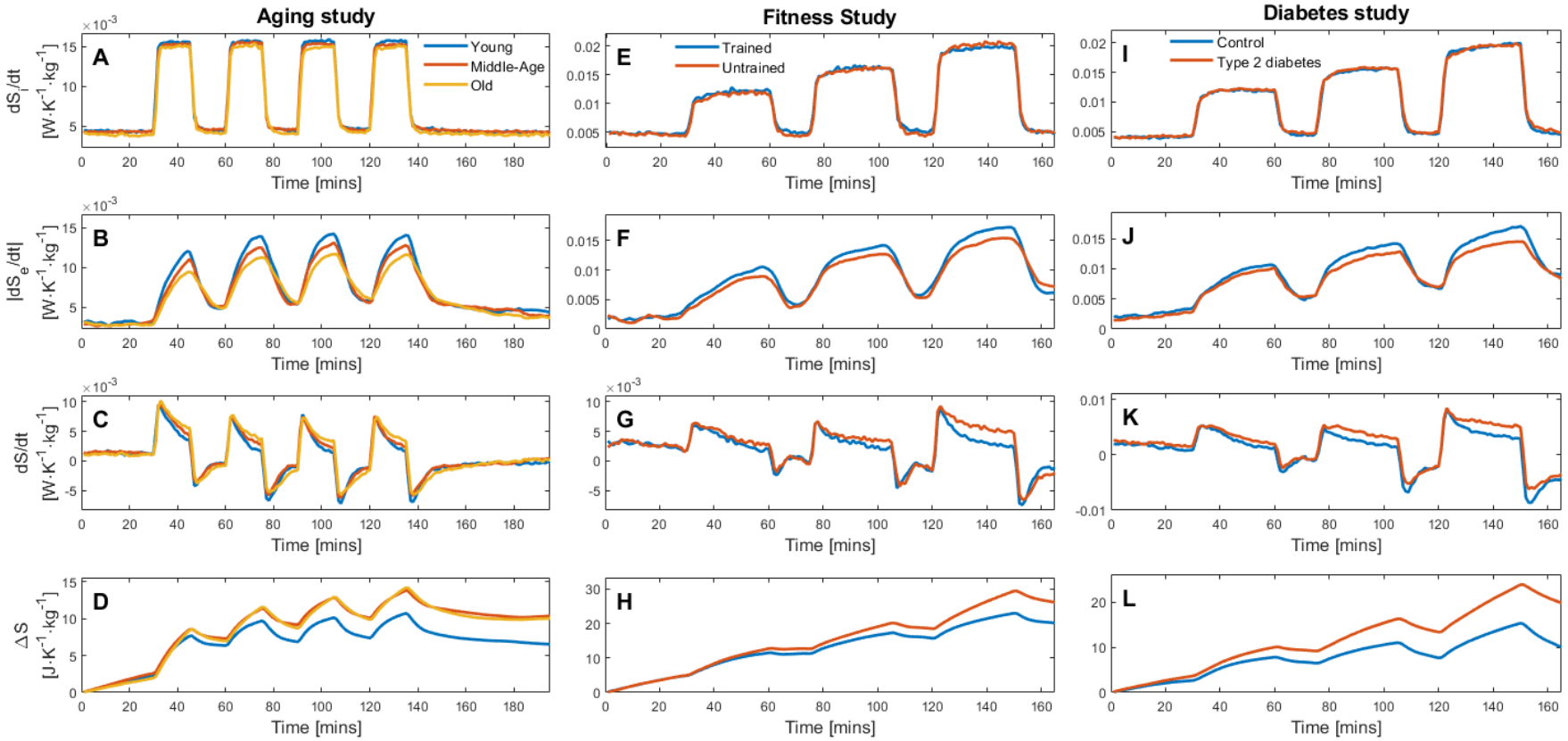

Figure 4.1: **Summary of the entropy rates and entropy accumulation for all studies.** The figure columns provide the entropy rates and entropy accumulation for the aging study (left), fitness study (middle) and diabetes study (right). The first row shows the average specific entropy production rate (dS_i/dt) as a function of time calculated from Equation (4.4). The second row shows the absolute value of the average specific entropy export rate (dS_e/dt) as a function of time calculated from equation (4.5). The third row shows the average rate of specific entropy change (dS/dt) obtained by summing the entropy production and export rates. The fourth row shows the entropy accumulation, which corresponds to the cumulative specific entropy change over time as calculated from equation (4.6). Individual curves are normalized using the participants' weights prior to computing the group averages shown here.

The bottom row of figure 4.1 shows the cumulative entropy change, or entropy accumulation, as calculated from equation (4.6). Entropy accumulation can be interpreted as a thermodynamic measure of biological stress [35, 39]. We found that young participants were able to stabilize their entropy accumulation by the second exercise period, as their level of entropy accumulation at the end of the first recovery period (at 60 min) and that at the end of the experiment (at 195 min) were essentially equal. Therefore, young participants showed no net gain in entropy during the last three exercise periods and their associated recovery periods. Entropy accumulation for middle-aged and older participants was significantly higher than that of their younger counterparts, with a consistently growing difference attributed to a net gain of entropy following each cycle of exercise/recovery. A similar behavior was observed in the entropy accumulation time series for trained and untrained participants (figure 4.1H) and participants with and without diabetes (figure 4.1L), especially during the last exercise period at higher intensity levels. A statistical comparison of the total entropy accumulation after each exercise period, shown in figure 4.2 for all studies, reveals that entropy accumulation is strongly associated with age, sedentary lifestyle, or the presence of diabetes.

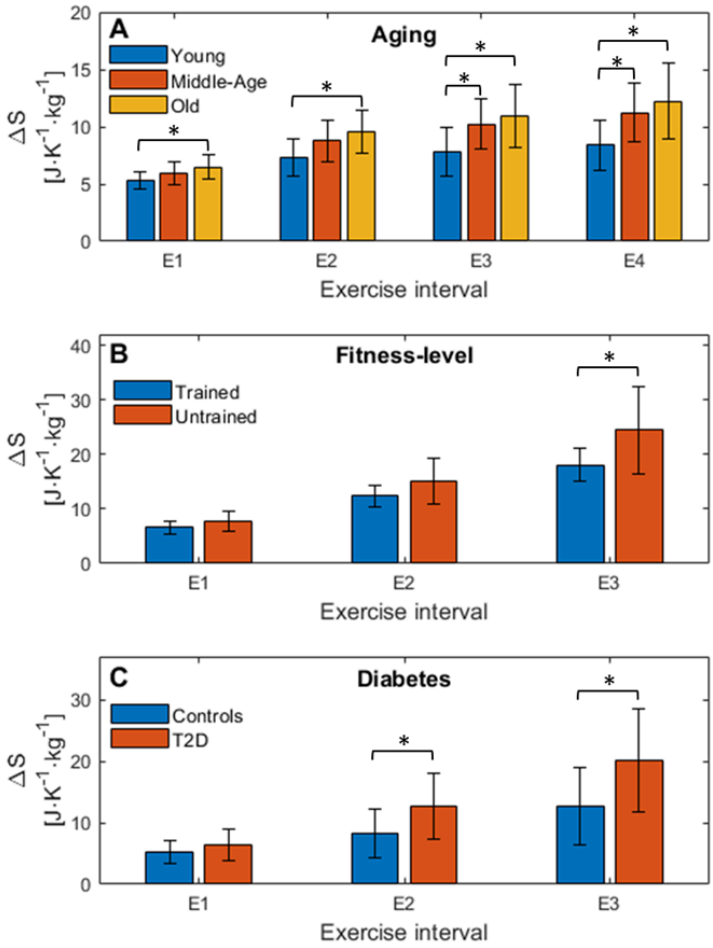

Figure 4.2: **Cumulative specific entropy change for all studies.** Cumulative specific entropy change at the end of every exercise period in association with age (top panel), fitness-level (middle panel) and diabetes (bottom panel). Statistically significant differences between groups ($p < 0.05$) are indicated by an asterisk. Error bars represent the standard deviation for group averages.

Figure 4.3 shows the correlation and linear regression analysis between entropy accu-

mulation and maximal oxygen consumption (i.e., $\dot{V}O_2^{\max}$), a common marker of cardiovascular fitness [133]. We found a slight negative correlation across age groups ($R = -0.26$), a moderate negative correlation between trained and untrained participants ($R = -0.40$), and a weak negative correlation between participants with and without diabetes ($R = -0.18$). In the latter case, the weaker correlation can be attributed to a broad distribution of $\dot{V}O_2^{\max}$; the diabetic group tended to have a higher entropy accumulation across similar $\dot{V}O_2^{\max}$ compared to the control group. Overall, we found a trend of negative correlation between $\dot{V}O_2^{\max}$ and entropy accumulation, which suggests that higher cardiovascular fitness (i.e., higher $\dot{V}O_2^{\max}$) is associated with lower entropy accumulation during intense exercise across various demographic and health conditions.

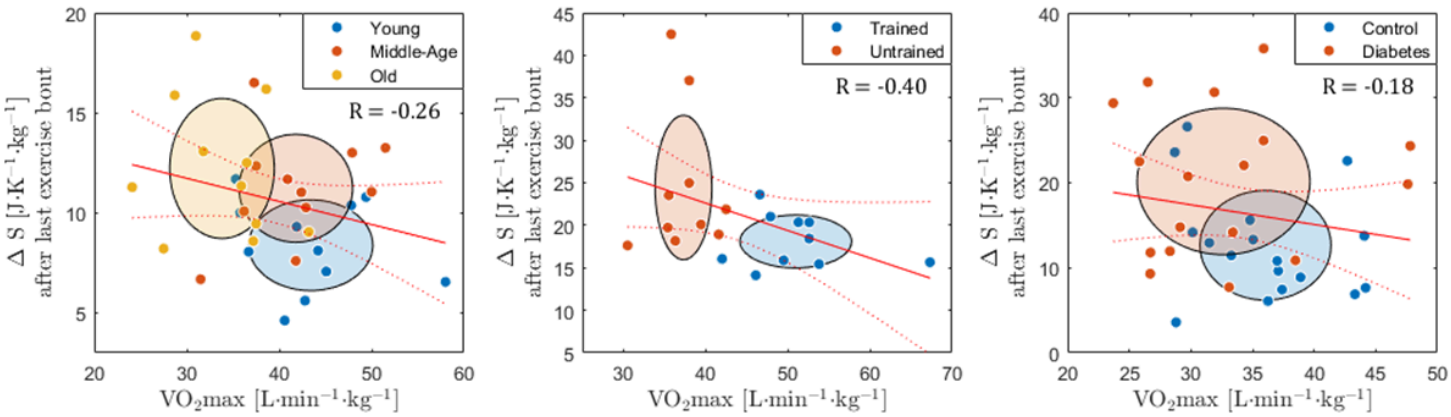

Figure 4.3: **Correlation analysis between $\dot{V}O_2^{\max}$ and cumulative specific entropy change.** Correlation analysis between the individual cumulative specific entropy change at the end of the last exercise bout and the individual $\dot{V}O_2^{\max}$ value for the aging study (left panel), fitness study (middle panel) and diabetes study (right panel). Individual data points are shown for the different groups within each study. Results of the linear regression are shown by the straight red lines with their associated confidence interval (95%) shown as the dashed red lines and the correlation coefficients R. Using the same color code as shown in the legend, the ellipses are centered on the average value of each group with their major/minor axis representing the standard deviation along each dimension.

4.4 Discussion

Result summary

We measured the rates of internal entropy production and external entropy export in humans exercising under heat stress using concurrent indirect and direct calorimetry, respectively. In conditions set to have a standardized rate of internal entropy production, we observed progressive impairment of external specific entropy export and associated entropy accumulation under three separate conditions: with increasing age, reduced fitness level, and the presence of a common chronic disease (i.e., type 2 diabetes). Furthermore, a trend of negative correlation between $\dot{V}O_2{}^{\max}$ and entropy accumulation was found for all these clinical conditions. Such a negative correlation is also present between $\dot{V}O_2{}^{\max}$ and heat accumulation (not shown), and constitutes a novel finding in thermoregulatory physiology under heat stress. These observations support the hypothesis that the capacity to produce and export entropy to the environment may be associated with or even offer a novel measure of health.

Previously, extensive research has been done on the thermoregulation of humans under various environmental conditions and exercise-induced heat stress in healthy and pathological conditions [78]. For example, it is known that older adults display a greater vulnerability to heat stress primarily due to a reduction in sweating capacity caused by a lower sweat output per gland [134]. In the case of diabetes, the impaired temperature regulation is commonly attributed to two main causes: (1) an attenuated capacity for evaporative heat loss that originates from a neuropathy in peripheral nerves [135] (including sudomotor nerves) and (2) a reduced skin blood flow response due to a neuropathy in vasodilator nerves [136] and microvascular dysfunction [137]. These biological explanations provide a mechanistic understanding for the observed impairment in thermoregulation. However, it is also possible to investigate the homeostatic control of the body from a physics perspective under the unifying thermodynamic principles of complex non-equilibrium systems.

The human body is an open thermodynamic system that exchange matter and energy with its environment. Chemical energy, work and heat are all distinct forms of energy that are on an equal footing with regards to the First Law of Thermodynamics. However, there exists an asymmetry in that it is possible to fully convert chemical energy and work into heat, but the reverse is not possible. This inherent irreversibility of heat generation within a system, often referred to as energy export or energy degradation, is the manifestation of the Second Law of Thermodynamics. In general, for systems that are far from equilibrium, the more complex and robust the underlying system is (e.g., metabolism), the more energy export and entropy production are expected for basic operation and maintenance. However, the production of entropy and its associated idea of converting energy into forms of lesser quality (e.g., thermal energy) doesn't contradict the evolutionary principle of energy efficiency. Indeed, living systems are rather incentivized to maximize the amount of work that can be extracted from an energy source [24], which implies a maximal degradation of energy. The production of entropy all along the cascade of metabolic processes is both a requirement and an inevitable consequence of continuously maintaining a dynamical steady state in non-equilibrium conditions.

Non-equilibrium Thermodynamics in Health

A basal rate of internal entropy production refers to the minimum rate at which entropy must be generated within the body to sustain the basic physiological functions and is closely related to the energy expenditure or basal metabolic rate. The entropy production rates presented in table 4.3 are not formally basal rates, but rather resting rates in these experiments in participants being subjected to heat stress (i.e., not a thermally neutral environment) without performing exercise and work. Consequently, the entropy production rate is expected to be slightly elevated compared to basal conditions, as physiological mechanisms are actively engaged in dissipating the extra heat. Considering that older people are typically less efficient at dissipating internal heat [88], it is possible that their resting metabolic rate must increase further compared to that of their younger counterparts when subjected to heat stress, as more energy must be utilized to dissipate the same amount of heat. This situation could explain why the resting rate of entropy production appears

to be constant irrespective of age.

Nonetheless, it has been hypothesized that higher basal rates of entropy production are beneficial in terms of health and fitness [71]; while they might not be the direct *cause* of health and fitness, they at least *enable* the maximization of work output, which is a necessary condition for a system to efficiently fight perturbations around homeostatic states. This idea is exemplified in athletes who have both elevated basal and maximal rates of energy expenditure, and consequently, entropy production, compared with non-athletes [138]. In this sense, health and fitness can be viewed as the ability to utilize resources at a greater rate to either have a faster response to a perturbation or being able to output more work. Both cases are associated with a high cardiopulmonary capacity ($\dot{V}O_2^{\max}$), which was found hereby to be negatively correlated with entropy accumulation. More generally, there appear to be some minimal requirements in energy consumption to even sustain the possibility of achieving high levels of work, related to the ability to maximally increase their energy export rate when needed; however, this is only possible at the cost of having a higher basal rate of entropy production. Thus, one could expect that aging and disease are associated with a diminishment in (either or both) the capacity for basal and maximal internal entropy production, as suggested previously [98].

Given that the specific rates of internal entropy production were kept approximately constant across all participants in each study, most of the differences in the specific rates of entropy change can be attributed to differences in the specific rates of external entropy export. Therefore, elevated rates of specific entropy change at the end of exercise periods can be associated with one's inability to export the entropy produced within the body following the elevation of the metabolic rate. The ability to return to a dynamic equilibrium state (where external export equals internal production) faster, as observed in younger participants, physically trained participants, and participants without diabetes, is thus indicative of greater fitness and general health. Thermodynamically, stationarity is obtained when heat and entropy flows are exactly balanced such that there is no net gain or loss of entropy within the body.

This perspective offers potential advances in physiologic and therapeutic temperature manipulation. For example, a relevant clinical example could be therapeutic temperature management for patients with fever. The human body has a highly constrained range of internal temperatures for normal operation, typically between 36 and 38 °C at rest, which represents less than 1% variation when expressed in Kelvin units (the natural temperature unit of entropy). Any further variations in temperature require immediate care, as in the case of fever. Although fever increases body temperature, the increase in metabolic heat production and dissipation can be proportionally larger, leading to elevated resting rates of entropy production (i.e., heat divided by temperature). The clinical question then becomes: in what circumstances are elevations in internal temperature beneficial or harmful for a patient's recovery? Based on entropic principles, we argue that letting body temperature rise is beneficial if it increases the rate of entropy production, that is, if it increases metabolic activity in greater proportion than the rise in temperature. Thus, clinical interventions could be tailored to improve metabolic and physical resilience based on entropic principles.

An additional relevant quantitative measure of the inability to cope with perturbations (e.g., environmental or exercise-induced heat stress) that can be derived from the results presented here is the specific entropy accumulation, calculated from equation (4.6). Indeed, lower specific entropy accumulation is associated with higher maximal oxygen consumption ($\dot{V}O_2{}^{\max}$), suggesting that individuals with higher cardiovascular fitness may be able to handle higher exercise intensities with lower physiological stress. Specific entropy accumulation could then serve as an indicator of the effectiveness of the physiological response to stimuli (e.g., exposure to an environmental heat load or heat load generated by exercise), otherwise thought of as the system's capacity for adaptation or general robustness. If the measurement of entropy rates can be helpful in monitoring changes in health, it can also provide valuable information for performance optimization in athletes. One could expect that reducing entropy accumulation as a physiological variable over time could lead to enhanced long-term performance, especially in young athletes. Although the effect of excessive entropy accumulation at the molecular or cellular level remains to be elucidated

by future studies, preventive measures against long-term entropy accumulation can be implemented. For example, strategies to maintain higher basal and maximal rates of entropy production are hypothesized to be beneficial for long-term health provided that the entropy export response remains equally efficient. The clinical evidence of the impairment in entropy export presented here opens the door for the development of clinical studies, which would be required to further validate the effectiveness of entropy accumulation as an indicator of health.

Limitations

Several limitations of this work merit discussion. First, the use of indirect calorimetry to estimate metabolic heat production rate assumes that the expired gases are the product of the oxidation of carbohydrates, thus considering that only aerobic metabolism is involved. However, exercise periods were kept relatively short (<30 mins) and the recovery periods long enough (>15 mins) to avoid depletion of aerobic substrates during exercise and allow replenishment during recovery, thus minimizing anaerobic metabolism. For an in-depth discussion about the limitations of direct and indirect calorimetry to estimate entropy production and export, the reader is referred to our previous work [39].

Second, although the combined methods of indirect and direct calorimetry remain the most accurate approach to estimate the total amount of heat stored (from the balance of heat flows), our approach does not provide information about the temperature distribution within the body. Indeed, temperature is known to be heterogeneous across the different tissues, depending on their blood perfusion, and especially during exercise where muscles temperature can reach up to 40 °C while core temperature is closer to 38.5 °C [37,122,125]. Nevertheless, calorimetry-derived temperature measurements are more reliable compared to the traditional use of temperature probes as thermometry was found to be inaccurate for the calculation of entropy time-series [39] due to the limited number of localized probes that do not reflect the whole-body temperature [94]. Additionally, each study presented here contained a relatively small number of participants in each group, which leads to moderate errors in the determination of the group averages (as seen in figures 4.2 and 4.3).

Indeed, the modified Snellen air calorimeter has an accuracy of ±2.3 W (approximately 1% error) [38]. Thus, the uncertainty in the group averages is mostly attributable to the biological variability among participants rather than the measurement error.

The entropy balance analysis presented here considers heat production and transfer as the main contributions to the entropy change. A more complete tally could eventually include contributions associated e.g. with the formation and elimination of metabolic byproducts. Furthermore, limiting the entropy contributions to heat production and transfer also implies that our entropy analysis is not considerably different from the heat balance analysis conducted in traditional studies of human thermoregulation. Indeed, body temperature in homeothermic organisms is highly constrained to operate within a very narrow range, typically between 36-38 °C, leading to temperature variations of less than 1% when expressed in Kelvin units. In turn, this implies that entropy rates, obtained by dividing the rates of heat production and heat loss by core or skin temperatures, remain largely unaffected by these small temperature variations. However, thermoregulation studies involve the analysis of heat fluxes solely from the perspective of the First Law of Thermodynamics, namely the conservation of energy. The inefficiency of biological systems to convert chemical energy (low entropy) into heat (high entropy) is not only interesting from a First Law perspective, but naturally extends to involve the Second Law, that is the increase of entropy associated with irreversible processes.

Finally, the datasets used for our entropy analysis involve uniquely male participants. While sex-related differences in thermoregulation have been studied in the past [139–141], it is still debated whether there exist true physiological differences between sexes in heat management [37, 78]. The difficulty in identifying absolute differences stems from the different morphological characteristics between male and female (e.g., body mass, surface area, body composition, etc.), all of which play a significant role in how heat is produced, managed internally and eventually dissipated. However, compared to males, it is known that females typically have a lower $\dot{V}O_2{}^{\max}$. Therefore, in experiments where metabolic heat production is fixed (i.e., not a fixed relative intensity in terms of percentage of $\dot{V}O_2{}^{\max}$), females would be exercising at a higher relative intensity compared to males, which can

be viewed as a higher physiological stress in females. Additionally, females have a lower sweat output during high-intensity exercise [142], which implies a reduced capacity for evaporative heat loss and thus a smaller entropy export rate. Overall, one could expect that females, in the context of the experiment protocols presented here, would accumulate entropy at a faster pace than males under comparable absolute heat stress conditions due to their typically lower body mass (i.e., smaller heat sink) and lower maximal sweating capacity. In the light of these biological differences, further research is crucially needed to investigate the entropy dynamics in females, and especially if the ultimate goal is to develop tailored therapeutic approaches.

Different Insights from the Entropy Perspective

The design of our experiment allows us to only measure heat related irreversibility and oxygen consumption. The heat fluxes and entropy rates show qualitatively similar behaviours, but they are not precisely the same, since heat flux and temperature variations (by which the fluxes are divided) differ. Our method thus enables us to frame the joint heat flux-temperature results in terms of an imbalance in entropy production and export during exercise and recovery. This perspective is new, and relates to the growth of entropy in the body while it struggles to re-establish heat and, as we suggest, entropic balance. After the last exercise bout, the body does apparently eventually fully recover from the points of view of calorimetry and heat export. But it is clear that an integral of the rate of total entropy change over time signifies an increase in entropy in the body, i.e. it is larger after the exercise regime. Past flux-based analyses did not consider this possibility, and in that sense this is a divergence from an approach based on energy metrics.

Further, differences between energy conservation (an equality) and the increase in the entropy (an inequality about the quality of energy) are fundamentally different concepts. *The fact that we have carried out an experiment in which the energy balance and entropic balance viewpoints produce quantitatively similar trends, especially because of the use of absolute temperature units, does not negate the fact that these are different laws.* Entropy production still exists as an additional law, even in the case of the conduction of a minute

amount of heat across two systems only a couple of degrees apart (see Introduction of this chapter). It could give insight into e.g. efficiency of energy use and Onsager's transport theory, and variants thereof further away from equilibrium.

One must also distinguish between the fact that we consider two thermodynamic laws, and the issue of limited experimental accuracy to measure heat fluxes and temperature variations described above. Our paper will provide incentive to the community to devise improved or alternative experimental designs with higher accuracy for certain variables, e.g. to see changes in specific (per body surface area) or absolute entropy rates that reflect skin-vs-core temperature changes. For example, it may be telling to control for the work rate instead of the metabolic rate as done here. Our foundational technical contribution can promote the establishment of relationships with minimal or maximal entropy production ideas that permeate the non-equilibrium thermodynamics literature. By design, our analysis with controlled entropy production highlights differences in entropy export rates, and these are found to span a wider range of values (dynamic range) for the fittest, youngest, and non-diseased, with associated lesser changes in entropy accumulation.

While the concept of heat is more tangible and intuitive, entropy is arguably more fundamental in delineating how dissipative structures operate far from equilibrium. The fact that the temperature fluctuates weakly on the Kelvin scale makes results of our study from the perspectives of the first and second laws qualitatively similar. Yet, our experimental design which integrates human thermoregulation and heat exchange enables us to make such statements about two fundamental thermodynamic aspects of these biological systems, and opens further avenues for quantifying the efficacy of far-from-equilibrium biological systems in different states to perform work, and to generate and export entropy. Consequently, the exploration of health and fitness through the Second Law constitutes a next step beyond the first law to deepen our understanding of biological systems' ability to respond to perturbations that are either internal (e.g. chronic disease) or external (e.g. environmental heat stress).

A further insight afforded by the entropic perspective is as follows. While dissipating

the same amount of heat, entropy export in the human body can be markedly enhanced by maintaining a lower skin temperature, since a smaller denominator in equation (4.5) implies a larger entropy export and thus a lesser entropy accumulation within the body. However, a lower skin temperature can also be a sign of pathological thermoregulation (such as occurs with individuals with type 2 diabetes [90, 143]) if it originates from the inability to increase blood flow to the skin, in which case heat is ineffectively transferred from the core to the skin and accumulates internally. This situation leads to a smaller numerator $\dot{Q}_{out}$ in equation (4.5) and, despite having a lower skin temperature, this results in greater entropy accumulation within the body. Similarly, generating metabolic heat $\dot{Q}_{int}$ at a lower core temperature implies a greater internal production of entropy which, from a thermodynamic perspective, is beneficial in non-equilibrium systems as long as they retain the ability to export it. Thus, it is beneficial for the body to maintain a lower core temperature, which aligns with the strict control observed over the increase of core temperature [78]. The scenarios discussed above provide concrete examples where the entropy analysis would diverge from the sole analysis of heat flux. And while the foundational measurement framework presented here could allow these investigations, further explorations are needed to generate a more entropically-informed physiological and clinical picture.

The present study provides an alternative framework for understanding and evaluating thermodynamic flows in the human body and their alteration in association with health, disease and age. It demonstrates the feasibility of real-time monitoring of entropy production and export across a range of physiological states. Indeed, it is experimentally very challenging to accurately measure heat flows and temperature changes simultaneously in the body, both quantities needed to derive entropy rates. This explains the very limited number of published experimental results related to entropy in humans, despite its central nature in the self-organization of living systems as recognized by Schrodinger more than 80 years ago [57]. Our unique experimental instrumentation will allow further thermodynamic exploration of the human body during different acute disturbances in physiological state created by exercise and or exposure to environmental stressors. For example, future work could extensively quantify across clinical status the real-time mechanical efficiency

based on the first law, i.e. work divided by metabolic energy. Our approach also opens the door to the application of non-equilibrium thermodynamics measures, involving e.g. system fluctuations and efficiencies, to human clinical data [64, 114].

4.5 Conclusions

In summary, we provided experimental evidence for the impairment of entropy export and, consequently, entropy accumulation in association with increased age, reduced fitness level, and presence of diabetes during exercise under heat stress using direct and indirect calorimetry. We also found a trend of negative correlations between the maximal oxygen consumption rate ($\dot{V}O_2^{\max}$) and entropy accumulation after a series of exercise bouts at vigorous intensity. More generally, the inability to export the entropy produced internally is indicative of a lack of adaptability to external stimuli (e.g., exposure to hot environments and exercise), with potentially severe clinical consequences. Our results suggest that thermodynamic principles can be useful to guide clinical decision-making by identifying therapeutic interventions involving the optimization of resting and maximal entropy production rates, such as the management of physiological strain associated with fever during acute illness or following exposure to hot and cold environments. By continuing to explore the role of entropy production and export in human health, we work towards a novel understanding of physiology based on non-equilibrium physics, which could lead to the development of therapeutic approaches that will transform and improve patient care.

Chapter 5

Stochastic Modeling of Entropy Regulation in Humans

Abstract

Biological organisms are far from equilibrium systems that breakdown chemical energy gradients to sustain their internal structural and functional order. While entropy-generating processes are necessary for self-organization, growth and healing, entropy export is required to prevent entropy accumulation within the body. Health is conceptualized as the capacity to maintain entropic balance by rapidly augmenting external entropy export during periods of increased internal entropy production. This study introduces a model of entropy regulation in humans that is in good agreement with experimental calorimetric data for young, middle-aged and older adults exercising under heat stress. It assumes an asymmetry in the response time between exercise and rest periods. Our model is based on the hypothesis that the human organism regulates its entropy export rate according to the current net rate of entropy change of the body. A significant age-related increase in response times is found during both exercise and recovery, indicating diminished physiological adaptability

in older (n = 11, age 63 ± 3) relative to young (n = 11, age 26 ± 2) individuals. The model was further expanded to incorporate the effect of temporal additive noise to characterize the individual variability in the entropy export response. Our analysis revealed a lower strength of additive dynamical noise for the older participants during physical exercise, reinforcing the case for a reduction in thermoregulatory resilience associated with aging. Additionally, since the model has the form of an Ornstein-Uhlenbeck process in the static situation prior to the exercise regimen, a Fokker-Planck analysis of the entropy export dynamics could be performed. This enabled estimates from baseline fluctuations of both the additive noise strength and the response time. The response time estimates were compatible with those under dynamic exercise conditions, but static noise increased with age. Our stochastic thermodynamical analysis offers a useful fluctuation-dissipation perspective in this far-from-equilibrium physiological system, and more generally on the entropic and thermoregulatory control in endothermic biological organisms across the life span.

5.1 Introduction

The ability of complex living systems to maintain a stable internal dynamic state, such as that associated with health in humans, can be understood fundamentally as the successful regulation of thermodynamic flows such as energy, heat and entropy. Living systems actively extract free energy in the form of energy-dense (low entropy) food and oxygen to sustain the necessary metabolic processes, while exporting higher entropy wastes (e.g., CO_2, stools) to the environment. This irreversible transformation of energy is known to be quite inefficient in the human body as more than 80% of the chemical energy extracted from glucose and fat storage is ultimately converted into heat [37], while the remaining can be used to perform useful work (e.g. walking, lifting an object, etc.). Part of this heat also enables the chemical reactions to occur within tight temperature bounds for warm-blooded animals (endotherms), but much is irreversibly lost for the execution of mechanical work. This purely mechanical inefficiency, which conjures up comparisons to steam engines, should however be put in perspective since the human body performs a remarkable range of tasks of varying complexity in order to maintain its internal order

over the lifespan. Nevertheless, this transformation of energy also comes at the cost of an increase in entropy, which, once produced, must be exported to the environment to prevent its accumulation within the body. Interestingly, biological organisms share striking similarities with dissipative structures [32], that is, self-organized systems for which structures and functions emerge from the entropy-generating processes that govern them [16].

The application of nonequilibrium thermodynamics to biological systems has a long history [5, 8, 144], but the experimental investigation of entropy production and export still remains limited, apart from an early significant contribution from Aoki that provided foundational understanding of entropy flows in humans in basal conditions [33]. Recently, we have shown the feasibility of real-time monitoring of the entropy production and export during exercise under heat stress using indirect and direct calorimetry [39]. Our approach produced results in good agreement with Aoki's work regarding the measurement of entropy production rate at rest. It offers the potential to further study health and illness using nonequilibrium thermodynamic principles. Here we pursue this direction by formulating a dynamical model for the deterministic and stochastic aspects of entropy responses to exercise and heat perturbations across the lifespan. In complex living systems, healthy steady states implicate balanced thermodynamic flows where e.g. the entropy produced internally by the metabolic processes is in balance with the entropy exported to the environment.

Specifically, when the human body is perturbed out of a steady state, for example at the onset of physical exercise or exposure to a hot environment, or both as in our study, a transient period of imbalanced entropy flows is expected as the sudden increase in entropy production rate is not immediately matched by an increase in the entropy export rate. This situation leads to entropy accumulation within the body which promotes structural and functional breakdown. Recent work has shown that this impairment in capacity to export entropy worsens with age, fitness level and chronic disease [40]. Therefore, the study of entropy production and export might enhance our understanding of how various physiological and pathological conditions impact health stability, and lead to novel clinical interventions for improved metabolic and physical resilience.

As pointed out by Katchalsky & Curran, regulation mechanisms in living systems operate on external perturbations to re-establish a steady state in a way that is often analogous to a restoring force [5]. The mass-spring system is a typical analogy in which the force acting on the mass is larger the further it is displaced from the equilibrium position – or in other words, the equilibrium lies at the minimum of some effective potential. Also, free energy is minimized under equilibrium conditions. But for systems near equilibrium, according to the field of stochastic thermodynamics, the quantity being minimized is the difference between the free energy and the work done by external driving forces [64,145,146]. These are open questions for complex biological systems. Yet, the responses of these systems are typically characterized by a first-order linear differential equation for which, under a constant driving term, the mathematical solution is an exponential function that decays asymptotically to a steady state.

For example, such a model has been used to study the deterministic and stochastic constriction-dilation dynamics of the human pupil light reflex during alternating epochs of light and dark [147]. In that system, there exists an asymmetry in response times between constriction and dilation which involve, respectively, parasympathetic and sympathetic mechanisms and associated muscle dynamics in the iris. This kind of asymmetry is also seen and modeled in the current study of exercise in heat stress. More generally, one can formulate a linear response analysis of the biological system driven by a time-varying input to account for changes in the activity mean and variance compared to the non-driven state.

In the field of human thermoregulation, a similar first-order model was used by Malchaire to predict the response in evaporative heat loss under fluctuating thermal conditions [148]. Moreover, it is known that during exercise, humans regulate themselves through various physiological mechanisms [78], e.g. enhancing heat export to the environment through increased sweating and peripheral blood flow. Upon cessation of exercise, the relaxation of the heat export rate towards stationarity results from a restoring force that is proportional to the deviation from homeostasis [106]. Models of temperature control combine physical laws and phenomenological relations to predict the behaviour of e.g. sweat rate and skin blood flow as a function of body core temperature [106]. In parallel,

much work has been devoted to formulating models of different geometrical complexity for the equilibration of heat between different body compartments [104].

It has nevertheless proven challenging to predict the actual time course of e.g. core temperature following heat stress and exercise as these are determined from the combination of both neural responses to physiological sensors and the evolving heat fluxes between body compartments and with the environment. In particular, those studies cite age as a factor that negatively affects thermoregulation, and this will be the case below. This is in line with other recent studies that account for loss of function by the impaired integration of regulatory mechanisms at multiple hierarchical scales (see e.g. Cohen et al [149]).

Therefore, given the central nature of entropy in self-organized systems such as the human body, there remains a need to develop a working model that can properly and accurately describe the dynamic interplay between entropy production and entropy export. Here we do just that in the context of heat stress and exercise. Such a model could make predictions in situations beyond those presented below for which our model is developed. Our work contrasts with more classic bioheat exchange models by focusing not on the spatial-temporal distribution of temperature within the body [109, 150] (although it assumes core and skin compartments), but rather on the dynamical response of the whole body under various conditions such as exercise in the heat. Moreover, current thermoregulation studies and their heat flux analyses are ultimately based on the conservation of energy (i.e. first law of thermodynamics), which conceals the fact that complex living systems emerge from the entropy-generating irreversible processes associated with the second law of thermodynamics. Thus, our objective is to model the entropy export rate response following experimentally controlled changes in entropy production rate.

This study introduces a model of entropy regulation in humans, with experimental validation by direct comparison with data from a study on healthy young, middle-aged, and older adults exercising under heat stress [88]. The model describes the dynamics of entropy export response to changes in entropy production based on the **hypothesis that the body regulates its entropy export rate according to the current net rate**

of entropy accumulation of the body. Fitting the simple stochastic dynamical model to the data identifies intuitive and potentially clinically relevant health parameters. Our approach offers insights into the stochastic thermodynamics of this and possibly other far-from-equilibrium system.

5.2 Material and Methods

5.2.1 Data collection and experimental design

That data in the present study were chosen from a larger body of work assessing the effect of aging on whole-body heat exchange in young and older males during moderate-intensity exercise in the heat. Full, detailed descriptions of trial procedures and outcomes can be found elsewhere [88]. The joint consideration of heat fluxes and temperature measurements is new to this study. Briefly, heat transfer was measured employing a whole-body direct air calorimeter during and following exercise under heat stress in healthy and physically active males of three different age groups: 11 young (26 $\pm$ 2 years), 11 middle-aged (43 $\pm$ 2 years), and 11 older (63 $\pm$ 3 years) males with similar physical characteristics except for the percentage of body fat, which was positively correlated with age. The experimental design consisted of four 15-min exercise bouts of cycling on an upright seated cycle ergometer at a constant rate of metabolic heat production equal to 400 W. Each bout was followed by a 15-min inactive period with a final recovery period of 60 min. The temperature inside the calorimetry chamber (see figure 2.5) was set to 35 °C and a relative humidity of 20%.

5.2.2 Measurement of heat flows, temperature and entropy flows

The internal heat production rate, or metabolic heat production rate $\dot{Q}_{int}$, was measured continuously using indirect calorimetry. Metabolic energy expenditure $\dot{M}$, which represents the rate of chemical energy liberated from metabolic processes (measured in Watts), is transformed into external work rate (e.g., cycling) and metabolic heat production rate. Metabolic energy expenditure rate was estimated spirometrically by directing the expired air from the participants into a metabolic gas analysis system and measuring the respira-

tory exchange ratio between the rate of carbon dioxide production and the rate of oxygen consumption [37]. In these experiments, the external work rate $\dot{W}$ done on the cycle ergometer was continuously adjusted by changing the cycling resistance to ensure that the targeted values of metabolic heat production remained constant during the exercise periods. From energy conservation and accounting for the work done on the cycle, metabolic energy expenditure ($\dot{M}$) is equal to metabolic heat production ($\dot{Q}_{int}$) added to the work done during the exercise cycle. Indirect calorimetry is regarded as the gold standard, the reference standard and clinically recommended method for accurate measurement of energy expenditure ($\dot{M}$). By measuring $\dot{M}$, and subtracting the work performed, one can calculate the internal metabolic heat [91, 92].

$$\dot{Q}_{int} = \dot{M} - \dot{W} \quad . \tag{5.1}$$

The external heat dissipation rate to the surroundings, denoted by $\dot{Q}_{out}$, was measured by direct calorimetry using a modified Snellen calorimeter [38], which is a state-of-the-art whole-body air calorimeter, as shown in figure 2.5. The two main contributions of heat dissipation by the body are: (1) dry heat loss resulting from heat exchange with the environment via conduction, convection, and radiation at the skin surface, calculated using the temperature difference between the outflow and inflow of air in the calorimeter, and (2) evaporative heat loss resulting from the evaporation of sweat on the skin, calculated from the change in absolute humidity within the calorimeter.

The heat produced internally (i.e., metabolic heat production) is partly dissipated to the environment through various physiological mechanisms (e.g., increase in blood flow to the skin and increase in sweat production), and in the case of insufficient heat dissipation, is partly stored within the body. Generally, the balance between the rate of metabolic heat production and the rate of heat dissipation corresponds to the rate of heat storage $\dot{Q}_{st}$, such that $\dot{Q}_{st} = \dot{Q}_{int} - \dot{Q}_{out}$.

Body temperature, measured during the initial resting period, was estimated using a weighted average of the core temperature (90%) and mean skin temperature (10%), both determined thermometrically. Core temperature was measured by inserting a thermocouple probe into the rectal cavity. Skin temperature was calculated using a weighted average of four skin temperature probes located on the upper back (30%), chest (30%), quadriceps (20%) and back calf (20%). Changes in whole-body temperature during exercise are best estimated by calorimetry using the rate of heat storage (i.e., the balance of heat flow) [37]. Therefore, thermometry was used to obtain the baseline body temperature (prior to exercise) and then temperature changes were calculated using calorimetry.

A two-compartment core-skin entropy flow model was used to derive an expression for the rate of entropy change of the body dS/dt. For a detailed derivation of the entropy flow model, please refer to Brodeur & al [39]. Starting from the entropy balance equation from the body's perspective, which states that the rate of entropy accumulation within the body corresponds to the entropy produced internal minus the entropy exported to the environment, we have

$$\left(\frac{dS}{dt}\right)_{body} \approx \frac{dS_i}{dt} - \frac{dS_e}{dt} \tag{5.2}$$

where dS_i/dt and dS_e/dt corresponds to the rates of entropy production and export, respectively. The negative sign on the right-hand side of equation equation (5.2) indicates that we consider the entropy export rate to be positive for an entropy outflow, which is contrary to the physical conventional, but more practical from an experimental and modeling perspective. Considering that the dominant contributions of entropy change correspond to heat generation and thermal exchange (i.e., neglecting the entropy change associated with the exchange of mass), we obtained the following equations for the rate of entropy production and export:

$$\frac{dS_i}{dt} = \frac{\dot{Q}_{int}}{T_b} \tag{5.3}$$

and

$$\frac{dS_e}{dt} = \frac{\dot{Q}_{out}}{T_s} \tag{5.4}$$

where $\dot{Q}_{int}$ is the rate of metabolic heat production, $\dot{Q}_{out}$ is the external heat dissipation rate (the outflow is positive-definite), T_b is the calorimetry-derived whole-body temperature estimate and T_s is the thermometry-derived mean skin temperature. Note that we do not expect the changes in temperature during work to contribute any extra entropy production since such terms have been estimated [35] to vary as $(dT/dt)/T^2$, and the rate of change of temperature is slow. Thus, entropy changes simply track the slow temperature changes.

All the data and modeling results for the entropy rates dS_i/dt, dS_e/dt and dS/dt in our study are normalized by the resting rate of entropy production, measured as an average of dS_i/dt for each participant during the first 30 minutes of initial rest. This normalization allows for a standardized comparison across individuals and age groups by accounting for baseline differences in entropy production, making it easier to identify and interpret physiological responses to heat stress. This approach enables us to quantify relative changes in entropy rates during exercise and recovery periods while minimizing the impact of inter-individual variations in body composition, fitness level, and other factors that might influence absolute entropy production rates. By using this normalization method, we can more accurately assess the dynamic entropy regulation capabilities of participants in response to exercise-induced heat stress, relative to their baseline metabolic states.

5.2.3 Modeling methods without stochastic noise

In the absence of exercise, there is a discrepancy where the aforementioned normalized dS_i/dt fluctuates near 1, while dS_e/dt is slightly below that value (see figure 5.3 when pre-exercise dS_i/dt is assumed constant). Observations show that this gap, which reflects an imbalance between entropy production and export to the environment, decreases over a time scale of hours as the subjects acclimatize to the heat stress in the calorimeter. This gap also essentially disappears following alternating epochs of exercise and recovery. We hypothesize that the body regulates its current entropy export rate according to the current rate of entropy change. In other words, the body either increases or decreases dS_e/dt proportionally to the current value of dS/dt. Using the entropy balance equation, the differential equation governing this behavior can be written as

$$\frac{d^2 S_e}{dt^2} = \alpha \cdot \frac{dS}{dt} = \alpha \left(\frac{dS_i}{dt} - \frac{dS_e}{dt} \right) \quad , \tag{5.5}$$

which has the general form

$$y'(t) = \alpha \, [x(t) - y(t)] \tag{5.6}$$

where $y(t)$ corresponds to the entropy export rate dS_e/dt and $x(t)$ corresponds to the entropy production rate dS_i/dt. Given that dS_i/dt is fixed by experimental design, $x(t)$ acts as a driving term corresponding to the schedule of alternating exercise and recovery periods. In reality this driving term exhibits fluctuations in time (as we shall see in figure 5.10), and across subjects, and has its own dynamical characteristics, which we investigate further below; in particular, the fluctuations are smaller than for dS_e/dt, and the response times to exercise onset and offset are shorter (corresponding to larger rate constants). The parameter α is interpreted as a responsiveness or adaptation coefficient that quantifies how fast the body can change its current entropy export rate given its current rate of

entropy accumulation. Larger α values lead to a faster response to a change in entropy accumulation. The reciprocal of α corresponds to a time constant. Exponential behavior is expected from a first-order differential equation during periods in which the driving term is time-independent. The analytical solution in such case is given by equation (5.7) and a graphical representation is shown in figure 5.1).

$$y(t) = \begin{cases} (\gamma_3 - \gamma_1)\, e^{-\alpha t} + \gamma_1 & \text{during exercise} \quad (t < t^*) \\ \\ (\gamma_2 - \gamma_3)\, e^{-\alpha t} + \gamma_3 & \text{during recovery} \quad (t > t^*) \end{cases} \tag{5.7}$$

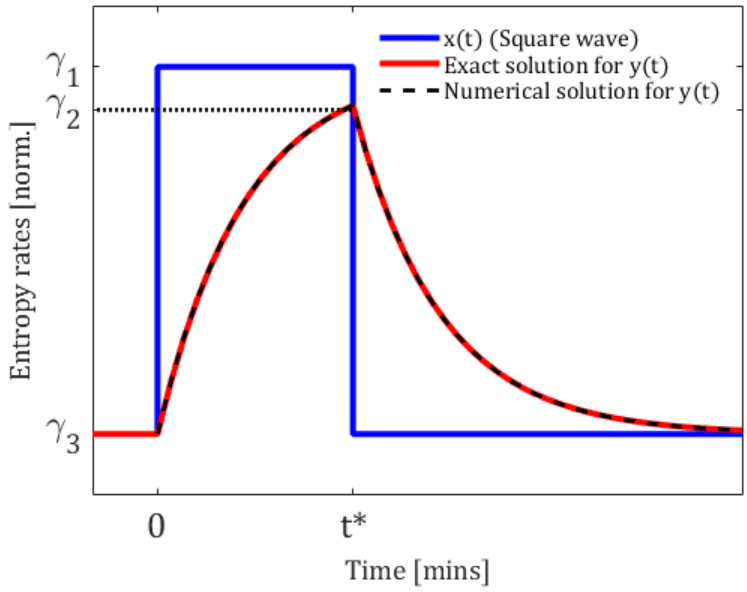

Figure 5.1: Analytical (red) and numerical (dashed black) solutions for the entropy export rate as given by equation (5.6). The entropy production rate corresponds to the driving term $x(t)$, here modeled as a step function (blue). The parameters γ_1 and γ_3 represent the entropy production rate during exercise (fixed by experimental design) and recovery periods, respectively. The parameter γ_2 represents the value of the entropy export rate reached by the participant at the end of the exercise period. The rate constant α for the data and our modeling will take on a different value during the exercise and rest periods.

This approach is equivalent to stating that in the absence of exercise, there is a constant mean rate of entropy production, which causes a baseline or steady state rate of entropy export. But upon exercising, this production rate increases, and the ensuing changes in export can be modeled through linear response theory. Given the noise in the dynamics, the variable y is merely the difference between the steady state and driven ensemble-averaged rates of entropy export (i.e. averages over the noise ensemble), and we neglect higher order terms in powers of the input drive:

$$y(t) \equiv \langle y \rangle_{x=0} - \langle y(t) \rangle_x = y(0)\, e^{-\alpha t} + \alpha \int_0^t x(t')\, e^{-\alpha(t-t')}\, dt' + O(x^2) \tag{5.8}$$

It is known that during intermittent exercise at a fixed rate of metabolic heat production, whole-body heat loss exhibits a slower response during the first exercise period compared to the subsequent exercise periods, leading to a consistent reduction in heat stored in the body during the following exercise periods [151]. This behavior, in which a body that is already warm has less thermal inertia upon reactivation, has been referred to as the priming effect [152]. To account for these expected differences in the dynamics of the entropy export response, we consider here the α exponents to be state-dependent and assign different α values for the following states: initial rest (α) (see also Appendix A), first exercise bout (α_1), first recovery bout (α_2), subsequent exercise bouts (α_3) and subsequent recovery bouts (α_4). In other words, we consider the dynamics of the entropy export response to be different when the body is at rest under heat stress (first 30 minutes of the experiment) and during the first exercise and recovery period, but the same α_3 and α_4 are applied for the all the following exercise and recovery periods, respectively. The model is thus a piecewise linear differential equation whose rate constant depends on the drive $x(t)$, as well as on the history of the drive (i.e. how many exercise bouts have occurred). The best-fitting α coefficients were obtained through a genetic algorithm that optimizes the model's prediction to the experimental data (group averages) based on least-square method. The data analysis was performed using an in-house program written in MATLAB R2023a (The MathWorks, Natick, MA, USA).

5.2.4 Modeling methods with stochastic noise

We studied the noise level in the individual entropy export rate time series by adding an additive noise term to equation equation (5.6). We then obtained the following stochastic differential equation

$$y'(t) = \alpha\ [x(t) - y(t)] + \sigma\, \xi(t) \tag{5.9}$$

where σ represents the noise strength and $\xi(t)$ is an additive Gaussian white noise (the time derivative of a Wiener process) with zero mean $\langle \xi(t) \rangle = 0$ and delta-correlation $\langle \xi(t)\xi(s) \rangle = \delta(t - s)$. Equation (5.9) is interpreted in the Ito sense. This stochastic differential equation was integrated numerically using the Euler-Maruyama method. Since the signal that the model is meant to reproduce is an average over subjects in a given age group, and that the individual noises $\xi_i(t)$ are independent between subjects, the noise strength in the stochastic model will be a factor $1/\sqrt{N}$ smaller than the actual noise affecting individual subjects (see Appendix A.1). Our conclusions below, derived from the analysis of averaged time series, nevertheless hold subject-wise keeping in mind this factor. Below this model is applied to the pre-exercise as well as exercise regimes.

In the pre-exercise regime where $x(t)$ is a constant that counterbalances the entropy export (which can be taken as zero without loss of generality for the calculation of the fluctuation properties), the model becomes an Ornstein-Uhlenbeck process with drift (α) and diffusion σ. Here α has a value specific to this steady state, which is determined by some combination of the asymmetric processes that are more clearly exposed during exercise and recovery. Fokker-Planck analysis then leads to a Gaussian stationary probability density of the entropy export rate $P(y)$ with variance $\sigma^2/(2\alpha)$ and stationary autocovariance function $A(\tau) = A_0 \exp(-\alpha\, \tau)$ where $A_0 = \mathrm{var}(y)$. The values of α and σ can be determined by detrending each individual time series data, computing the population-averaged autocovariance, and fitting it to the formula above to extract A_0 and α, along with their uncertainty using the covariance matrix. The mathematical details and derivations are

shown in the Appendix of this manuscript (section 5.6). This approach enables us to estimate a response time and noise strength of the entropy regulation in the static regime based on the associated fluctuations.

5.3 Results

5.3.1 Experimental evidence for entropy regulation in humans

The basis of our proposed model can be first validated experimentally by recognizing that the left-hand side of equation (5.5) corresponds to the slope of the entropy export rate, while the right-hand side corresponds to the rate of entropy change. Consequently, the value of the slope of the entropy export rate during each 1-min interval can be plotted as function of the rate of entropy change during the same interval. The resulting scatter plot is shown in figure 5.2 (top row) for all age groups. This figure highlights the fact that when the current rate of entropy change is large, that is when entropy is accumulating within the body, the body increases its entropy export rate; inversely, if the rate of entropy change is negative, that is when $dS_i/dt < dS_e/dt$, then entropy export is reduced (i.e., negative slope of dS_e/dt). Rates of change in entropy export were correlated with the current rate of entropy change, with Pearson's correlation coefficients R close to 0.8 for all age groups.

More interestingly, equation (5.5) also implies that an average α coefficient can be extracted from the slope of a linear regression, as shown in figure 5.2. The resulting experimental α-values demonstrate a clear and statistically significant decreasing trend in association with age. This observation suggests that older participants are not simply limited in their maximal entropy export rate, but also in the rate at which they can increase their entropy export. We found that their physiological response to entropy accumulation is systematically and uniformly lower than that of younger participants.

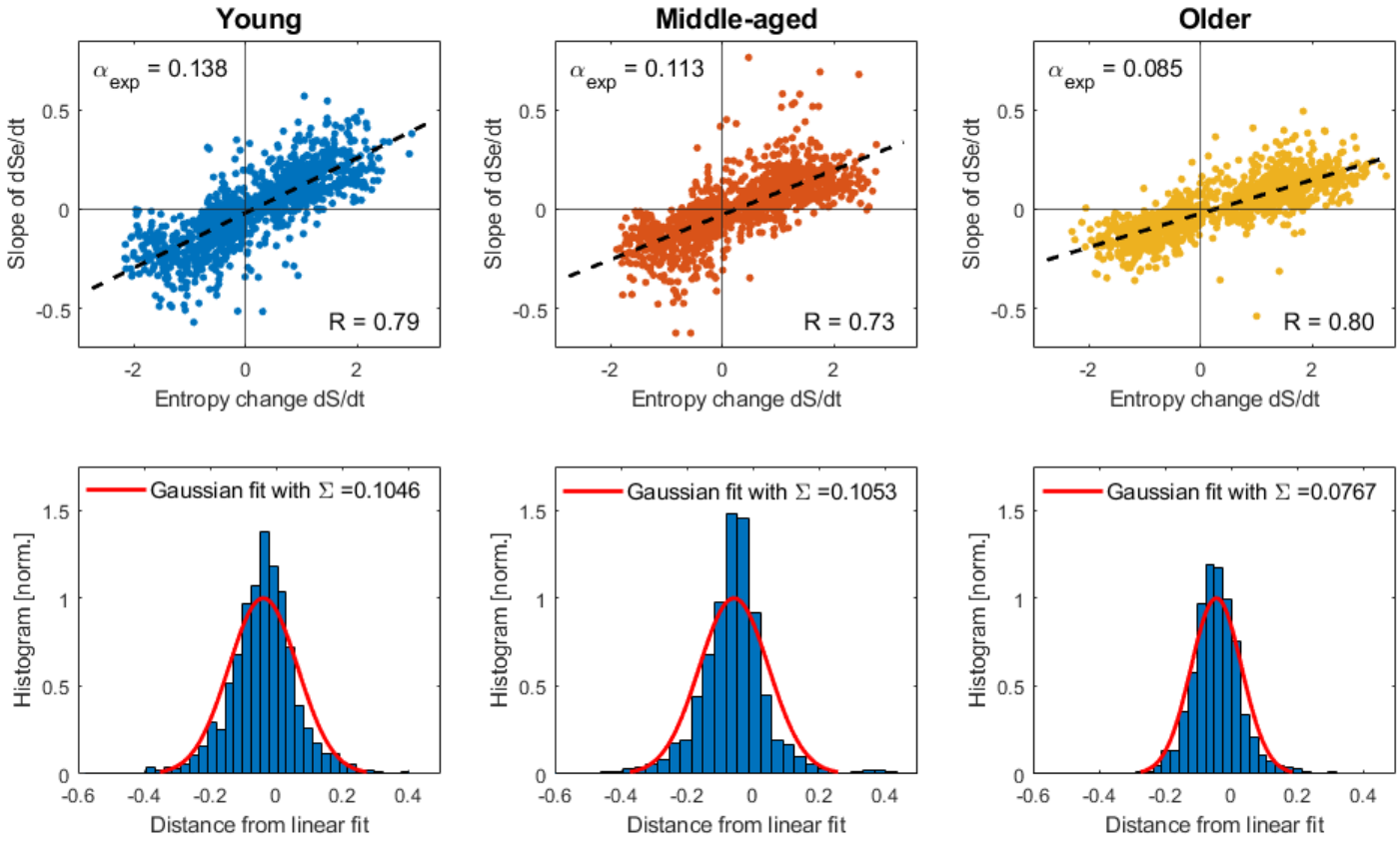

Figure 5.2: **Top row** shows a scatter plot of the slope of the entropy export rate as a function of the entropy change from the experimental data. This plot can be interpreted as one's efficiency at increasing its current rate of entropy export based on the amount of entropy being currently accumulated (i.e., magnitude of dS/dt). As such, we refer to this plot as an adaptation plot considering it provides information on how quickly a participant can adjust its entropy export rate in the face of perturbation. Values of entropy change (x-axis) are positive during exercise (i.e., when entropy in accumulating in the body) and negative during recovery periods (i.e., when entropy export is larger than entropy production). Black lines correspond to a linear regression where the obtained slope value corresponds to the adaptation coefficient α_{exp} and the Pearson's correlation coefficients R are indicated at the bottom right. Adaptation coefficients show a decreasing trend with increasing age, indicating a slower response to perturbation (onset and offset of exercise) with age. **Bottom row** shows the distribution of distances from the linear fit shown in the top row. The standard deviation Σ of the resulting gaussian fit was extracted and used with the calibration curve to obtain the noise strength σ.

5.3.2 Modeling results without noise (to reproduce the average behaviour)

Comparison of the entropy export rates between the experimental data (colored line) and our model (dashed black) is shown in figure 5.3. The resulting modeled entropy export response curves are obtained by first generating an array for the σ coefficients at each time point, then solving equation (5.6) iteratively while optimizing to find the best-fitting σ's through a genetic optimization algorithm. The entropy production rate values used to generate the square wave were obtained by averaging the experimental data of entropy production during the respective intervals. Hence, the height of the plateaus during the different periods can differ slightly in the driving term of equation (5.6) to best replicate the experimental conditions. Overall, the proposed model is in good agreement with the experimental data as it closely captures the dynamics of the entropy export response.

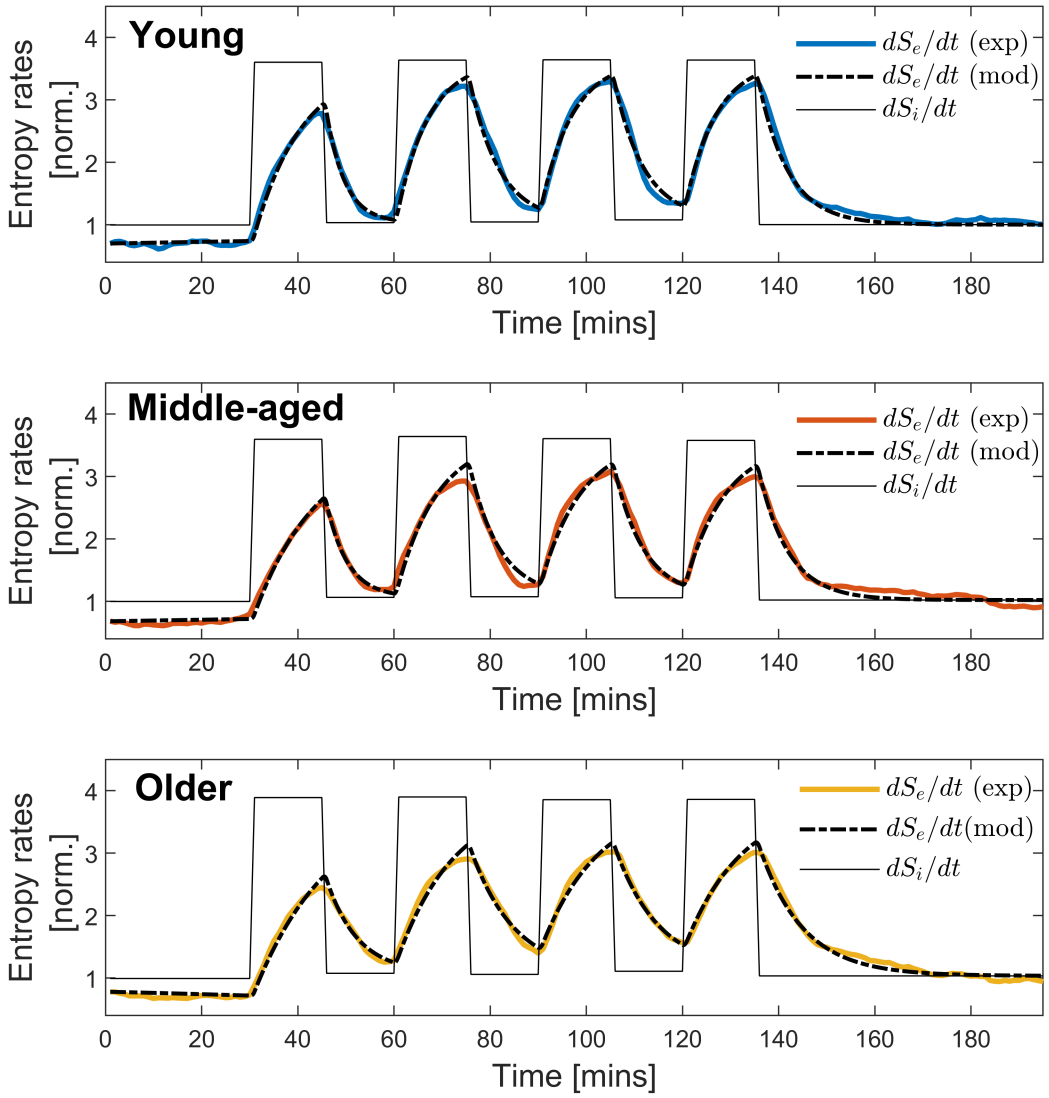

Figure 5.3: **Comparison between experimental data and modeling results.** Comparison of the entropy export rates between the experimental data (solid colored lines) and our model (black dashed lines) in young (26 $\pm$ 2 yrs), middle-age (43 $\pm$ 2 yrs) and older (63 $\pm$ 3 years) males performing intermittent, moderate-intensity exercise in the heat. The resulting model curves are obtained by solving the equation (5.5) and optimizing the coefficients using a genetic algorithm. The best-fitting α coefficients are shown in table 5.1 for all age groups. The entropy production rate dS_i/dt, shown as a solid black line above, corresponds to the driving term $x(t)$ in our model. The entropy rates (i.e., both dS_e/dt and dS_i/dt) were normalized by each individual's resting entropy production rate measured, as an average over the first 30 minutes of initial rest, prior to calculating the group averages.

The best-fitted α values are shown in Table table 5.1 for all groups. The values for $\langle\alpha\rangle$ correspond to weighted averages of all the coefficients α_1 to α_4, with the weight being the total time Δt_i for which the α_i is active, such that $\langle\alpha\rangle = \sum \alpha_i \Delta t_i / \sum \Delta t_i$. Results indicate a clear progressive decrease in coefficient values from young to older age groups that is consistent across individual values during all periods (α_1 to α_4), averaged values $\langle\alpha\rangle$ over all periods and experimental value, indicating a systematic decline in physiological adaptation with aging. Comparison between α_1 and α_3 for all groups indicates that the entropy export response at the onset of the first exercise bout is consistently lower compared to the response of the following exercise periods (i.e., $\alpha_1 < \alpha_3$), which supports the idea that the body can be considered in a different state. On the other hand, we found the α coefficients to be larger during the first recovery period compared to the subsequent recovery periods (i.e., $\alpha_2 > \alpha_4$). We also found that middle-aged participants, while being slower to respond to the increase in entropy production rate for the second exercise period and onward compared to their younger counterparts as indicated by a smaller α_3 value, have a similar value for the entropy export response during the recovery periods (i.e., α_4). Overall, these results suggest a reduced adaptative capability associated with age and that impairments in the entropy export response are apparent both during exercise and recovery.

Groups	α_1 Exc. 1	α_2 Rec. 1	α_3 Exc. 2-4	α_4 Rec. 2-4	$\bar{\alpha}$	α_{exp}
Young	0.0990	0.258	0.151	0.157	0.159	0.138 ± 0.003
Middle-aged	0.0763	0.211	0.115	0.155	0.136	0.113 ± 0.003
Older	0.0695	0.140	0.098	0.102	0.100	0.085 ± 0.002

Table 5.1: Comparison of the model and experimental adaptation parameters α.

5.3.3 Modeling results with noise

The previous results relate to the deterministic model (given by equation (5.5)) that accurately describes the average behavior of the entropy export response within a population

(i.e., different age groups). Now, the objective of transforming the deterministic model into a stochastic differential equation provided by equation (5.9) is to characterize the statistical fluctuations (quantified by the noise strength σ) in the individual time series of entropy export rate. Figure 5.4 shows the resulting individual trajectories (colored lines) and average trajectories (black lines) when solving the stochastic differential equation (5.9) for increasing noise strength σ. For small σ, all the individual trajectories overlap and tend to the model solution without noise. As σ increases, greater fluctuations are observed when the system nears the stationary state, that is, during the initial rest and at the end of every exercise and recovery periods. Mathematically, this is explained by the fact that near equilibrium, the first term in equation (5.9) becomes small and thus the noise term dominates. On the other hand, when the body is further from the stationary state (i.e. onset of exercise and recovery), fluctuations are comparatively small as the first term then dominates.

The intuition that led us to quantify the noise in the entropy export response came from the observed differences in the spread of the data points around the linear regression in the adaptation plots. As shown in the second row of figure 5.4, we modeled the entropy export response using equation (5.9) with a known and unique α=0.13 min^{-1} for increasing values of σ. We observed that the thickness of the distribution of points increases with increasing noise strength σ in modeled responses. The objective is then to build a calibration curve that allows us to establish a relationship between the data spread and the value of noise strength. To accomplish this, we detrended the adaptation plot such that the slope of the linear fit becomes zero, and then made a projection of the data distribution on the y-axis. The resulting distribution, shown in the third row of figure 5.4, thus allows us to quantify the spread of the data points which is assumed to come from the noise.

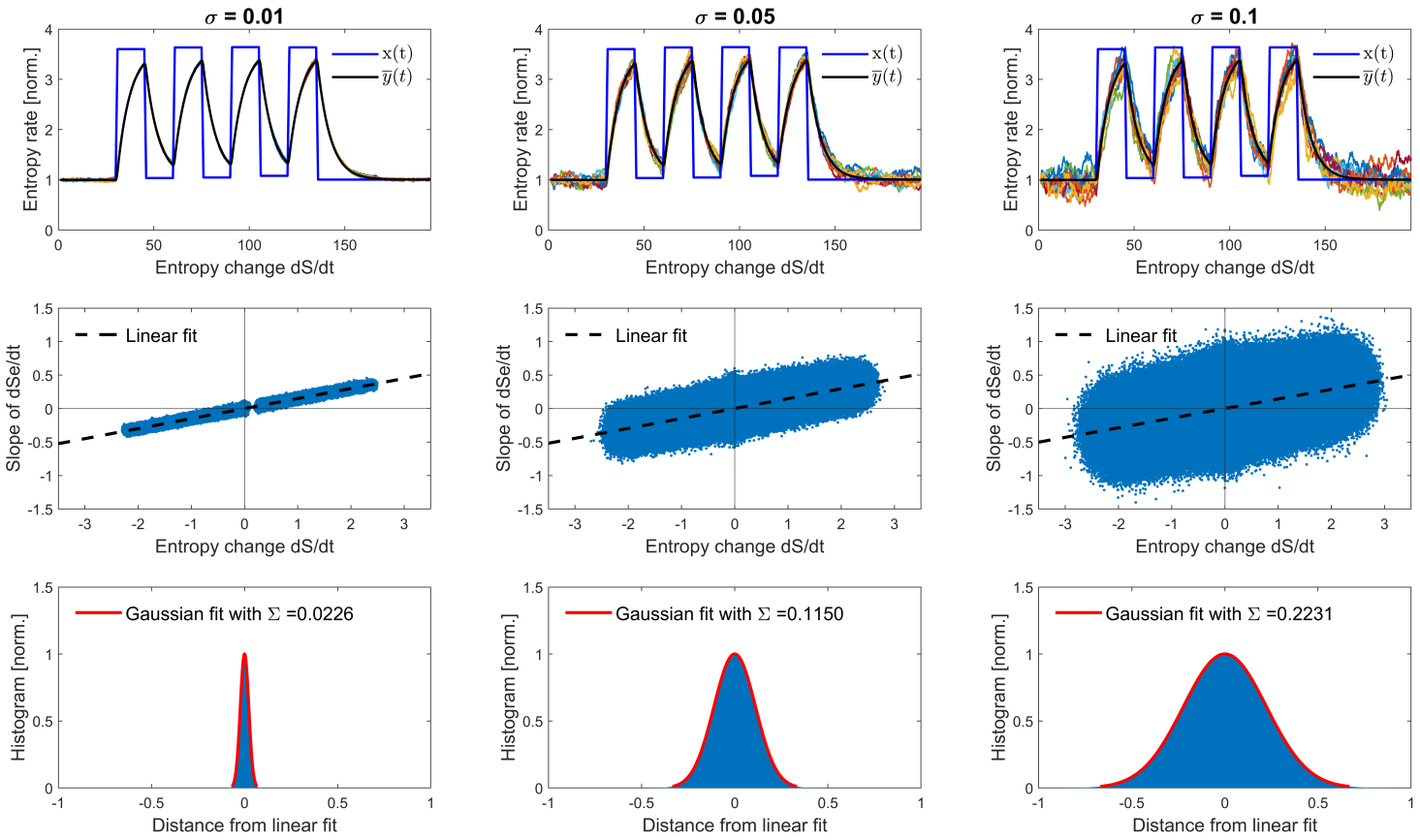

Figure 5.4: Effect of the stochastic noise on the dynamics of the entropy export response. The top row shows the modeled entropy export response for increasing noise strength with $\sigma = 0.01$ (low noise), $\sigma = 0.05$ (moderate noise) and $\sigma = 0.1$ (high noise). The colored lines correspond to individual trajectories of entropy export response (we show 10 trajectories selected at random out of the 5000 individual trajectories that were simulated), the black lines correspond to the group average of the 5000 trajectories of the entropy export response, and the blue lines correspond to the entropy production rate (i.e., the driving term $x(t)$ in the model). The modeled curves were obtained by using a single value of $\alpha = 0.15$ min^{-1} for all the exercise and recovery periods. The middle row shows the scatterplots of the slope of the entropy export response as a function of the entropy change as calculated from equation (5.2). As the noise strength increases, there is a noticeable thickening of the linear trend, which can be quantified by removing the linear trend (i.e., detrending) and projecting the distribution on the y-axis. The standard deviations of the resulting distributions, shown in the bottom row, are shown to increase linearly with noise strength (see figure 5.5 for the calibration curve).

Given that we used additive Gaussian white noise, the resulting distributions from modeled time series are also Gaussians. We found a linear relationship between the standard deviations of the resulting Gaussian distributions, which quantify the data spread in adaptation plots, and the noise strength σ (see figure 5.5 where this linear relationship between both quantities is used as a calibration curve). Interestingly, the calibration curve is independent of the α value used to generate the modeled response. The same procedure was applied to experimental data to calculate the standard deviation on the detrended distributions and obtain the noise strength σ for all age groups. Table 5.2 shows the resulting noise strength values, which were analyzed independently for the initial rest (static phase) using a Fokker-Planck analysis (see Appendix A.2) and the alternating schedule of exercise and recovery (dynamic phase) using the calibration curve method described above. It should be noted that the addition of noise in the model does not significantly affect the determination of the α coefficients in the region of smaller noise strength values obtained, as shown by figure 5.5 With this distinction between the static and dynamic phase, we expect the system's dynamics to be quantitatively different in both phases, and thus we allow the noise strength values to be different.

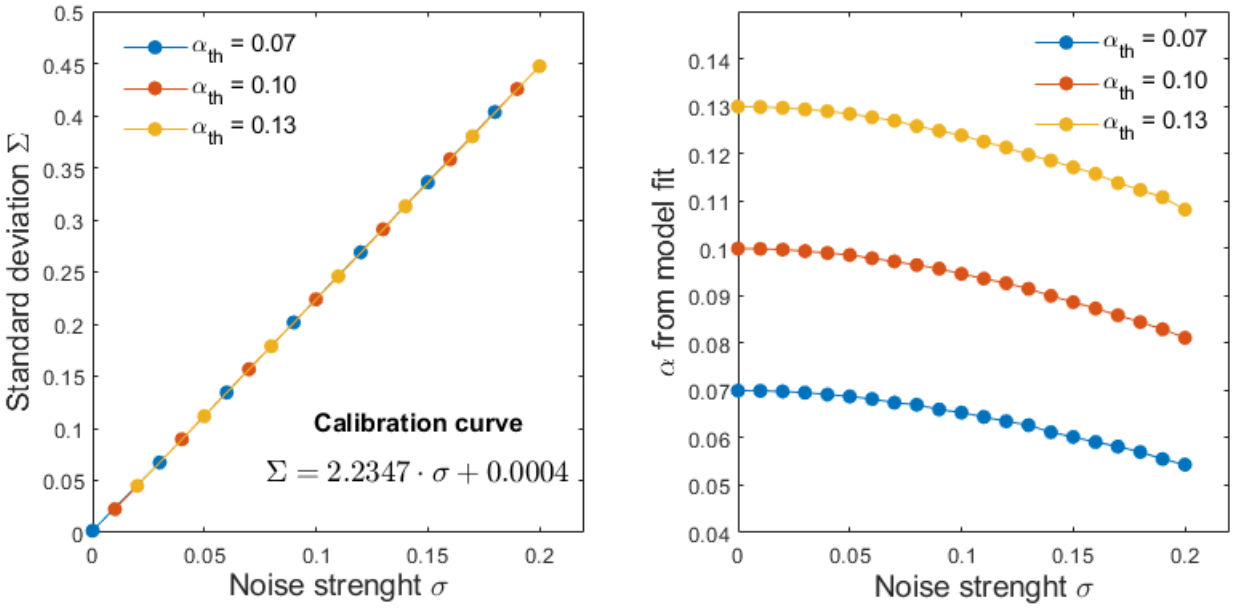

Figure 5.5: **Calibration Curves.** The left panel shows the calibration curve used to obtain the noise strength from the calculated standard deviation of the experimental time-series following the detrended distribution process. The calibration curve is conveniently independent of the α value, thus allowing direct comparison for all entropy export response. The right panel shows the noise dependency of the α value obtained from fitting the model knowing the theoretical value of α inputted. We observed a monotonous decrease in the calculated α value as the noise strength increases. As expected, the calculated α value retrieves its theoretical value as the noise strength tends to zero.

Firstly, let's consider the dynamic case where the noise values were obtained using the calibration curve method. We found that the young and middle-aged participants exhibited a similar level of noise of $\sigma = 0.047 \pm 0.001$ min$^{-1/2}$ and $\sigma = 0.047 \pm 0.002$ min$^{-1/2}$, respectively, whereas the older participants showed a significantly lower noise strength of $\sigma = 0.034 \pm 0.001$ min$^{-1/2}$. The uncertainties on the values of noise strength have been obtained from the bootstrapping method and statistical significance was confirmed using a one-way ANOVA test. Finally, it should be noted that the intergroup differences observed for noise strength is independent of the choice of normalization for the entropy rates;

differences remained even if the entropy rates were normalized by the participant's weight, body surface area, or no normalization was applied.

Secondly, let's consider the static case where the adaptation coefficients α and noise level σ were obtained from the Fokker-Planck analysis. The top row of figures 5.6, 5.7 and 5.8 show the individual raw and detrended time series for each subject in each age group, while the bottom row displays the individual as well as averaged autocovariances. The exponential behaviour of the correlation between successive points is apparent in these plots, and thus we are able to directly recover an average parameter α from the static data, in contrast to the differing rates during exercise and recovery periods in the dynamic regime. The parameters obtained from this method are shown in table 5.2. Qualitatively, and even quantitatively, they are generally close to those found during the subsequent dynamic exercise phase of the experiment, although the latter were estimated using a different technique. The reason for this difference is the difficulty of performing a Fokker-Planck analysis on an OU process driven by a square wave process that causes increases and decreases in the entropy production. A further complication that precluded this approach is the fact that the drift coefficient changes between the exercise and recovery phase. A thorough analysis of Fokker-Planck type in the dynamic regime is well beyond the scope of our study.

We first notice in the static case that the same qualitative behaviour is seen for this coefficient, namely, that it is decreases monotonically with age. Thus, the conclusion that age slows down the response of the entropy export also comes out of the static analysis. The noise levels also compare favorably to the dynamic case, with very close values for the young and middle-aged groups. However, in contrast to the dynamic case, the noise level is now 23% larger for the older subjects, rather than smaller. Older age thus increases the baseline fluctuations but reduces their strength when the system is adapting to the successive exercise and recovery phases. One expects the variability to be less visible during the dynamic phases as a significant portion of the response is driven by the "stimulus" (exercise). Nevertheless, the underlying variability appears to be relatively smaller or "quenched" by the exercise regime in the older subjects, suggesting a property that is a

correlate of the diminished capacity to export entropy.

Table 5.2: Results for the noise strength σ for the different age groups during the static phase (initial rest) and dynamic phase (exercise and recovery periods).

Groups	**Static Phase**			**Dynamic Phase**
	α [min^{-1}]	σ [min$^{-1/2}$]	η [nd]	σ [min$^{-1/2}$]
Young	0.20 ± 0.09	0.061 ± 0.002	-0.004 ± 0.002	0.047 ± 0.001
Middle-aged	0.13 ± 0.03	0.057 ± 0.001	-0.007 ± 0.002	0.047 ± 0.002
Older	0.11 ± 0.06	0.0737 ± 0.0005	-0.013 ± 0.001	0.034 ± 0.001

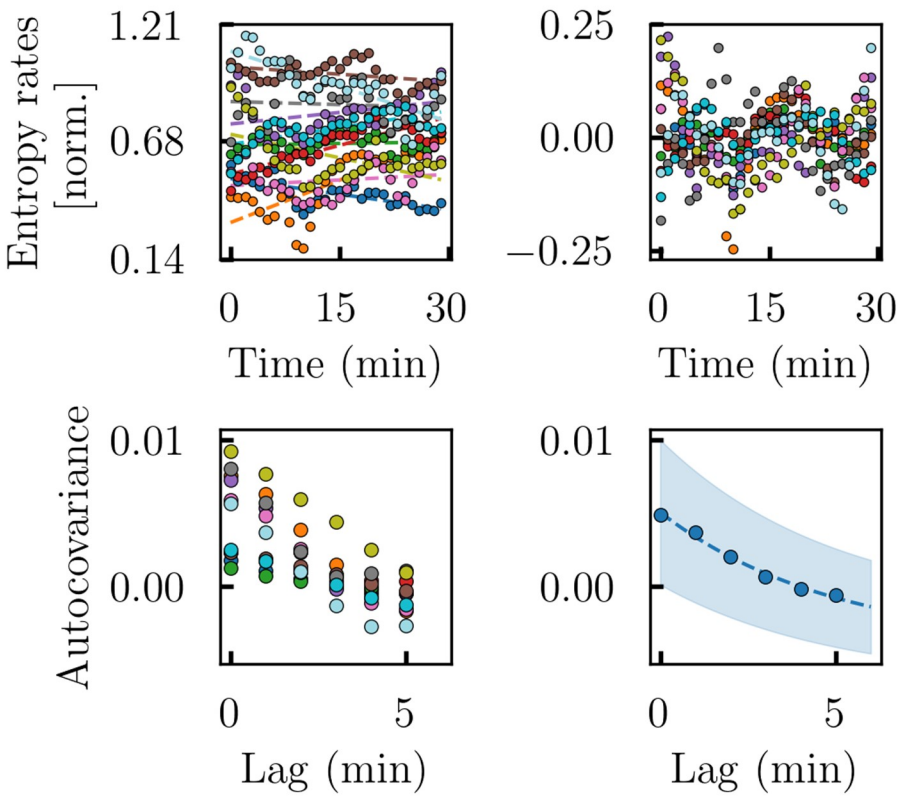

Figure 5.6: Ornstein–Uhlenbeck (OU) process parameters estimation during resting phase for the young age group. **Top panels**: The participants' entropy export rate time series (top left). The detrended time series (top right) were obtained by using linear regression such that they are all centered around 0. **Bottom panels**: Autocovariance of each participant (bottom left) is computed using the detrended samples and then averaged over all participants of the age group (bottom right). The fit to recover the parameters of the OU process is made on the group averaged autocovariance. The light blue area is the error on the autocovariance due to fitted parameter uncertainty. It is computed using the total differential of equation (5.17). As is standard practice, lags are limited to a fifth of the data set to avoid larger statistical fluctuations in correlation due to decreasing overlap between the time series and its lagged version.

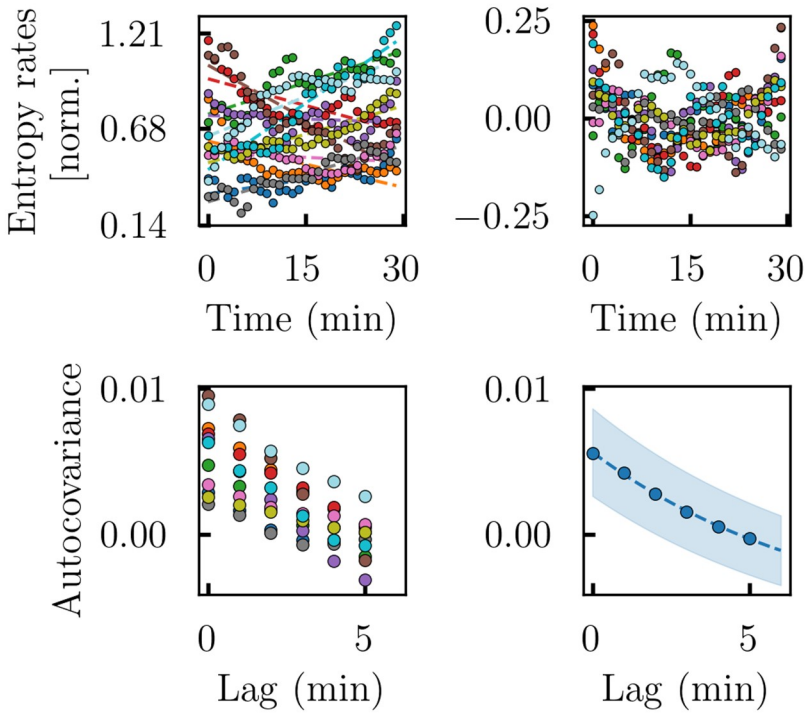

Figure 5.7: Ornstein–Uhlenbeck (OU) process parameters estimation during resting phase for the middle-aged group. **Top panels**: The participants' entropy export rate time series (top left). The detrended time series (top right) were obtained by using linear regression such that they are all centered around 0. **Bottom panels**: Autocovariance of each participant (bottom left) is computed using the detrended samples and then averaged over all participants of the age group (bottom right). The fit to recover the parameters of the OU process is made on the group averaged autocovariance. The light blue area is the error on the autocovariance due to fitted parameter uncertainty. It is computed using the total differential of equation (5.17).

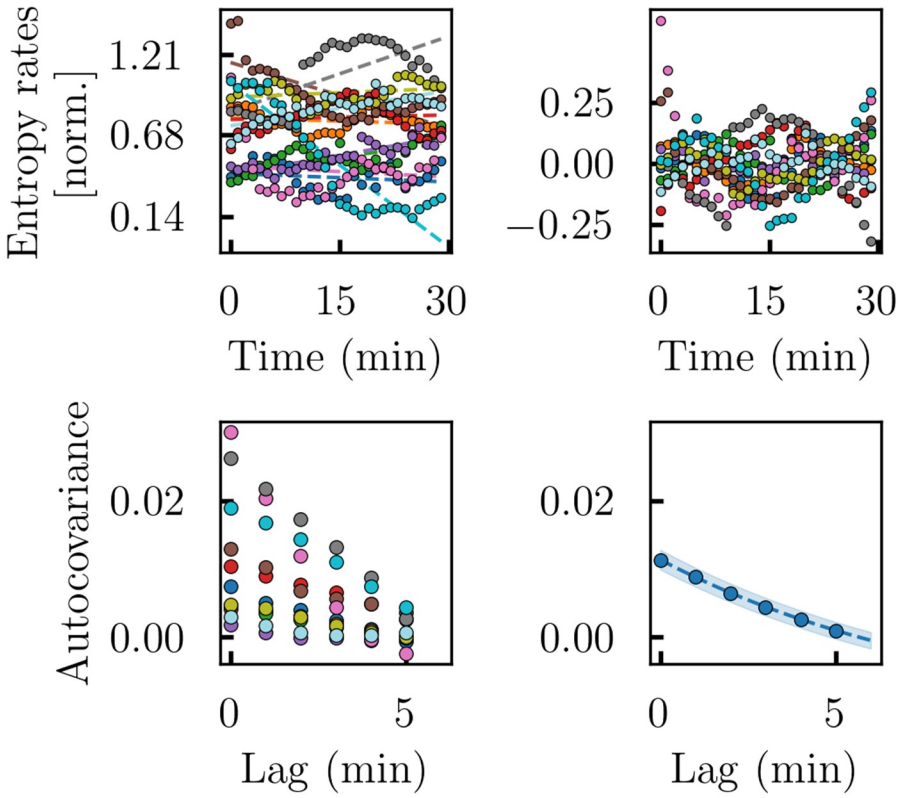

Figure 5.8: Ornstein–Uhlenbeck (OU) process parameters estimation during resting phase for the older age group. **Top panels**: The participants' entropy export rate time series (top left). The detrended time series (top right) were obtained by using linear regression such that they are all centered around 0. **Bottom panels**: Autocovariance of each participant (bottom left) is computed using the detrended samples and then averaged over all participants of the age group (bottom right). The fit to recover the parameters of the OU process is made on the group averaged autocovariance. The light blue area is the error on the autocovariance due to fitted parameter uncertainty. It is computed using the total differential of equation (5.17).

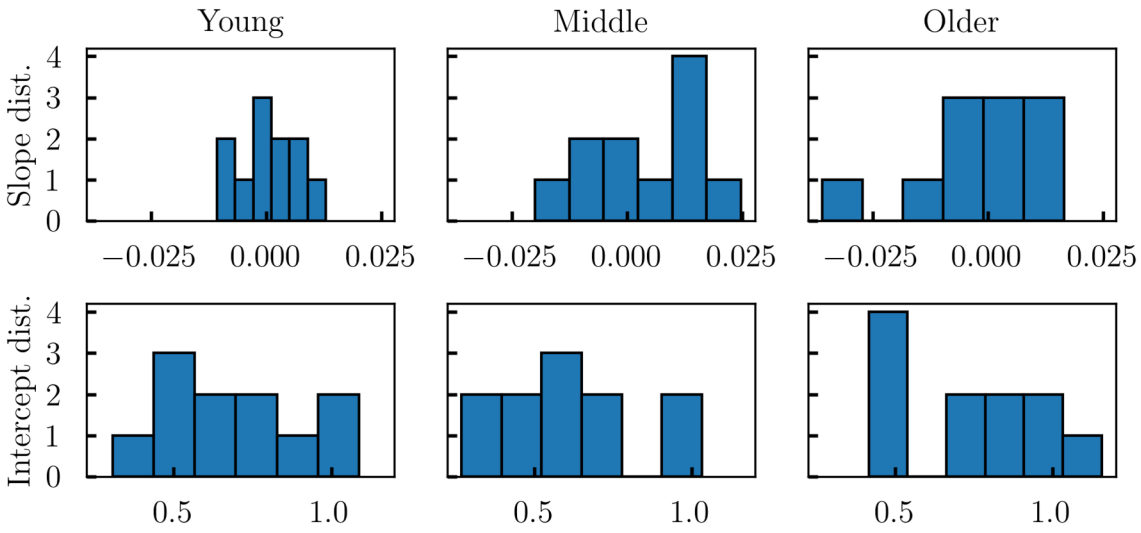

Figure 5.9: Distribution of linear trend parameters for each age group. In all three groups, 5 participants have a negative slope. The distributions are similar amongst all age groups, with the exception of the slope distribution for the young participants which is narrower.

5.4 Discussion

We provide a novel, simple yet reasonable model of the entropy export response for humans exercising under heat stress at fixed metabolic heat production rates. Comparison between our model and experimental data supports the hypothesis that humans regulate their rate of entropy export to maintain entropy balance in a way analogous to a restoring force while exercising under heat stress. The model coefficients α_i introduced here correspond mathematically to inverse time constants characterizing the exponential decay of the entropy export response to the stationary state (i.e., increasing or decrease entropy export until matching the entropy production). These coefficients can be interpreted as adaptation coefficients describing the body's efficiency at changing its current rate of entropy export. Results indicate a clear trend of decreasing α coefficients with increasing age. Furthermore, introducing additive Gaussian white noise in the model revealed that

older participants have a lower noise strength compared to their younger counterparts during physical exercise and their following recovery periods, which suggests a lower level of biological variability. In contrast, the noise strengths were found to be larger during rest compared to the alternating exercise/rest regime for each age group.

5.4.1 From the first law to the second law of thermodynamics

While thermoregulation studies are based on the First Law of Thermodynamics, i.e. the conservation of energy, the inefficiency associated with the conversion of chemical energy (low entropy) into mostly heat (high entropy) relates to the Second Law, which describes a system's natural tendency toward entropy increase. The analyses of heat balance and entropy balance thus offer complementary perspectives on health and fitness, with entropy balance being potentially valuable to deepen our understanding of biological systems. Heat flow analysis recognizes the importance of thermoregulation in homeothermic organisms, whereas entropy analysis attempts to bridge physiological considerations to the realm of non-equilibrium thermodynamics in which the organisms are viewed as dissipative structures. Within the latter framework, entropy production is a necessary condition for self-organization (maintenance and healing), while entropy export is required to prevent internal entropy accumulation.

Although the entropy perspective is conceptually different from the heat perspective, it is quantitatively quite similar in the context of our study since the main contributions to entropy production and export come from heat production and transfer (either internally between compartments or with the external environment). Human body temperature is highly constrained, typically between 36-38 °C up to a few degrees higher during greater heat stress. Thus, entropy rates obtained by dividing heat production and heat loss by core and skin temperatures in degrees Kelvin thus undergo relatively small changes. The analysis of entropy fluxes is thus numerically close to that of heat fluxes in this context. As a consequence, our modeling efforts are also relevant to the traditional perspective of thermoregulation [78]. Nevertheless, our setup enables us to make statements about entropy rates even when the body is driven away from its normal steady state including in

its core and skin temperatures.

While we observed clear differences in the dynamics between young and older participants, the mechanistic explanation for the decrease in adaptation associated with age remains to be elucidated. For example, we observed that older participants decrease their entropy export rate more slowly at the onset of the recovery periods, as indicated by consistently smaller values of α_2 and α_4, even though they accumulated more entropy during the exercise periods due to their impairment in entropy export [39]. This slower decrease in entropy export can be explained two ways: (1) they reduce their entropy export rate more slowly after exercise as a way to compensate for the additional entropy accumulated during the exercise; alternately, or in addition, (2) they are simply slower at adjusting their dynamics in both directions (i.e. onset of exercise and onset of recovery). Further investigation is needed to identify the most accurate explanation and explore the potential physiological mechanisms behind the observed differences in the dynamics of the entropy export response between older and younger individuals. For example, it may be related to the metabolic cost of maintaining an elevated physiological activity to sustain the active dissipation of heat and entropy export to the environment. Increasing disruption in the hierarchical regulatory systems with age are likely at play while involving genetic and other factors [130, 149].

5.4.2 State dependence of the model

Our modeling approach is based on the notion that the body can effectively be considered in different "states" over the course of the experiment: the pre-exercise quasi-steady state phase in which the subjects are still slowly accommodating to the environment of the calorimeter; the first exercise bout without warm up; and the subsequent exercise phases. These exercise phases can be viewed as slowly evolving steady states, as seen in the entropy and temperature time series. In addition, the model distinguishes between the exercise phase per se, i.e. the physical exertion, and the recovery phase; different physiological control mechanisms are at play in each phase. Accordingly, and for simplicity, exercise bouts have been divided into an exertion state and a recovery state. This allows us to

assign a different adaptation coefficient α_i to each state. The dynamics of the entropy export response over specific exercise and recovery periods is thus governed by discrete state-dependent coefficients α_i where transitions between the different states are assumed to be instantaneous. Alternatively, one could think of the α coefficient to be a time-dependent function based on the history of previous events, with explicit dependence on recent events (e.g. exercising right after warming up) as well as more distant or sustained events (e.g., regular exercise and healthy habits).

We believe the state-dependent view provides a simpler and biologically plausible description of the dynamics if the exercise periods are kept relatively short (< 30 mins), such that each period encapsulates a single state during exercise and another during recovery. Mechanistically, the faster dynamical response in entropy export at the onset of exercise periods (i.e. larger α) when the body has been warmed up by previous exercise could originate, at the whole-body level, from the pre-activation of heat loss mechanisms (e.g. increased peripheral blood flow), as well as the increased metabolic activity which makes the energy more readily available for conversion (e.g. faster recruitment of biomolecular machinery) [153, 154].

The model assumes a unidirectional coupling between the entropy export response (dS_e/dt) and the entropy production rate (dS_i/dt). As shown in equation (5.5), changes in the entropy export rate depend explicitly on the entropy production rate. A relation in the opposite direction is also conceivable; such bidirectional coupling has not been modeled at this point and could be explored in the future. For example, one could expect that for smaller rates of entropy export (e.g., during rest or low-intensity exercise), the body can effectively dissipate its excess heat without a massive mobilization of thermoregulatory mechanisms, a situation which could be described as a semi-passive return to the stationary state. In contrast, for larger rates of entropy export (e.g., during high-intensity exercise), the body must actively engage numerous regulatory mechanisms to ensure that the excess heat produced internally is properly directed to the skin region and eventually dissipated to the environment. Consequently, the physiological and metabolic requirements associated with a larger dissipation of heat and export of entropy bear a greater energetic cost which,

in turn, lead to an increase in metabolic heat production and entropy production. In the present experiment, metabolic heat production is fixed during the exercise periods and, therefore, the entropy production rate is also highly constrained. However, it would be interesting to study the bidirectional coupling between entropy production and export rate in an experimental design where both quantities can vary freely.

The entropy export response was generated by inputting an array of randomly generated α values (α_1 to α_4) into equation (5.5), solving this differential equation using these α values for their respective exercise/recovery periods and optimizing the response's fit with experimental data by adjusting the α values through a genetic algorithm. This approach ensures that the resulting time series for the entropy export rate does not exhibit discontinuities at the transition between the different periods (exercise to recovery and vice-versa) (see also figure 5.12). Indeed, solving the model piecewise on the different periods leads to discontinuities at the end of each period because it is unlikely that the last value of a period matches the starting value of the following period. There is also a relatively small delay in the response that has not been model explicitly. Our continuous approach thus models a dynamical response rather than simply characterize the exponential decay using the experimental data, but this does come with an interpretive downside: the α value of a specific period or state depends slightly on the dynamics of the previous and the following periods through its starting and ending points. While it is arguably good that the present α value depends on the previous period as a mean of taking the body's history into account, it is not intuitive that the body's response also slightly depends on events that are yet to come (i.e. the following period).

5.4.3 Differences in dynamics during rest and physical exercise

The body is close to but not quite in a steady state during the initial resting period prior to the onset of the first exercise. Indeed, Meade & al. found that heat balance is achieved after 2.4 hours and 2.6 hours for young and older adults respectively [155]. The dynamics of the entropy export response exhibits significant fluctuations in spite of a slow deterministic approach to a stationary steady state of entropic balance. Our detrending

analyses in figures 5.6, 5.7 and 5.8 in fact show trends with positive and negative slopes. The dominance of noise, i.e. of the diffusion term, is expected when a dynamical system is around a steady state that corresponds to the fixed point of the deterministic dynamics. Table 5.2 shows in fact that the noise strengths under these conditions are between 20 and 50% higher than during the exercise regime. Upon entry in the calorimeter chamber and for the first 30 minutes, the imbalance between entropy production and entropy export leads to entropy accumulation with the body. This result suggests that initially the body adjusts its entropy export rate on a much slower timescale when subjected to environmental heat/entropy stress compared to its faster response during exercise-induced heat/entropy stress. In other words, the body appears to react more strongly if entropy accumulation originates from the increase in internal entropy production rate compared to a negative entropy export rate (i.e., inflow of entropy from the environment).

The comparison of the two analyses of noise and time constants for the static and dynamic regimes reveals a good consistency, where numerical values are at times quite close while others differ at most by about 40%. This is so even though these two regimes likely involve a number different biophysical entropy-generating processes, and that the analyses to extract the parameters are quite different. We note that the error for the parameter alpha for the young group in the static regime is relatively large compared to the other groups. However, the data for that group reveal more significant deviations from exponential correlation; in contrast the fits give more accurate values for the noise strength.

Our covariance analysis during this rest period was able to extract the rate constants for the dynamics of the different age groups in the absence of forcing by the exercise regime (i.e. for $x = 0$). These values where in the range of those for the later exercise and recovery phases. The picture that emerges is again of an entropy regulation that acts like a restoring force in a quadratic potential around a fixed point $y = 0$, which is precisely the same as for an Ornstein-Uhlenbeck process. This analogy carries over to the driven case with comparable parameters.

5.4.4 Thermodynamics and regulatory behavior in living systems

The analysis of stochastic noise in the entropy export response aligns with the well-established concept of biological variability inherent in physiological systems [156, 157]. While our deterministic model (i.e. equation (5.5)) effectively captures the average behavior of entropy export rate, incorporating a stochastic element provides a more realistic representation of individual responses. This biological variability can stem from numerous sources, including fluctuations in metabolic processes or in the autonomous nervous system response [158]. Similarly to the complexity metrics used to analyze other physiological signals [157], such as heart rate variability for cardiovascular fitness [159] or variability in electroencephalography to predict epilepsy events [160], the parameter σ for noise strength introduced here could serve as a quantifiable measure of the individual's biological variability. Through this lens, the lower noise strength observed in older participants during exercise, which can be interpreted as a loss of biological variability, suggests a potential age-related reduction in thermoregulatory resilience and thus greater vulnerability to heat and entropy stress.

It should be noted that the values of dynamical noise strength for the export dynamics obtained here are slightly overestimated, since they include the noise in the experimental time-series of dS_i/dt, i.e. of the driving term. Furthermore, our model conflates all sources of fluctuations including measurement noise into one compound dynamical noise term. Heat flows and local temperature variables have their individual sources of fluctuations, which may overlap and thus be correlated. Our experimental design does provide measures of these variables, and in principle one could try to tease apart their deterministic and stochastic components in future work. Likewise, we have made the common simplifying assumption that the compound fluctuation is Gaussian white noise, although in reality, it likely has an average finite correlation time of many seconds. It can nevertheless be seen as quasi-white, compared to the slow time scale of the heat and temperature responses. Energy fluctuations of equilibrium systems have also been viewed through the lens of temperature fluctuations even in the canonical ensemble [161], and this picture may be all the more useful in the far-from-equilibrium context of spatially distributed biological

systems.

While greater noise strength may indicate greater biological variability when the system is perturbed out of a steady-state, fluctuations may play the opposite role when the system is near or in a steady-state. Indeed, at small scales, thermodynamic uncertainty relations in stochastic thermodynamics showed that fluctuations in a current J (e.g. heat flow in a thermal gradient, or entropy production itself which is the most relevant current in our case) is bounded by the system's entropy production Φ, for non-equilibrium steady-states, such that [64]

$$\frac{\langle J^2 \rangle}{\langle J \rangle^2} \geq \frac{2k_B}{\Phi} \quad . \tag{5.10}$$

This equation can be interpreted as follows: the larger the entropy production Φ is, the smaller are the relative fluctuations $\langle J^2 \rangle$ within the system. This thermodynamic uncertainty relation was derived within the framework of large deviation theory for jump processes and therefore was not intended for large, complex, far-from-equilibrium systems such as biological systems. Direct evaluation of this expression in our context, using the steady state entropy production data that precedes the exercise bouts, yields $5\text{x}10^{-3}$ for the ratio of entropy production variance to the square of its mean, and of the order of 10^{-22} for the right-hand side evaluated with Φ as the average entropy produced during these 30 minutes. Given the scale of the Boltzmann constant, it is clear that this inequality is satisfied, but not very informative for the complex macroscopic dissipative structure that is the human body.

Nonetheless, the idea of stability through production of entropy may be a reasonable hypothesis and guiding principle that could help understand physiological processes, based on the flow of energy and matter, within the framework of stochastic thermodynamics. Interestingly, during the initial rest where participants are near a dynamical steady state, we found a larger noise strength value for older participants compared to the young and

middle-aged participants. Given that (1) a lower noise strength implies a smaller variance on the entropy export rate (i.e. l.h.s numerator of equation (5.10)) and (2) we previously found that older males have a lower basal entropy production rate compared to their younger counterparts (i.e. smaller entropy production Φ) [40], our results are very well consistent with equation (5.10).

Our first-order asymmetric (and piecewise linear) model of entropy control can be seen as a linear overdamped Langevin equation, with a stochastic driving force acting directly on the entropy rates rather than on the forces (such as drag forces) that drive the system out of equilibrium (such as a sheer force, i.e. a flow gradient in the context of fluids) [54, 146]. It is tempting to cautiously push the analogy further, and relate such a force to the excess work that causes non-equilibrium contributions, a kind of biological drag force with deterministic and stochastic components. We note however that far from equilibrium theories require precise knowledge of the probability densities of the relevant variables, which is difficult and perhaps impossible to properly estimate for biological systems at this point.

Recent developments in the field of stochastic thermodynamics have extended classical thermodynamics to nanoscale, non-equilibrium stochastic systems, providing a framework for quantifying energy, heat and work at the level of individual trajectories (e.g. probabilistic transitions between different states) [162–164]. In this microscopic realm where stochastic fluctuations are an integral part of the dynamics, the entropy production of a system is not limited to heat exchanges with a thermal reservoir, but also includes a contribution from the flow of information $\dot{I}$. For example, when a system is decomposed into coupled subsystems X and Y (e.g. bipartite system), information flow $\dot{I}_y$ can be understood as the rate at which the dynamics of a subsystem Y increase the mutual information $I[X, Y]$ between the two subsystems.

In this context, given that information flow corresponds to a legitimate form of free energy, it also constitutes a thermodynamic resource from which work can be obtained. As discussed by Leighton and Sivak [163], this implies that the information flow can allow a

subsystem X to *borrow* free energy from the correlation it builds with another subsystem Y, effectively reducing local heat dissipation (thus minimizing local entropy generation). In such a case, it appears that subsystem X is violating the second law by converting heat from its environment directly into output work. However, when accounting for the information flow, the validity of the second law remains. Information flow can be used by molecular machines to optimize their efficiency, especially in the case of isothermal machines which cannot rely on temperature differences to perform work, but instead support their functions using information flow [163].

The information flow could be the basis for entropy accumulation at the cellular and subcellular levels. While our study is interested in the macroscopic entropy dynamics, we must recognize that molecular machines are ultimately responsible for most of the conversion of free energy fueling the cellular functions. In a similar spirit to the transition from Boltzmann's statistical description to Clausius macroscopic description, it would be interesting to further study how information flow is involved in the entropy dynamics of the whole body through the interaction of its subsystems (i.e. organs). Concretely, this approach could provide a more theoretical background to the field of variability analysis of physiological signals [156, 157].

5.4.5 Limitations and future work

Our model has several limitations. First, given that the entropy production rate is modeled by an idealized square wave (i.e., no latency), the model assumes instantaneous transitions between the different states (exercise/recovery), which is not physiologically accurate. Experimentally, it takes between 2 or 3 minutes to reach and stabilize the targeted metabolic heat production rate. As the entropy production rate increases during the few first minutes of exercise, the entropy export rate also increases, but at a slightly slower rate compared to the model's prediction, leading to a slight underestimation for the α coefficients. Alternatively, the deviation from the square wave approximation for the entropy production rate during the first few minutes of exercise periods can be modeled by a sharp exponential rise to the experimental target value x_o using the following equation:

$$x'(t) = \beta_i \left(x_0 - x\right) \quad . \tag{5.11}$$

The coefficients β_i correspond to the inverse time constants that characterize the approach to the asymptotic value during exercise (β_1) and recovery (β_2) periods. The coefficients β_1 and β_2 can be obtained by fitting the solution of equation (5.11) on the experimental time series of entropy production rates. Then, the solution for $x(t)$ can be used as the input driving function to model the entropy export response according to equation (5.6). The resulting coefficients β_1 and β_2, obtained by fitting the experimental data, and the modeled entropy export responses are shown in figure 5.10 for all three groups. The resulting α coefficients for this transient model are show in table 5.3.

Out of curiosity, we additionally solved the model given by equation (5.6) (i.e. without stochastic noise) using the experimental time series of dS_i/dt as the driving term $x(t)$. Considering the relatively low sampling frequency (1 data point per minute), we used linear interpolation in the experimental time series to increase data resolution. The resulting adaptation coefficients α for the experimental driving function are shown in table 5.4.

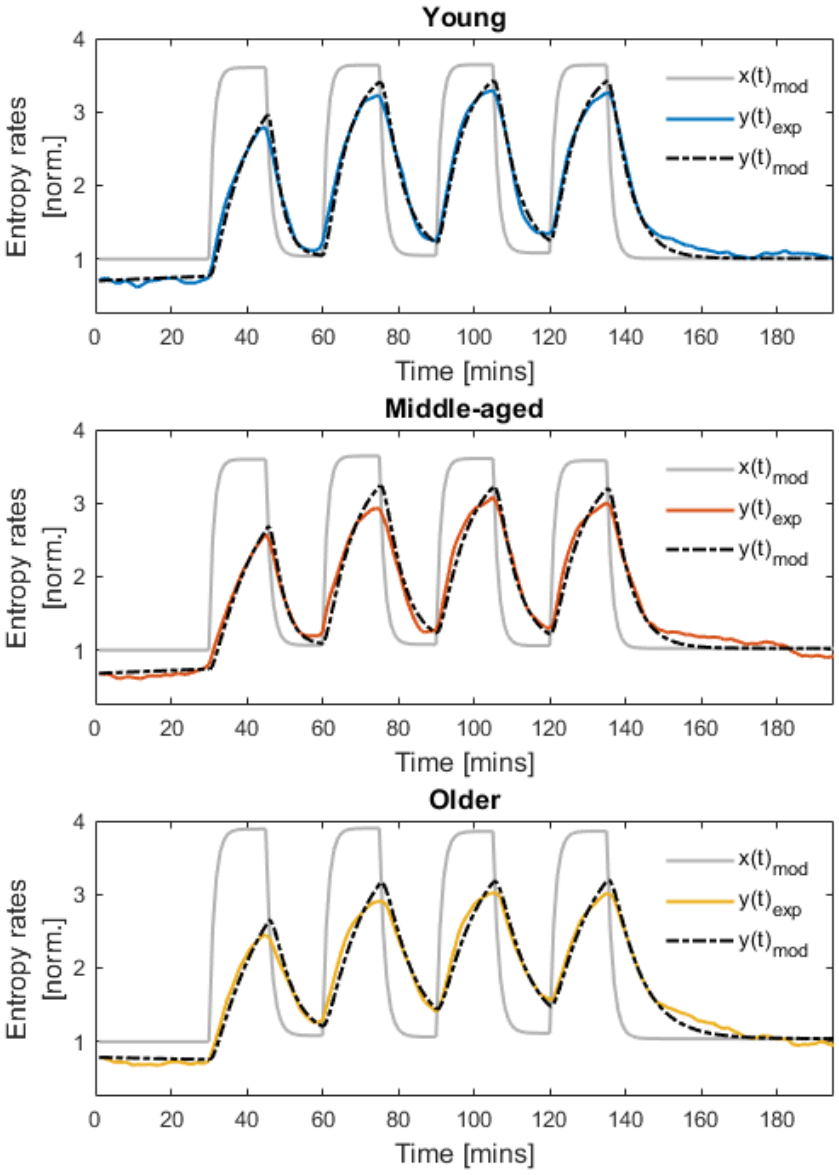

Figure 5.10: Entropy export response for a driving term $x(t)$ given by the solution to equation (5.6), which corresponds to a decreasing exponential function that approaches a fixed value. We refer to this situation as the transient model because the driving term (i.e. the entropy production rate) deviates slightly from the square wave case considered in the main text. The exponential approach can be characterized by the coefficients β_i (inverse time constants). Fitting the coefficients β_i from equation (5.11) on the experimental time series for dS_i/dt for the young (Y), middle-aged (M) and older (O) participants yields $\beta_1^Y = 0.87\ \text{min}^{-1}$, $\beta_2^Y = 0.74\ \text{min}^{-1}$, $\beta_2^M = 0.86\ \text{min}^{-1}$, $\beta_2^M = 0.73\ \text{min}^{-1}$, $\beta_1^O = 0.74\ \text{min}^{-1}$, $\beta_2^O = 0.65\ \text{min}^{-1}$. The resulting adaptation coefficients α for the transient driving function are shown in table 5.3.

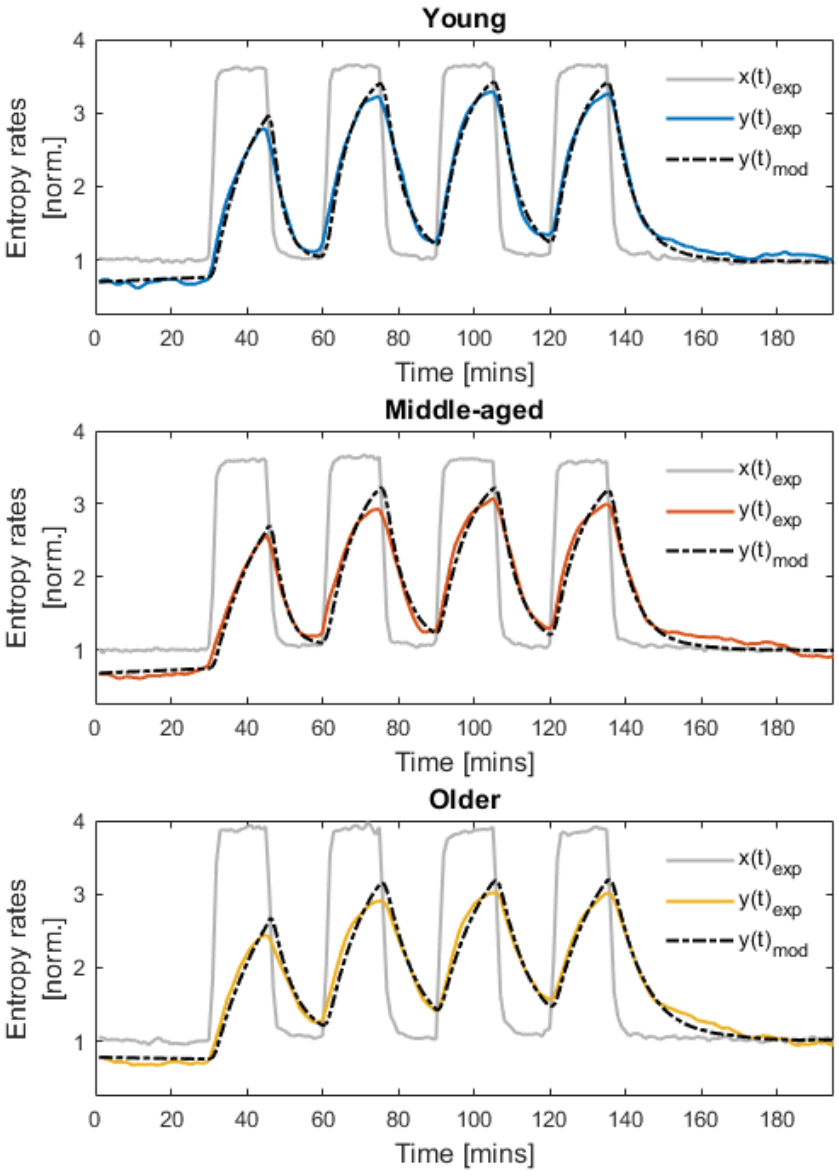

Figure 5.11: Entropy export response for a driving term $x(t)$ given by the experimental time-series of the entropy production rate. Interpolation between the experimental data was used to solve the model given by equation (5.6). The resulting adaptation coefficients α for the experimental driving function are shown in table 5.4.

Table 5.3: Estimated parameters α using the **transient** model for dS_i/dt.

Groups	α_1 Exc. 1	α_2 Rec. 1	α_3 Exc. 2-4	α_4 Rec. 2-4
Young	0.105	0.393	0.175	0.197
Middle-aged	0.079	0.3424	0.132	0.199
Older	0.064	0.204	0.094	0.133

Table 5.4: Estimated parameters α using the **experimental** time-series for dS_i/dt.

Groups	α_1 Exc. 1	α_2 Rec. 1	α_3 Exc. 2-4	α_4 Rec. 2-4
Young	0.102	0.363	0.171	0.195
Middle-aged	0.078	0.313	0.128	0.195
Older	0.062	0.183	0.091	0.131

From a control theory standpoint, this model can be seen as a simple open-loop control that aims to minimize the difference between the entropy production and export rates, i.e. where $y(t)$ aims to track $x(t)$. More elaborate schemes could be tested in future work, where e.g. the entropy balance is maintained via different kinds of feedback including tracking strategies that involve state estimation and filtering [165]. Such approaches could be inspired by existing elaborate thermoregulation models [104] and may lead to further insights.

Future work could investigate a mixed approach where one could use state-dependent α coefficients that also have a time-dependence, for example to model fatigue building up over time as participants exercise for longer time periods. Thus, building a dynamical

model in the form of equation (5.5), compared to a simple piecewise characterization of exponential coefficients, has the flexibility of adding a time-dependence on the coefficients, which has never been done to our knowledge. Moreover, the analytical solutions in the form of decreasing exponential functions are obtained only when the driving term $x(t)$ takes the shape of a step function, that is for alternating values of fixed entropy production rates.

However, our model can technically predict the entropy export response for any time-dependence of the entropy production rate (i.e., any shape of $x(t)$) and is thus not limited to the experimental design presented here. For example, one could design an experiment in which the entropy production rate is modulated in real-time as a sinusoidal function, with an expected entropy export response taking a similar sinusoidal form with a slight time delay and smaller amplitude. Such an experiment could further validate the predictive power and general usefulness of our entropy regulation model. This approach could possibly benefit from recent theoretical extensions of the thermodynamic uncertainty relation to periodically forced systems, which is the experimental context we are dealing with albeit in far from equilibrium conditions [166].

While additive noise provides a reasonable model for the observed noise, it does not capture the whole behavior of individual trajectories, especially during the first few minutes of exercise and recovery where the observed noise amplitude is greater than our model's prediction. Alternative (and combination of) types of noise could be considered to improve the model such as multiplicative noise applied on the α coefficient itself, which would model a fluctuating α coefficient and thus could explain the observed deviation from pure exponentially decaying functions. A comparison between data and the modeled negative exponentials can be appreciated visually in figure 5.12 where a semi-log plot of the entropy export response is shown.

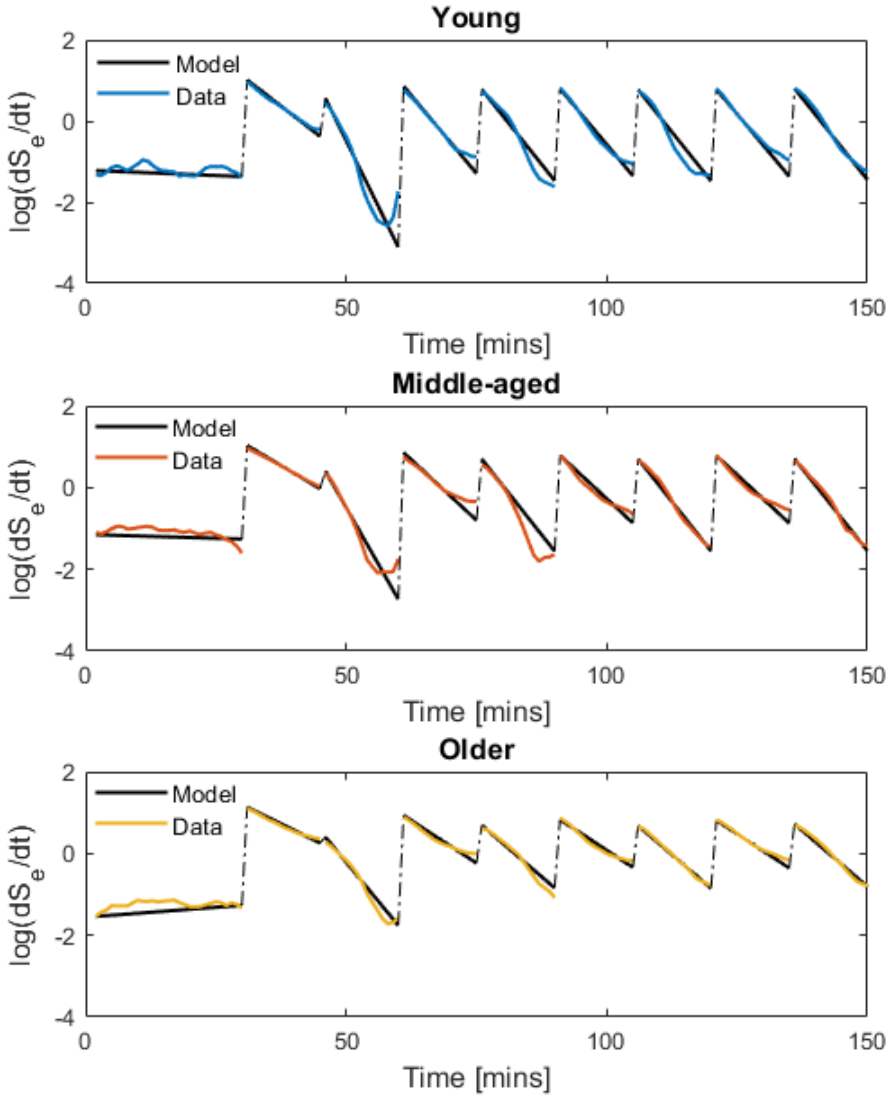

Figure 5.12: Semi-log plot of the entropy export response as a function of time for the young (blue), middle-aged (red) and older (yellow) participants. For a constant driving term $x(t)$, the analytical behavior for the entropy export response is a decaying exponential function which, on a semi-log plot, takes the form a straight line with negative slope (in black). The discontinuous black lines represent each interval, that is the initial rest followed by the alternating schedule of exercise and recovery, with their negative slope corresponding to the calculated α value given in table 5.1.

Additionally, our stochastic term does not distinguish between intrinsic thermodynamic fluctuations and the measurement noise (experimental uncertainty). Although the modified Snellen whole-body air calorimeter has an incredible accuracy of ± 2.3 W for the measurement of total body heat loss ($\dot{Q}_{out}$), which represents a measurement error that is smaller than 1% [38], future work could focus on providing a tighter estimate of the nonequilibrium fluctuations. Despite these limitations, the model provides valuable insights into entropy regulation dynamics and age-related changes in thermoregulatory capacity.

Finally, the two-compartment entropy model used here greatly simplifies the heterogeneous nature of temperature distribution and heat transfers within the body. While distinguishing only the core and skin compartments leads to more direct calculation of internal entropy production and external entropy export, the two-compartment model is known to underestimate changes in mean body temperature, particularly during physical exercise [93]. For example, during physical exercise, temperature increases are most notable within muscles and adjacent tissues (e.g., tendons which further suffer temperature increase from the conversion of elastic energy into heat [167, 168]). Quantitatively, if most of the heat is generated within the muscles (at a higher temperature T), then our two-compartment entropy model may overestimate the entropy production rate (i.e., a larger denominator in $dS_i/dt = \dot{Q}_{int}/T$ for the same $\dot{Q}_{int}$ leads to a smaller dS_i/dt). However, it remains unclear how the subsequent transfer of heat to the other organs, primarily through blood circulation, would impact the total entropy accumulation within the body. With regards to heat dissipation, given that the overwhelming majority of heat loss occurs at the skin region, a traditional multi-compartment model would not improve the accuracy of entropy export rates, unless the skin region is itself compartmentalized (e.g., head, torso, legs, etc.) to account for the differences in heat loss across different locations on the skin. To our knowledge, there are no experimental approach capable of measuring simultaneously both the evaporative and dry heat loss for different skin locations independently.

Additionally, a two-compartment model is highly practical given our methodology based on calorimetry measurements. Indeed, calorimetry cannot differentiate where the

heat is produced and stored within the body, but it provides a very accurate assessment of the overall heat content. As such, the calorimetry approach to the measurement of entropy rates is currently limited to a two-compartment model. A multi-compartment model would most likely require the use of thermometry (i.e. temperature probes) for the continuous measurement of internal temperatures. However, the invasive nature of inserting probes in different organs to increase the spatial resolution of internal temperatures has obvious practical limitations. Therefore, further improvements in the measurement of entropy rates could involve a combination of whole-body calorimetry data, the use of strategically placed and minimally invasive temperature probes, and insights from multi-compartment modeling to account for known heat transfer processes.

5.4.6 Relation to other modeling approaches

Our work builds on the extensive research on thermoregulation in humans under various environmental conditions, including exercise-induced heat stress in healthy and pathological conditions [78, 79]. For example, our approach relates to previous work done by Larose & al. where they approximated the time constants of exponential decay in the rate of evaporative heat loss during alternating schedule of exercise and recovery as the time needed to reach 63.2 % of the total amplitude [88]. Based on the modeling work of Malchaire [148], Kenny & al. similarly reported the time constants associated with the exponential fitting of the rate of total heat loss in young participants (27 ± 7 yr, 6 males and 4 females) [151], which are in good agreement with our α values. The α values that we obtained are in good agreement with the time constants. Nonetheless, both previous approaches differ from our work by focusing more on the piecewise characterization of experimental time series rather than a mathematical description of the system's dynamical response to single and repeated perturbations.

Recently, Joshi & al. compared four thermoregulation models of varying complexity and, most notably, provided an update to the Stolwijk-1971 model [105, 107]. Their updated Stolwijk-2024 model, which considers six body segments and four tissue types (core, muscle, fat, skin), produced efferent sweat signal that exhibit exponential-like behaviour

with two distinct regimes (i.e., different dynamics for short and long timescales). Similarly, a six-cylinder thermoregulatory model (SCTM) was developed by Xu & al. to predict core temperatures during high-intensity exercise in warm environments [169]. The main advantage of using such multi-segmented models with multiple concentric layers is that this allows a greater detailed spatial resolution of the thermoregulatory analysis. As noted by Sawka & Castellani, there is no one uniform core temperature and the relationship between internal tissues temperatures can vary as a function of physical exercise and environmental exposure [94]. Thus, compared to our simpler two-compartment model, multi-segmented models reduce the uncertainty associated with the heterogeneous distribution of internal temperatures.

The model presented here provides a simplified representation of the complex thermoregulatory processes captured in typical bioheat equation models [106, 150, 170]. While bioheat equations often involve detailed descriptions of heat transfer mechanisms within the body (e.g., conduction, convection, and blood perfusion), our model focuses on the overall balance of entropy flows as the driving force for health stability. The adaptation coefficients α can be seen as a coarse-grained representation of the numerous physiological processes involved in heat exchange, encompassing heat loss mechanisms such as sweating and vasodilation and other nonthermal factors that can modulate the regulation of heat loss responses (e.g., baroreceptors, metaboreceptors, etc.) [37].

In essence, our model is based on the principle that the body regulates its entropy export rate in proportion to the rate of entropy change, effectively reducing the multiple coefficients of bioheat models into a single, state-dependent adaptation coefficient. Indeed, the adaptation coefficient, hereby calculated from experimental data, embodies the effective contribution of all the rate constants used in traditional thermoregulation models [130]. Interestingly, the values we obtained for the adaptation coefficients are similar to the illustrative values used by Hajnova & al. [171]. The simplification associated with our model allows for a more tractable analysis of entropy regulation while still capturing the essential dynamics of the system, as evidenced by the model's agreement with experimental data.

The body is a far-from-equilibrium thermodynamic system that exchanges heat and matter with its environment, processes governed by heat and chemical gradients. A comprehensive description of its thermodynamic behaviour, including asymmetries in transition probabilities between states and fluctuations in thermodynamic currents, is currently out of reach. It would entail heat and material exchanges between myriad internal reservoirs, perhaps each with its local approximate temperature and chemical potentials, as well as the body's environment. As in studies of non-living mesoscopic systems, it may prove useful to split entropy changes between equilibrium contributions and non-equilibrium corrections in the form of generalized work [146]. Such thermal and chemical work contributions keep the system out of equilibrium even if the control parameters that can do work on the system are kept fixed, and the system relaxes to some non-equilibrium steady state. Perturbing the steady state heat flows as well as core and skin temperatures through exercise bouts can ultimately guide a stochastic thermodynamic understanding of the human body, with possible attendant fluctuation theorems and thermodynamic uncertainty relations. Our approach makes a first step in this direction by quantifying the deterministic and stochastic components of the control mechanisms that govern entropy accumulation and relaxation following perturbations away from the steady state balance.

5.5 Conclusion

In summary, we presented a novel model for entropy regulation in humans during exercise under heat stress. The model accurately captures the dynamics of the entropy export response across different age groups using state-dependent coefficients that can be interpreted as adaptation coefficients. A clear age-related decline in adaptation coefficients was observed, indicating reduced physiological adaptability in older individuals. The model was extended to include stochastic noise, allowing the characterization of individual variability in entropy export responses. The model provides insights into how humans may regulate entropy during exercise and recovery, with implications for understanding age-related changes in thermoregulatory capacity. Our initial findings suggest the model is a good agreement with experimental calorimetric data, however further evaluation using

different and variable exercise and heat stress are required to validate this model. Future exploration of this thermodynamic framework for analyzing human physiological response and the proposed mechanistic hypothesis for human entropy regulation is warranted.

5.6 Appendix to this manuscript

Autocovariance for the Ornstein-Uhlenbeck process

During rest, i.e. prior to the successive exercise-recovery periods, the entropy production can be assumed approximately constant. Our model then becomes an Ornstein–Uhlenbeck (OU) process centered around μ with parameters α and σ as defined previously:

$$y'(t) = \alpha\ (\mu - y(t)) + \sigma\, \xi(t) \tag{5.12}$$

where $y(t) = dS_e/dt$ and $\xi(t)$ is standard Gaussian white noise.

Assuming for now that μ is a constant, a Fokker-Planck analysis on this Langevin equation yields a steady state average $\langle y(t) \rangle = \mu$ and steady state covariance [115]

$$\langle (y(t) - \mu)(y(t - \tau) - \mu) \rangle = \frac{\sigma^2}{2\alpha}\, e^{-\alpha\tau} \quad . \tag{5.13}$$

However, the thirty minutes of rest data show linear trends in most participants. These can be increasing or decreasing, depending on the fluctuations (see figures 5.6, 5.7 and 5.8 for the trends, and figure 5.9 for the distribution of linear fit parameters for detrending). We attribute these trends to very slow equilibration dynamics of the body which would eventually (e.g. a few hours later) reach a steady state with $y = 1$. When slow enough, we model this trend by defining the steady state of the OU process with an adiabatic variation of an effective drive

$$\mu(t) = ct + \mu_0 \quad . \tag{5.14}$$

This drive is a simple way to account for the slow pre-exercise drift in the entropy export rate y, and encompasses the long-term variations of the entropy production and export that occur while the subject becomes accustomed to the slightly elevated temperature in the calorimeter. Because each participant might not be at the same stage of this very slow process, we need to detrend each participant's sampled data separately. Using linear regression on the $n = 30$ samples (taken each minute for 30 minutes) of participant i, we find an estimate of $\mu_i(t)$ which we define as $\tilde{\mu}_i(t)$. Defining y_i^k the data sample of participant i at time k and, similarly, $\tilde{\mu}_i^k = \tilde{\mu}_i(k)$, we detrend each data point with $\tilde{y}_i^k = y_i^k - \tilde{\mu}_i^k$ as shown in figures 5.7 (top panels). The distributions of estimated linear parameters are shown in figure 5.9. We then compute the centered autocorrelation, i.e. the autocovariance using the individual detrended time series:

$$\begin{aligned}
A_i(\tau) &= \frac{1}{n-\tau} \sum_{k=1}^{n-\tau} \tilde{y}_i^k \cdot \tilde{y}_i^{k-\tau} \\
&= \frac{1}{n-\tau} \sum_{k=1}^{n-\tau} \left(y_i^k - \tilde{\mu}_i^k\right) \cdot \left(y_i^{k-\tau} - \tilde{\mu}_i^{k-\tau}\right) \\
&= \frac{1}{n-\tau} \sum_{k=1}^{n-\tau} \left(y_i^k - \tilde{\mu}_i^k + \mu_i^k - \mu_i^k\right) \cdot \left(y_i^{k-\tau} - \tilde{\mu}_i^{k-\tau} + \mu_i^{k-\tau} - \mu_i^{k-\tau}\right) \\
&= \frac{1}{n-\tau} \sum_{k=1}^{n-\tau} \left(y_i^k - \mu_i^k\right) \cdot \left(y_i^{k-\tau} - \mu_i^{k-\tau}\right) + \eta_i \quad .
\end{aligned} \tag{5.15}$$

Here,

$$\eta_i = \frac{1}{n-\tau}\sum_{k=1}^{n-\tau}\left[\left(\mu_i^{k-\tau}-\tilde{\mu}_i^{k-\tau}\right)\left(y_i^k-\mu_i^k\right)+\left(\mu_i^k-\tilde{\mu}_i^k\right)\left(y_i^{k-\tau}-\mu_i^{k-\tau}\right)+\left(\mu_i^{k-\tau}-\tilde{\mu}_i^{k-\tau}\right)\left(\mu_i^k-\tilde{\mu}_i^k\right)\right] \tag{5.16}$$

quantifies how different the estimate $\tilde{\mu}_i$ is from the actual μ_i underlying the OU process. We then pool all N participants in an age group to compute the average autocovariance

$$\begin{aligned} A(\tau) &= \frac{1}{N}\sum_{i=1}^{N} A_i(\tau) \\ &= \frac{1}{N}\sum_{i=1}^{N}\left[\frac{1}{n-\tau}\sum_{k=1}^{n-\tau}\left(y_i^k-\mu_i^k\right)\cdot\left(y_i^{k-\tau}-\mu_i^{k-\tau}\right)\right]+\frac{1}{N}\sum_{i=1}^{N}\eta_i \quad . \end{aligned} \tag{5.17}$$

Assuming all participants of an age group can be modeled by the same parameters α and σ, we expect the first term to tend towards the actual autocorrelation (equation (5.13)) as the number of participants increases. Similarly, the second term of equation (5.17) will tend towards a value dependent on some average difference between the sample and real linear trends. The scale of the second term is uniquely dependent on the finite sample size in time n. Increasing the number of participants N will not reduce this quantity; therefore, it can not be ignored while fitting our parameters α and σ. To estimate these parameters for the different age groups, we fit the function

$$f(\tau) = \frac{\sigma^2}{2\alpha}\,e^{-\alpha\tau}+\eta \tag{5.18}$$

to the average autocovariance of detrended samples using the *curve_fit* function from the *scipy* package in Python. This function yields the optimal parameters α, σ and η alongside

a covariance matrix from the linearization around this optimum, allowing us to compute the goodness of fit. We take the error as the square root of the diagonal terms associated to the fit parameters of this covariance matrix.

Chapter 6

Conclusion

This thesis sits on the central hypothesis that the principles of non-equilibrium thermodynamics, particularly the balance between entropy production and export, are fundamental to understanding the physiological state, adaptability, and resilience of the human body. More generally, we argued for a paradigm shift in how we view biological systems through the lens of entropy, moving beyond speculative notions towards a more rigorous and intellectually honest assessment of the application of non-equilibrium thermodynamics to complex living systems. The initial skepticism often associated with the application of entropy to macroscopic biological systems provided the core motivation for this rather exploratory endeavor.

Nonetheless, we built a coherent and progressive research narrative, starting with the establishment of a novel methodology for measuring entropy rates in humans, followed by experimental investigations into the physiological and clinical relevance of entropy dynamics, and culminating in the development and validation of a modeling framework to shed light on the underlying regulatory mechanisms. The common thread of applying the principles of the second law of thermodynamics to the study of living systems provides a strong and unifying framework for the entire body of work.

Summary

In Chapter 3, we addressed the first central research question: How can we measure entropy production and entropy flow in humans? To this end, we introduced an experimental approach leveraging existing data from studies employing state-of-the-art whole-body calorimetry on humans exercising under heat stress. The rationale was that complex living systems are characterized by self-organized and dissipative behaviours, necessitating the continuous internal production of entropy and its subsequent export to the environment.

This chapter detailed the methodologies of direct and indirect calorimetry, which were used to quantify internal metabolic heat production (and thus internal entropy production) and external heat dissipation (and thus external entropy flow). A two-compartment entropy flow model, considering the core and skin as distinct thermodynamic entities with respective temperatures, was developed to calculate these entropy rates. The balance between the entropy produced internally and entropy exported externally provides an estimate of the entropy change within the body, the accumulation of which can be interpreted as a thermodynamic measure of physiological stress. It is likely a lower bound to the changes in entropy rate since we are currently able to only quantify heat-based contributions, in contrast to e.g. degradation of internal tissues and regulatory mechanisms. Although these additional sources of entropy production are present, we measure their effects via their impact on heat and gas exchange mechanisms.

In one of our studies (Chapter 3), eleven middle-aged men performed alternating exercise and recovery bouts under environmental heat stress. During the initial resting period (prior to any exercise), we measured a resting internal entropy production rate consistent with prior, albeit limited, measurements. Furthermore, the comparison between entropy changes estimated using calorimetry and thermometry highlighted the superior reliability of calorimetry for continuous monitoring over short intervals, mostly due to the limitations of localized temperature probes in reflecting whole-body temperature dynamics. This methodological foundation established the feasibility of real-time monitoring of entropy production and entropy flow in humans, providing a crucial step towards a

thermodynamics-based understanding of human physiology and, most interestingly, clinical applications which were discussed in the following chapter.

In Chapter 4, we delved into the second research question: How is entropy involved in the thermodynamic stability (or homeostasis) of humans from a physiological and clinical perspective? This chapter presented a retrospective analysis of data from studies investigating the effects of aging, fitness level, and type 2 diabetes on entropy regulation during exercise under heat stress. By applying the previously established methodology for quantifying entropy production and export, we uncovered significant impairments in entropy export, leading to increased entropy accumulation, in association with increased age, decreased fitness level (as quantified by $\dot{V}O_2^{\max}$), and the presence of a chronic disease (type-2 diabetes). Specifically, older individuals, less fit individuals, and those with diabetes exhibited a reduced capacity to export the entropy generated by metabolic processes during exercise, indicating a diminished adaptability to physiological stress.

These findings suggested that the balance of entropy production and export is a critical factor in maintaining physiological stability and can serve as a potential indicator of health status. The observed correlations between entropy accumulation and $\dot{V}O_2^{\max}$ further linked this thermodynamic perspective with traditional measures of physiological capacity. This chapter underscored the clinical relevance of considering entropy dynamics in understanding physiological responses to stress and in potentially identifying novel therapeutic targets based on non-equilibrium thermodynamics. Moreover, the study on fitness level where we compared the entropy regulation in trained and untrained middle-aged men also highlights a peculiar characteristic of living systems: not only do they suffer from the wear-and-tear of everyday use (e.g. aging), they also suffer, to a greater extent than machines, from the lack of use (e.g. sedentary lifestyle and lower fitness) [27]. Indeed, this principle of *use it or lose it* appears to be ubiquitous in living systems, for example with cognitive decline in humans [172], and could provide the incentive to maintain elevated basal and maximal rates of entropy production to counter the effects of aging [71].

It would also be interesting to investigate the entropy dynamics in diverse conditions

beyond heat stress (both exercise-induced and environmental) to provide a more comprehensive picture of human thermodynamics. For example, future studies could explore the entropy production and export in conditions where lower entropy rates (compared to normal resting state) are expected such as during sleep, fasting and exposure to cold environments. These experiments could provide interesting insights on the clinical application of therapeutic hypothermia to prevent neurological deficits in patients that suffered from acute brain injuries [173] or cardiac arrest [174].

Finally, in Chapter 5, we addressed the third research question: How does the human body regulate its entropy production and entropy flow from a modeling perspective? To explore the underlying mechanisms of entropy regulation, a novel stochastic model was introduced. This model posited that the entropy export rate dynamically adjusts in response to the net rate of entropy change which, under the conditions of our experiments, corresponds to the net rate of entropy accumulation. The model incorporated a state-dependent adaptation coefficient (α), representing the responsiveness of the system to deviations from entropy balance, and stochastic noise (σ) to account for intrinsic fluctuations and individual variability. By fitting this model to the experimental data from the aging study (revisited from Chapter 4), we quantified the adaptation coefficients across the different age groups (young, middle-aged and older participants) and physiological states (during static rest and dynamic exercise/recovery). The results revealed a clear age-related decline in these adaptation coefficients, indicating a reduced capacity for older individuals to effectively regulate their entropy export in response to exercise-induced perturbations. The inclusion of stochastic noise allowed for the characterization of individual variability in entropy export responses, providing a more comprehensive understanding of the system's dynamics. This modeling approach offers a mechanistic framework for interpreting the interplay between entropy production and export, which provides a different but complementary perspective to the traditional thermoregulation models. Unlike bioheat models that use primarly the First Law to analyze temperature distributions across a large number of compartments, our model incorporates insights from the Second Law to capture the essential aspects of the regulatory dynamics of entropy from a simplified whole-body perspective.

This Chapter 5 also initiates a larger reflection on what adaptation is and what it means for biological systems. Adaptation of living systems comes from their own ability to manufacture the non-equilibrium conditions in which they thrive and, subsequently, their ability to recover from a perturbation by returning to a dynamically stable steady state. To relate this adaptation behavior to a theoretical framework, we applied the Fokker-Planck method to analyze the stochastic fluctuations in the entropy export responses during resting conditions based on our model that is equivalent to an Ornstein-Uhlenbeck process. Given that the original data were not collected for this specific purpose, this analysis was limited by the relatively short time series (30 minutes). However, there exist calorimetric studies of resting individuals over multiple hours, or even day-long experiments, which could be easily repurposed to further investigate the adaptation and stochastic behavior in human response using the methods presented here, while making stronger connections to Fluctuation-Dissipation Relations [64,175,176], Control Theory [165] and Linear Response Theory [177]. Moreover, it would be interesting to keep monitoring entropy production and export rates for much longer (e.g., 6-12 hours) after physical exercise to investigate the full recovery to the resting steady-state, which also involves analyzing the dynamics of the steady-state itself given the different regimes observed between the static and dynamic phases. Longer studies are also required to investigate the timescale at which the entropy accumulated during physical exercise gets exported out of the body, if ever, or participates in a gradual lifetime accumulation in the form of structural damage at the subcellular level. Ultimately, this could provide valuable insights into the homeostatic regulation of entropy and its potential alterations in various physiological and pathological states.

Future perspectives

The experimental protocol used so far involves fixing the metabolic heat production, and thereby entropy production, which provides a controlled design to assess the capacity for entropy export under specific and standardized internally generated entropy. However, letting entropy production vary freely could yield complementary and highly relevant information about the entropy dynamics. For example, fixing the work rate performed by the participants instead of the entropy production rate could reveal feedback loops where

the body adjusts its entropy production rate in response to its capacity for entropy export (e.g. bidirectional coupling discussed in chapter 5). Additionally, letting the entropy production rate vary freely could help assess the full range of adaptability since healthier (or fitter) individuals might be able to sustain higher rates of entropy production while maintaining entropy balance due to more efficient export mechanisms. Fortunately, the stochastic model of entropy regulation (and its deterministic version) developed in chapter 5 allows for arbitrary and time-dependent entropy production driving terms, which can be modeled independently as exemplified by the transient model discussed in Section 5.4.4.

In this thesis, we explored the vital role of entropy production and export mainly from the metabolic perspective and its application in the thermodynamic stability of humans. However, we ignored so far possibly the most intriguing case of self-organized complexity: the highly complex dynamics of our brain from which emerge our cognition and consciousness. While the brain contributes significantly to the body's overall entropy production through its energetically expensive (and thus inherently dissipative) metabolic activity, our cognitive abilities might reveal a more profound connection to the production of entropy when viewed as an information processing unit. As recognized by Seely [71], the constant processing and synthesis of sensory information, which allow us to extract meaning and create abstract internal models of the world, also involve a significant *loss of information* that might be accompanied by heat generation (and thus entropy) following Landauer's principle [178, 179].

While this hypothesis of entropy generation through information reduction in the brain remains to be proven experimentally, potentially using the same calorimetric approach described in this thesis, it offers an elegant way to reconcile the thermodynamic and informational definitions of entropy [180, 181]. Reinforcing the relation between cognition and thermodynamics, Kondepudi suggested that high entropy production rates may be a necessary condition for the emergence of *physical intelligence* in a system with a large number of non-equilibrium states between which the system can make transitions as it interacts with its environment [182]. This perspective raises the interesting question of whether the human body has achieved the maximal state of metabolic complexity given the

current constraints and evolutionary trajectory such that Nature, through the Maximum Entropy Production Principle, is now venturing into the realm of information processing within our brain to continue its mission of energy degradation and entropy generation.

This intriguing hypothesis naturally prompts a deeper dive into the underlying physical principle that might be orchestrating this drive towards increased entropy production and complexity across biological scales. Indeed, the Maximum Entropy Production Principle (MEPP) mentioned above posits that non-equilibrium systems will tend to organize themselves in a way that maximizes the rate of entropy production given the constraints acting on them [183]. But must entropy production be maximized on all spatial scales in order to maximize the entropy production of the whole system? In other words, how does the MEPP manifests itself across the different levels of organization, from the scale of individual biochemical reactions and cellular processes to the integrated functions of organs and entire organism? It appears reasonable to assume that subsystems naturally achieve an *optimal* entropy production rate, as opposed to a *maximal* rate, that allows for (1) the minimal energy consumption to sustain the necessary functions due to evolutionary pressure and (2) ensures the stability of the system (or systems) at larger scales.

For example, individual cells in our body don't appear to maximize entropy production; rather, there exists some sort of social contract where each cell limits its energy consumption and replication to maintain the tissue's integrity. However, the accumulation of DNA damage and ensuing genomic instability can lead to a drastically different behavior, that of cancer cells, which maximize their energy consumption and replication at the detriment of the organism [184, 185]. As such, the invisible hand of Adam Smith seems to be invalid in the case of self-interested cancer cells; in favoring the metabolism of their subsystem at the expense of the whole, these cells disrupt the orchestrated equilibrium necessary for the greater good, with cancer now being one of the leading causes of death [186]. This increased metabolic activity of cancer cells is also exploited for diagnostic purposes in the positron emission tomography (PET scan) [187].

Paradoxically, cancer cells may hold key insights into the self-organization of living

systems as examples of life gone pathologically wrong with a potentially profound connection to thermodynamics. First, we must note the fascinating observation that living and non-living systems can adopt oddly similar structures, for example hydrographic networks that resemble anatomical networks like the vascular bed or the tracheobronchial tree. This shared propensity for self-organization in response to non-equilibrium conditions suggests a *universal* or *optimal* way for Nature to organize elements of dynamical systems, regardless of the spatial scale. And at the root of all these phenomena, we consistently observe fractal structures [158].

Thus, making connection between the expected constraints on entropy production and the observed fractality in self-organized systems, future research could be motivated by the following question: is there a functional relation between the entropy production of living systems and the way they spatially organize themselves? The objective would be to determine whether fractal geometry represents the optimal spatial configuration allowing the maximization of entropy production in living systems. To do so, one could compare the fractal dimension (i.e., a measure of spatial complexity) and the metabolic activity (i.e., proxy for entropy production) of tumors. In this context, the hypothesis can be reformulated as follows: cancer cells with an enhanced metabolism develop into a solid tumor exhibiting a more complex spatial organization (i.e., larger fractal dimension of tumor contour) related to their efficiency at producing entropy. The proposed idea is to understand the thermodynamic behavior of cancer cells and shed light on their increased adaptability over normal cells. Ultimately, this thermodynamic profiling of tumors could provide a useful clinical tool to assess the malignancy of tumors (and the urgency of treatments) through a simple image analysis of their spatial complexity.

Closing remarks

Finally, this work provides the first steps to move past the current status quo by providing evidence of the constructive role of entropy production and entropy flow in complex living systems. Compared to the more traditional energy-based analysis, we believe the entropy analysis offers a complementary and potentially more fundamental perspective

on how living systems operate given their profound connection to dissipative structures. Unfortunately, entropy still suffers from the lack of a satisfactory theoretical definition in out-of-equilibrium conditions and remains experimentally challenging to measure even in equilibrium conditions [58, 74, 183].

As a result, significant progress in the study of complex living systems has been hindered in the past decades by the following epistemological hurdle: potentially relevant experimental findings were dismissed given their lack of proper theoretical basis and, concurrently, theoretical advances were deem as excessively speculative given their lack of experimental support. In other words, theorists struggled to formulate hypotheses that can be validated, while experimentalists struggled to provide results that do not seem overly simplistic. Hopefully, the contributions presented here will help the field break free from this impasse by establishing a more robust and mutually reinforcing connection between experimental, modeling and, to a smaller extent, theoretical work. In doing so, we aim to inspire further research at the intersection of health and thermodynamics.

References

[1] Donald Miller. Thermodynamics of Irreversible Processes: The Experimental Verification of the Onsager Reciprocal Relations. *Chemical Reviews*, 60(6), 1960.

[2] Dilip Kondepudi and Ilya Prigogine. *Modern Thermodynamics: From Heat Engines to Dissipative Structures*. Wiley, 2015.

[3] Maria Ribeiro, Teresa Henriques, Luísa Castro, André Souto, Luís Antunes, Cristina Costa-Santos, and Andreia Teixeira. The entropy universe. *Entropy*, 23(2):1–35, 2021.

[4] L. M. Martyushev and V. D. Seleznev. The restrictions of the maximum entropy production principle. *Physica A: Statistical Mechanics and its Applications*, 410:17–21, 2014.

[5] A. Katchalsky and Peter F. Curran. *Nonequilibrium Thermodynamics in Biophysics*. Harvard University Press, 1975.

[6] Eric Smith and Harold J. Morowitz. *The Origin and Nature of Life on Earth: The Emergence of the Fourth Geosphere*. Cambridge University Press, 2016.

[7] R Swenson. Autocatakinetics, evolution, and the law of maximum entropy produc-

tion: a principled foundation towards the study of human ecology. *Advances in Human Ecology, Vol. 6*, 6:1–48, 1997.

[8] G. Nicolis and Ilya Prigogine. *Self-organization in nonequilibrium systems : from dissipative structures to order through fluctuations*. New York : Wiley, 1977.

[9] Bong Jae Chung, Benjamin De Bari, James Dixon, Dilip Kondepudi, Joseph Pateras, and Ashwin Vaidya. On the Thermodynamics of Self-Organization in Dissipative Systems: Reflections on the Unification of Physics and Biology. *Fluids*, 7(4):1–23, 2022.

[10] Michael J. Russell, Laura M. Barge, Rohit Bhartia, Dylan Bocanegra, Paul J. Bracher, Elbert Branscomb, Richard Kidd, Shawn McGlynn, David H. Meier, Wolfgang Nitschke, Takazo Shibuya, Steve Vance, Lauren White, and Isik Kanik. The drive to life on wet and Icy Worlds. *Astrobiology*, 14(4):308–343, 2014.

[11] Abhishek Sharma, Dániel Czégel, Michael Lachmann, Christopher P. Kempes, Sara I. Walker, and Leroy Cronin. Assembly theory explains and quantifies selection and evolution. *Nature*, 622(7982):321–328, 2023.

[12] Sebastian Raubitzek, Alexander Schatten, Philip König, Edina Marica, Sebastian Eresheim, and Kevin Mallinger. Autocatalytic Sets and Assembly Theory: A Toy Model Perspective. *Entropy*, 26(9):808, sep 2024.

[13] Michael P. Robertson and Gerald F. Joyce. The origins of the RNA World. *Cold Spring Harbor Perspectives in Biology*, 4(5):1, 2012.

[14] Raffaele Saladino, Giorgia Botta, Samanta Pino, Giovanna Costanzo, and Ernesto Di Mauro. Genetics first or metabolism first? The formamide clue. *Chemical Society Reviews*, 41(16):5526–5565, 2012.

[15] Daniel R. Brooks, John Collier, Brian A. Maurer, Jonathan D.H. Smith, and E. O. Wiley. Entropy and information in evolving biological systems. *Biology and Philosophy*, 4(4):407–432, 1989.

[16] Dilip Kondepudi, Bruce Kay, and James Dixon. Dissipative structures, machines, and organisms: A perspective. *Chaos*, 27(10), 2017.

[17] Ervin Laszlo. *The New Evolutionary Paradigm*. Routledge, New York, 1991.

[18] Charles H. Lineweaver, Paul C.W. Davies, and Michael Ruse. *Complexity and the Arrow of Time*. Cambridge University Press, New York, 2013.

[19] Dilip K. Kondepudi, Benjamin De Bari, and James A. Dixon. Dissipative structures, organisms and evolution. *Entropy*, 22(11):1–19, 2020.

[20] Seymour Garte, Perry Marshall, and Stuart Kauffman. The Reasonable Ineffectiveness of Mathematics in the Biological Sciences. *Entropy*, 27(280), 2025.

[21] Ilya Prigogine and Isabelle Stengers. *La nouvelle alliance*. Gallimard, 1986.

[22] Roderick C. Dewar, Charles H. Lineweaver, Robert K. Niven, and Klaus Regenauer-Lieb. *Beyond the Second Law: Entropy Production and Non-equilibrium Systems*. Springer-Verlag Berlin Heidelberg, 2014.

[23] Karo Michaelian. Entropy Production and the Origin of Life. *Journal of Modern Physics*, 02(06):595–601, 2011.

[24] R. E. Ulanowicz and B. M. Hannon. Life and the Production of Entropy. *Proc. R. Soc. Lond.*, 232:181–192, 1987.

[25] Peter T Macklem and Andrew Seely. Towards a Definition of Life. *Perspective in*

Biology and Medicine, 53(3):330–340, 2010.

[26] Bernard Brunhes. *La dégradation de l'énergie*. Flammarion, 1909.

[27] Eric D. Schneider and Dorion Sagan. *Into the cool: energy flow, thermodynamics, and life*. The University of Chigago Press, Chicago, 2005.

[28] Jan-peter Meyn. A Contemporary View on Carnot ' s Réflexions. *Entropy*, 26, 2024.

[29] Alex B. Kiefer. Intrinsic motivation as constrained entropy maximization. *Entropy*, 27(372), 2025.

[30] William James Sidis. *The animate and the inanimate*. The Gorham Press, Boston, Mass., USA, 1925.

[31] Robert Rosen. *Life itself: a comprehensive inquiry into the nature, origin, and fabrication of life*. Columbia University Press, New York, 1991.

[32] Ilya Prigogine. *Introduction to thermodynamics of irreversible processes*. Wiley, 1968.

[33] Ichiro Aoki. Entropy Flow and Entropy Production in the Human Body in Basal Conditions. *Journal of Theoretical Biology*, 141:11–21, 1989.

[34] Ichiro Aoki. Effects of exercise and chills on entropy production in human body. *Journal of Theoretical Biology*, 145(3):421–428, 1990.

[35] Julie Bienertová-Vašků, Filip Zlámal, Ivo Nečesánek, David Konečný, and Anna Vasku. Calculating Stress: From Entropy to a Thermodynamic Concept of Health and Disease. *PLoS ONE*, 11(1):1–13, 2016.

[36] Filip Zlámal, Peter Lenart, Daniela Kuruczová, Tomáš Kalina, Gabriel De la Torre, Miguel A. Ramallo, and Julie Bienertová-Vašků. Stress entropic load: New stress

measurement method? *PLoS ONE*, 13(10):1–13, 2018.

[37] Glen P. Kenny and Ollie Jay. Thermometry, calorimetry, and mean body temperature during heat stress. *Comprehensive Physiology*, 3(4):1689–1719, 2013.

[38] Francis D. Reardon, Kalle E. Leppik, Ren Wegmann, Paul Webb, Michel B. Ducharme, and Glen P. Kenny. The Snellen human calorimeter revisited, re-engineered and upgraded: Design and performance characteristics. *Medical and Biological Engineering and Computing*, 44(8):721–728, 2006.

[39] Nicolas Brodeur, Sean R. Notley, Glen P. Kenny, André Longtin, and Andrew J. E. Seely. Continuous Monitoring of Entropy Production and Entropy Flow in Humans Exercising under Heat Stress. *Entropy*, 25(9):1290, 2023.

[40] Nicolas Brodeur, André Longtin, Glen P Kenny, and Andrew J E Seely. Real-time measurement of entropy production and export in humans : A step toward entropically informed medicine. *Annals of the New York Academy of Sciences*, pages 1–13, 2025.

[41] Nicolas Brodeur, Andrew J.E. Seely, Raphaël Lafond-Mercier, Glen P. Kenny, and André Longtin. The Second Law and Health: A Stochastic Model of Entropy Regulation in Humans (submitted). *Physics Review Research*, 2025.

[42] Thomas S. Kuhn. Energy Conservation as an Example of Simultaneous Discovery. In M. Clagett, editor, *Critical Problems in the History of Science*. Madison: University of Wisconsin Press, 1959.

[43] H.B. Callen. *Thermodynamics*. Wiley, 1960.

[44] Peter Coveney and Roger Highfield. *The Arrow of Time*. HarperCollins Publishers, London, 1991.

[45] Laurent Jodoin. Emergence et entropie : une analyse critique des stratégies explicatives émergentistes basés sur le concept d'entropie. 2015.

[46] Enrico Fermi. *Thermodynamics*. Prentice-Hall Compagny, 1937.

[47] A. Puglisi, A. Sarracino, and A. Vulpiani. Temperature in and out of equilibrium: A review of concepts, tools and attempts. *Physics Reports*, 709-710:1–60, 2017.

[48] Giovanni Gallavotti. Entropy production and thermodynamics of nonequilibrium stationary states: A point of view. *Chaos*, 14(3):680–690, 2004.

[49] Henning Struchtrup. Entropy and the second law of thermodynamics-The nonequilibrium perspective. *Entropy*, 22(7), 2020.

[50] Denis J. Evans and Gary Morriss. *Statistical Mechanics of Nonequilibrium Fluids*. Cambridge University Press, 2nd edition, 2008.

[51] Shin Ichi Sasa and Hal Tasaki. Steady state thermodynamics. *Journal of Statistical Physics*, 125(1):125–224, 2006.

[52] S.R. de Groot and P. Mazur. *Non-equilibrium Thermodynamics*. Dover Publications, 1984.

[53] Kim R Kristiansen and Bjørn Hafskjold. Local Equilibrium Approximation in Non-Equilibrium Thermodynamics of Diffusion. *Entropy*, 27(400), 2025.

[54] D. Reguera, J. M. Rubí, and J. M.G. Vilar. The mesoscopic dynamics of thermodynamic systems. *Journal of Physical Chemistry B*, 109(46):21502–21515, 2005.

[55] Elliott H. Lieb and Jakob Yngvason. The entropy concept for non-equilibrium states. *Proceedings of the Royal Society A: Mathematical, Physical and Engineering Sciences*,

469(2158), 2013.

[56] Vito Antonio Cimmelli, David Jou, Tommaso Ruggeri, and Péter Ván. Entropy principle and recent results in non-equilibrium theories. *Entropy*, 16(3):1756–1807, 2014.

[57] Erwin Schrödinger. *What is life?: The Physical Aspect of the Living Cell*. Cambridge University Press, United Kingdom, 1944.

[58] Georgy Lebon, David Jou, and José Casas-Vázquez. *Understanding Non-equilibrium Thermodynamics*. Springer-Verlag Berlin Heidelberg, 2008.

[59] David Jou, José Casas-Vázquez, and Georgy Lebon. *Extended Irreversible Thermodynamics*. Springer, 4th edition, 2010.

[60] Lars Onsager. Reciprocal Relations in Irreversible Processes. I. *Physical Review*, 37:405–426, 1931.

[61] Lars Onsager. Reciprocal Relations in Irreversible Processes. II. *Physical Review*, 38:2265–2279, 1931.

[62] L. M. Martyushev and V. D. Seleznev. Maximum entropy production principle in physics, chemistry and biology. *Physics Reports*, 426(1):1–45, 2006.

[63] Ilya Prigogine. *Étude Thermodynamique des Processus Irreversibles*. Desoer, Liège, 1947.

[64] Jordan M. Horowitz and Todd R. Gingrich. Thermodynamic uncertainty relations constrain non-equilibrium fluctuations. *Nature Physics*, 16(1):15–20, 2019.

[65] Roderick C Dewar. Maximum Entropy Production and Non-equilibrium Statistical

Mechanics. In *Non-equilibrium Thermodynamics and the Production of Entropy*, pages 41–55. 2006.

[66] S. N. Salthe. Maximum Power and Maximum Entropy Production: Finalities in Nature. *Cosmos and History: The Journal of Natural and Social Philosophy*, 6(1):114–121, 2010.

[67] Robert G. Endres. Entropy production selects nonequilibrium states in multistable systems. *Scientific Reports*, 7(1):1–13, 2017.

[68] Axel Kleidon and Ralph D. Lorenz. *Non-equilibrium Thermodynamics and the Production of Entropy: Life, Earth, and Beyond*. Springer-Verlag Berlin Heidelberg, 2005.

[69] Axel Kleidon and Ralph Lorenz. Entropy Production by Earth System Processes. In *Non-equilibrium Thermodynamics and the Production of Entropy*, pages 1–20. Springer, 2006.

[70] Leonid M. Martyushev. Life and Evolution in terms of maximum entropy production principle. *Preprints*, 2020.

[71] Andrew J. E. Seely. Optimizing Our Patients' Entropy Production as Therapy? Hypotheses Originating from the Physics of Physiology. *Entropy*, 22(10):1095, 2020.

[72] Keith R. Skene. Life's a gas: A thermodynamic theory of biological evolution. *Entropy*, 17(8):5522–5548, 2015.

[73] Robert C. Jennings, Erica Belgio, and Giuseppe Zucchelli. Does maximal entropy production play a role in the evolution of biological complexity? A biological point of view. *Rendiconti Lincei. Scienze Fisiche e Naturali*, 31(2):259–268, 2020.

[74] Ty N.F. Roach. Use and abuse of entropy in biology: A case for caliber. *Entropy*, 22(12):1–8, 2020.

[75] E.T. Jaynes and R.D. Rosenkrantz. *Papers on Probability, Statistics and Statistical Physics*. Reidel Publishing Company, Dordrecht, The Netherlands, 1983.

[76] Stuart J. Bartlett. *Why is Life? An Assessment of the Thermodynamic Properties of Dissipative, Pattern-forming Systems*. PhD thesis, University of Southampton, 2014.

[77] Paul Davidovits. *Physics in Biology and Medicine*. Elsevier, 4th edition, 2013.

[78] Matthew N. Cramer, Daniel Gagnon, Orlando Laitano, and Craig G. Crandall. Human Temperature Regulation Under Heat Stress in Health, Disease, and Injury. *Physiological Reviews*, 102(4):1907–1989, 2022.

[79] Julien D. Périard, Thijs M.H. Eijsvogels, and Hein A.M. Daanen. Exercise under heat stress: Thermoregulation, hydration, performance implications, and mitigation strategies. *Physiological Reviews*, 101(4):1873–1979, 2021.

[80] Robert D Meade, Fergus K O Connor, Brodie J Richards, and Emily J Tetzlaff. Validating new limits for human thermoregulation. *Proceedings of the National Academy of Sciences*, 122(14):1–11, 2025.

[81] Joseph L. Roti. Cellular responses to hyperthermia (40-46°C): Cell killing and molecular events. *International Journal of Hyperthermia*, 24(1):3–15, 2008.

[82] Y. Shapiro and D. S. Seidman. Field and clinical observations of exertional heat stroke patients, 1990.

[83] Irving P. Herman. Metabolism: Energy, Heat, Work, and Power of the Body. In *Physics of the Human Body*, pages 393–489. Springer Cham Heidelberg New York

Dordrecht London, 2016.

[84] J.H. Wilmore and D.L. Costill. *Physiology of Sport and Exercise*. Human Kinetics, Champaign, 3rd edition, 2004.

[85] Y. Nishi. Measurement of Thermal Balance of Man. In *Bioengineering, Thermal Physiology and Comfort*, chapter 2, pages 29–39. Elsevier, 1981.

[86] Glen P. Kenny, Sean R. Notley, and Daniel Gagnon. Direct calorimetry: a brief historical review of its use in the study of human metabolism and thermoregulation. *European Journal of Applied Physiology*, 117(9):1765–1785, 2017.

[87] Zachary J. Schlader, Deanna Colburn, and David Hostler. Heat Strain Is Exacerbated on the Second of Consecutive Days of Fire Suppression. *Medicine and Science in Sports and Exercise*, 49(5):999–1005, 2017.

[88] Joanie Larose, Heather E. Wright, Jill Stapleton, Ronald J. Sigal, Pierre Boulay, Stephen Hardcastle, and Glen P. Kenny. Whole body heat loss is reduced in older males during short bouts of intermittent exercise. *American Journal of Physiology - Regulatory Integrative and Comparative Physiology*, 305(6):619–629, 2013.

[89] Jill M. Stapleton, Martin P. Poirier, Andreas D. Flouris, Pierre Boulay, Ronald J. Sigal, Janine Malcolm, and Glen P. Kenny. Aging impairs heat loss, but when does it matter? *Journal of Applied Physiology*, 118(3):299–309, 2015.

[90] Sean R. Notley, Martin P. Poirier, Ronald J. Sigal, Andrew D'Souza, Andreas D. Flouris, Naoto Fujii, and Glen P. Kenny. Exercise Heat Stress in Patients with and Without Type 2 Diabetes. *JAMA - Journal of the American Medical Association*, 322(14):1409–1411, 2019.

[91] Laura E. Matarese. Indirect calorimetry: Technical aspects, 1997.

[92] Haifa Mtaweh, Lori Tuira, Alejandro A. Floh, and Christopher S. Parshuram. Indirect calorimetry: History, technology, and application. *Frontiers in Pediatrics*, 6:1–8, 2018.

[93] Ollie Jay, Francis D. Reardon, Paul Webb, Michel B. DuCharme, Tim Ramsay, Lindsay Nettlefold, and Glen P. Kenny. Estimating changes in mean body temperature for humans during exercise using core and skin temperatures is inaccurate even with a correction factor. *Journal of Applied Physiology*, 103(2):443–451, 2007.

[94] Michael N. Sawka and John W. Castellani. How hot is the human body? *Journal of Applied Physiology*, 103(2):419–420, 2007.

[95] Paul Webb. The physiology of heat regulation. *American Journal of Physiology - Regulatory Integrative and Comparative Physiology*, 268(37):R838–R850, 1995.

[96] Daniel Gagnon, Bruno B Lemire, Ollie Jay, and Glen P Kenny. Aural Canal, Esophageal, and Rectal Temperatures During Exertional Heat Stress and the Subsequent Recovery Period. *Journal of Athletic Training*, 45(2):157–163, 2010.

[97] Michael Zakharov and Michael Sadovsky. Model of thermal regulation of animals based on entropy production principle. *Journal of Siberian Federal University - Mathematics and Physics*, 6(3):381–405, 2013.

[98] Ichiro Aoki. Entropy production in living systems: from organisms to ecosystems. *Thermochimica Acta*, 1995.

[99] Abhijit Dutta and Himadri Chattopadhyay. A Brief on Biological Thermodynamics for Human Physiology. *Journal of biomechanical engineering*, 143, 2021.

[100] Carlos Silva and Kalyan Annamalai. Entropy generation and human aging: Lifespan entropy and effect of physical activity level. *Entropy*, 10(2):100–123, 2008.

[101] Carlos A. Silva and Kalyan Annamalai. Entropy Generation and Human Aging: Lifespan Entropy and Effect of Diet Composition and Caloric Restriction Diets. *Journal of Thermodynamics*, 2009:1–10, 2009.

[102] Ayşe Selcen Semerciöz-Oduncuoğlu, Sharon E. Mitchell, Mustafa Özilgena, Bayram Yilmazc, and John R. Speakman. A step toward precision gerontology: Lifespan effects of calorie and protein restriction are consistent with predicted impacts on entropy generation. *Proceedings of the National Academy of Sciences*, 120(37), 2023.

[103] Lütfullah Kuddusi. Thermodynamics and life span estimation. *Energy*, 80:227–238, 2015.

[104] Xiaojiang Xu, Timothy P Rioux, and Michael P. Castellani. Three dimensional models of human thermoregulation: A review. *Journal of Thermal Biology*, 112, 2023.

[105] Ankit Joshi, Bryce Twidwell, Michael Park, and Konrad Rykaczewski. Comparative analysis of thermoregulation models to assess heat strain in moderate to extreme heat. *Journal of Thermal Biology*, 127, 2025.

[106] George Havenith and Dusan Fiala. Thermal indices and thermophysiological modeling for heat stress. *Comprehensive Physiology*, 6(1):255–302, 2016.

[107] J. A. J. Stolwijk. A mathematical model of physiological temperature regulation. Technical Report NASA CR-1855, National Aeronautics and Space Administration, 1971.

[108] Dusan Fiala, Agnes Psikuta, Gerd Jendritzky, Stefan Paulke, David A. Nelson, Wouter D. van Marken Lichtenbelt, and Arjan J.H. Frijns. Physiological modeling for technical, clinical and research applications. *Frontiers in Bioscience*, 2010.

[109] Dusan Fiala and George Havenith. Modelling Human Heat Transfer and Temperature Regulation. *Studies in Mechanobiology, Tissue Engineering and Biomaterials*, 19(March):265–302, 2016.

[110] Henry C. Tuckwell. *Stochastic Processes in the Neurosciences*. Society for Industrial and Applied Mathematics, 1989.

[111] Paul C. Bressloff. *Stochastic processes in cell biology*. Springer, 1st edition, 2014.

[112] André Longtin and Ivan L'Heureux. Dynamical effects of noise on nonlinear systems. *Physics in Canada*, 57(2), 2001.

[113] Kurt Jacobs. *Stochastic Processes for Physicists: Understanding Noisy Systems*. Cambridge University Press, Cambridge, UK, 2010.

[114] Luca Peliti and Simone Pigolotti. *Stochastic Thermodynamics: An Introduction*. Princeton University Press, 2021.

[115] Crispin Gardiner. *Stochastic Methods - A handbook for the natural and social sciences*. Springer, Berlin, 4th edition, 2009.

[116] Philip Nelson. *Biological Physics: Energy, Information, Life*. W. H. Freeman Co, New York, 2007.

[117] James D. Hardy, Eugene F. Du Bois, and G. F. Soderstrom. Basal Metabolism, Radiation, Convection and Vaporization at Temperatures of 22 to 35°C. *The Journal of Nutrition*, 15(5):477–497, 1938.

[118] Kenneth Wark. *Thermodynamics*. McGraw-Hill, 1988.

[119] Hisashi Ozawa, Atsumu Ohmura, Ralph D. Lorenz, and Toni Pujol. The second law

of thermodynamics and the global climate system: A review of the maximum entropy production principle. *Reviews of Geophysics*, 41(4):1018, 2003.

[120] Delafield Du Bois and Eugene F. Du Bois. A Formula to Estimate the Approximate Surface Area if Height and Weight Be Known. *Arch Intern Med (Chic)*, XVII(6_2) : $863 - -871, 1916$.

[121] Daniel Gagnon, Ollie Jay, and Glen P. Kenny. The evaporative requirement for heat balance determines whole-body sweat rate during exercise under conditions permitting full evaporation. *Journal of Physiology*, 591(11):2925–2935, 2013.

[122] Nigel A.S. Taylor, Michael J. Tipton, and Glen P. Kenny. Considerations for the measurement of core, skin and mean body temperatures. *Journal of Thermal Biology*, 46:72–101, 2014.

[123] John S. Cuddy, Walter S. Hailes, and Brent C. Ruby. A reduced core to skin temperature gradient, not a critical core temperature, affects aerobic capacity in the heat. *Journal of Thermal Biology*, 43(1):7–12, 2014.

[124] Glen P. Kenny, Ollie Jay, and W. Shane Journeay. Disturbance of thermal homeostasis following dynamic exercise. *Applied Physiology, Nutrition and Metabolism*, 32(4):818–831, 2007.

[125] B. Saltin, A. P. Gagge, U. Bergh, and J. A. Stolwijk. Body temperatures and sweating during exhaustive exercise. *Journal of applied physiology*, 32(5):635–643, 1972.

[126] Piotr Bełdowski and Adam Gadomski. A quest to extend friction law into multiscale soft matter: experiment confronted with theory—a review. *Journal of Physics D: Applied Physics*, 55(483002), 2022.

[127] Maël Montévil and Matteo Mossio. Biological organisation as closure of constraints. *Journal*

of Theoretical Biology, 372:179–191, 2015.

[128] Alfred J. Lotka. Contribution to the Energetics of Evolution. *Proceedings of the National Academy of Sciences of the United States of America*, 8(6):147–151, 1922.

[129] Howard T. Odum and Richard C. Pinkerton. Time's Speed Regulator: The Optimum Efficiency for Maximum Power Output in Physical and Biological Systems. *American Scientist*, 43(2):331–343, 1955.

[130] H. Frederik Nijhout, Janet Best, and Michael C. Reed. Escape from homeostasis. *Mathematical Biosciences*, 257:104–110, nov 2014.

[131] U. von Stockar and J.-S. Liu. Does microbial life always feed on negative entropy? Thermodynamic analysis of microbial growth. *Biochimica et biophysica acta*, pages 191–211, 1999.

[132] N. L. Ramanathan. A new weighting system for mean surface temperature of the human body. *Journal of applied physiology*, 19:531–533, 1964.

[133] Megan N. Hawkins, Peter B. Raven, Peter G. Snell, James Stray-Gundersen, and Benjamin D. Levine. Maximal oxygen uptake as a parametric measure of cardiorespiratory capacity. *Medicine and Science in Sports and Exercise*, 39(1):103–107, 2007.

[134] Yoshimitsu Inoue, George Havenith, W. Larry Kenney, Joseph L. Loomis, and Elsworth R. Buskirk. Exercise- and methylcholine-induced sweating responses in older and younger men: Effect of heat acclimation and aerobic fitness. *International Journal of Biometeorology*, 42(4):210–216, 1999.

[135] Caitlin W. Hicks and Elizabeth Selvin. Epidemiology of Peripheral Neuropathy and Lower Extremity Disease in Diabetes. *Current Diabetes Reports*, 19(10), 2019.

[136] Aristidis Veves, Cameron M. Akbari, James Primavera, Valerie M. Donaghue, Dimitrios Zacharoulis, James S. Chrzan, Umberto Degirolami, Frank W. Logerfo, and Roy Freeman. Endothelial dysfunction and the expression of endothelial nitric oxide synthetase in diabetic neuropathy, vascular disease, and foot ulceration. *Diabetes*, 47(3):457–463, 1998.

[137] Eugene J Barrett, Zhenqi Liu, Mogher Khamaisi, George L King, Ronald Klein, Barbara E K Klein, Timothy M Hughes, Suzanne Craft, Barry I Freedman, Donald W Bowden, Aaron I Vinik, and Carolina M Casellini. Diabetic Microvascular Disease: An Endocrine Society Scientific Statement. *Journal of Clinical Endocrinology and Metabolism*, 102(December):4343–4410, 2017.

[138] K. R. Westerterp. Control of energy expenditure in humans. *European Journal of Clinical Nutrition*, 71(3):340–344, 2017.

[139] A. J. Frye and E. Kamon. Responses to dry heat of men and women with similar aerobic capacities. *Journal of Applied Physiology Respiratory Environmental and Exercise Physiology*, 50(1):65–70, 1981.

[140] Daniel Gagnon and Glen P. Kenny. Sex modulates whole-body sudomotor thermosensitivity during exercise. *Journal of Physiology*, 589(24):6205–6217, 2011.

[141] Daniel Gagnon and Glen P. Kenny. Sex differences in thermoeffector responses during exercise at fixed requirements for heat loss. *Journal of Applied Physiology*, 113(5):746–757, 2012.

[142] Luciana Gonçalves Madeira, Michele Atalla Da Fonseca, Ivana Alice Teixeira Fonseca, Kenya Paula De Oliveira, Renata Lane De Freitas Passos, Christiano Antônio MacHado-Moreira, and Luiz Oswaldo Carneiro Rodrigues. Sex-related differences in sweat gland cholinergic sensitivity exist irrespective of differences in aerobic capacity. *European Journal of Applied Physiology*, 109(1):93–100, 2010.

[143] Glen P. Kenny, Ronald J. Sigal, and Ryan McGinn. Body temperature regulation in diabetes, jan 2016.

[144] Anne Bernheim-Groswasser, Nir S. Gov, Samuel A. Safran, and Shelly Tzlil. Living Matter: Mesoscopic Active Materials. *Advanced Materials*, 30, 2018.

[145] James A. McLennan. Statistical mechanics of the steady state. *Physical Review*, 115(6):1405–1409, 1959.

[146] Robert Marsland III and Jeremy England. Limits of Predictions in Thermodynamic Systems: A Review. *Reports on Progress in Physics*, 81, 2018.

[147] André Longtin, John G. Milton, Jelte E. Bos, and Michael C. MacKey. Noise and critical behavior of the pupil light reflex at oscillation onset, 1990.

[148] Jacques B Malchaire. Predicted sweat rate in fluctuating thermal conditions Exponential weighting. *European Journal of Applied Physiology*, 63:282–287, 1991.

[149] Alan A. Cohen, Luigi Ferrucci, Tamàs Fülöp, Dominique Gravel, Nan Hao, Andres Kriete, Morgan E. Levine, Lewis A. Lipsitz, Marcel G.M. Olde Rikkert, Andrew Rutenberg, Nicholas Stroustrup, and Ravi Varadhan. A complex systems approach to aging biology. *Nature Aging*, 2(7):580–591, 2022.

[150] Katarina Katić, Rongling Li, and Wim Zeiler. Thermophysiological models and their applications: A review. *Building and Environment*, 106:286–300, 2016.

[151] Glen P. Kenny, Lucy E. Dorman, Paul Webb, Michel B. Ducharme, Daniel Gagnon, Francis D. Reardon, Stephen G. Hardcastle, and Ollie Jay. Heat balance and cumulative heat storage during intermittent bouts of exercise. *Medicine and Science in Sports and Exercise*, 41(3):588–596, mar 2009.

[152] Daniel Gagnon and Glen P. Kenny. Exercise-rest cycles do not alter local and whole body heat loss responses. *American Journal of Physiology - Regulatory Integrative and Comparative Physiology*, 300(4):958–968, 2011.

[153] Richie P. Goulding, Mark Burnley, and Rob C.I. Wüst. How Priming Exercise Affects Oxygen Uptake Kinetics: From Underpinning Mechanisms to Endurance Performance. *Sports Medicine*, 53(5):959–976, 2023.

[154] Anthony Gerbino, Susan A. Ward, and BrianJ. Whipp. Effects of prior exercise on pulmonary gas-exchange kinetics during high-intensity exercise in humans. *Journal of applied physiology*, 80(1):99–107, 1996.

[155] Robert D. Meade, Sean R. Notley, and Glen P. Kenny. Time to reach equilibrium deep body temperatures in young and older adults resting in the heat: a descriptive secondary analysis. *American journal of physiology. Regulatory, integrative and comparative physiology*, 327(3):R369–R377, 2024.

[156] Andrew J.E. Seely and Peter Macklem. Fractal variability: An emergent property of complex dissipative systems. *Chaos*, 22(1), 2012.

[157] Andrea Bravi, André Longtin, and Andrew J.E. Seely. Review and classification of variability analysis techniques with clinical applications. *BioMedical Engineering Online*, 10(1):90, 2011.

[158] Andrew Seely, Kimberley Newman, and Christophe Herry. Fractal Structure and Entropy Production within the Central Nervous System. *Entropy*, 16(8):4497–4520, 2014.

[159] Antonia Kaltsatou, Andreas D. Flouris, Christophe L. Herry, Sean R. Notley, Andrew J.E. Seely, Heather Wright Beatty, and Glen P. Kenny. Age differences in cardiac autonomic regulation during intermittent exercise in the heat. *European Journal of Applied Physiology*, 120(2):453–465, 2020.

[160] Imene Jemal, Amar Mitiche, and Neila Mezghani. A study of EEG feature complexity in epileptic seizure prediction. *Applied Sciences (Switzerland)*, 11(4):1–15, 2021.

[161] J.L. van Hemmen and André Longtin. Temperature Fluctuations for a System in Contact with a Heat Bath. *Journal of Statistical Physics*, 153(6):1132–1142, 2013.

[162] Gianmaria Falasco and Massimiliano Esposito. Macroscopic stochastic thermodynamics. *Reviews of Modern Physics*, 97(1):15002, 2025.

[163] Matthew P. Leighton and David A. Sivak. Flow of Energy and Information in Molecular Machines. *Annual Review of Physical Chemistry*, 76(1):379–403, 2025.

[164] Xingbo Yang, Matthias Heinemann, Jonathon Howard, Greg Huber, Srividya Iyer-Biswas, Guillaume Le Treut, Michael Lynch, Kristi L. Montooth, Daniel J. Needleman, Simone Pigolotti, Jonathan Rodenfels, Pierre Ronceray, Sadasivan Shankar, Iman Tavassoly, Shashi Thutupalli, Denis V. Titov, Jin Wang, and Peter J. Foster. Physical bioenergetics: Energy fluxes, budgets, and constraints in cells. *Proceedings of the National Academy of Sciences of the United States of America*, 118(26):1–10, 2021.

[165] John Bechhoefer. *Control Theory for Physicists*. Cambridge University Press, Cambridge, UK, 2021.

[166] Timur Koyuk, Udo Seifert, and Patrick Pietzonka. A generalization of the thermodynamic uncertainty relation to periodically driven systems. *Journal of Physics A: Mathematical and Theoretical*, 52(2), 2018.

[167] R. F. Ker. Dynamic tensile properties of the plantaris tendon of sheep (Ovis aries). *Journal of Experimental Biology*, 93:283–302, 1981.

[168] A. M. Wilson and A. E. Goodship. Exercise-induced hyperthermia as a possible mechanism for tendon degeneration. *Journal of Biomechanics*, 27(7), 1994.

[169] Xiaojiang Xu, Timothy P Rioux, Alexander P Welles, Ollie Jay, Brett R Ely, and Nisha Charkoudian. Modeling thermoregulatory responses during high-intensity exercise in warm environments. *Journal of Applied Physiology*, 136:908–916, 2025.

[170] Gimin Park, Jiyong Kim, Seungjai Woo, Jinwoo Yu, Salman Khan, Sang Kyu Kim, Hotaik Lee, Soyoung Lee, Boksoon Kwon, and Woochul Kim. Modeling heat transfer in humans for body heat harvesting and personal thermal management. *Applied Energy*, 323(August):119609, 2022.

[171] Veronika Hajnová, Filip Zlámal, Peter Lenárt, and Julie Bienertova-Vasku. Homeostatic model of human thermoregulation with bi-stability. *Scientific Reports*, 11(1):1–8, 2021.

[172] David F. Hultsch, Christopher Hertzog, Brent J. Small, and Roger A. Dixon. Use it or lose it: Engaged lifestyle as a buffer of cognitive decline in aging? *Psychology and Aging*, 14(2):245–263, 1999.

[173] H. Alex Choi, Neeraj Badjatia, and Stephan A. Mayer. Hypothermia for acute brain injury - Mechanisms and practical aspects. *Nature Reviews Neurology*, 8(4):214–222, 2012.

[174] Niklas Nielsen, Jørn Wetterslev, Tobias Cronberg, David Erlinge, Yvan Gasche, Christian Hassager, Janneke Horn, Jan Hovdenes, Jesper Kjaergaard, Michael Kuiper, Tommaso Pellis, Pascal Stammet, Michael Wanscher, Matt P. Wise, Anders Åneman, Nawaf Al-Subaie, Søren Boesgaard, John Bro-Jeppesen, Iole Brunetti, Jan Frederik Bugge, Christopher D. Hingston, Nicole P. Juffermans, Matty Koopmans, Lars Køber, Jørund Langørgen, Gisela Lilja, Jacob Eifer Møller, Malin Rundgren, Christian Rylander, Ondrej Smid, Christophe Werer, Per Winkel, and Hans Friberg. Targeted Temperature Management at 33°C versus 36°C after Cardiac Arrest. *New England Journal of Medicine*, 369(23):2197–2206, 2013.

[175] Gavin E. Crooks. Entropy production fluctuation theorem and the nonequilibrium work relation for free energy differences. *Physical Review E - Statistical Physics, Plasmas, Fluids, and Related Interdisciplinary Topics*, 60(3):2721–2726, 1999.

[176] Ken Funo, Tomohiro Shitara, and Masahito Ueda. Work fluctuation and total entropy production in nonequilibrium processes. *Physical Review E*, 94(6):1–12, 2016.

[177] Ryogo Kubo. Statistical-Mechanical Theory of Irreversible Process. I. *Journal of the Physical Society of Japan*, 12(6), 1957.

[178] Rolf Landauer. Irreversibility and Heat Generation in the Computing Process. *IBM Journal of Research and Development*, (July):183–191, 1961.

[179] Edward Bormashenko. Landauer's Principle : Past, Present and Future. *Entropy*, 27(437), 2025.

[180] S. Curilef, A. R. Plastino, R. S. Wedemann, and A. Daffertshofer. Landauer's principle and non-equilibrium statistical ensembles. *Physics Letters, Section A: General, Atomic and Solid State Physics*, 372(14):2341–2345, 2008.

[181] A. Daffertshofer and A. R. Plastino. Landauer's principle and the conservation of information. *Physics Letters, Section A: General, Atomic and Solid State Physics*, 342(3):213–216, 2005.

[182] Dilip Kondepudi. Self-Organization, Entropy Production, and Physical Intelligence. *Ecological Psychology*, 24(1):33–45, 2012.

[183] Leonid Martyushev. Entropy and Entropy Production: Old Misconceptions and New Breakthroughs. *Entropy*, 15(4):1152–1170, 2013.

[184] Douglas Hanahan and Robert A Weinberg. The Hallmarks of Cancer. *Cell*, 100:57–70, 2000.

[185] Douglas Hanahan and Robert A Weinberg. Hallmarks of cancer: the next generation. *Cell*, 144(5):646–74, 2011.

[186] Freddie Bray, Mathieu Laversanne, Elisabete Weiderpass, and Isabelle Soerjomataram. The Ever- Increasing Importance of Cancer as a Leading Cause of Premature Death Worldwide. *Cancer*, 127(16):3029–3030, 2021.

[187] Gerd Muehllehner and Joel S. Karp. Positron emission tomography. *Physics in Medicine and Biology*, 51(13), 2006.

APPENDICES

Appendix A

Useful derivations from stochastic dynamics

A.1 Averaged fluctuations in the entropy export response

The stochastic control model presented in Chapter 5 aims at replicating the *average* response over a number N of participants in each age group. The entropy export response for each participant i is expressed as $y_i(t)$. Modeling the average entropy export response $\bar{y}(t)$ over all N participants leads to

$$\bar{y}(t) = \frac{1}{N} \sum y_i(t) \quad . \tag{A.1}$$

We are interested in finding the relationship between the individual noise and the noise of the averaged response over N participants. By definition, the variance on $\bar{y}$ is given by $\mathrm{var}(\bar{y}) = \sigma_y^2 = \langle \bar{y}^2 \rangle - \langle \bar{y} \rangle^2$ and similarly for $\mathrm{var}(\xi_i) = \sigma_{\xi_i} = \langle \xi_i^2 \rangle - \langle \xi_i \rangle^2 = \langle \xi_i^2 \rangle$. The second

moment of $\bar{y}$ is given by

$$\langle \bar{y}^2 \rangle = \langle \frac{\sigma^2}{N^2} \sum \xi_i \xi_j \rangle = \frac{\sigma^2}{N^2} \sum \langle \xi_i^2 \rangle = \frac{\sigma^2}{N^2} \sum \sigma_{\xi_i}^2 = \frac{\sigma^2}{N^2} N \sigma_{\xi_i}^2 = \frac{\sigma^2 \sigma_{\xi_i}^2}{N} \quad . \tag{A.2}$$

Therefore, the variance on the averaged response σ_y^2 is related to the variance on the individual response $\sigma_{\xi_i}^2$ by

$$\sigma_y^2 = \frac{\sigma^2}{N} \sigma_{\xi_i}^2 \quad . \tag{A.3}$$

A.2 Model's relation to Fokker-Planck equation

Let the Gaussian white noise be the time derivative of the Wiener process with zero mean and delta-correlated noise:

$$\xi(t) = \frac{dW}{dt} \qquad \text{with} \quad \langle \xi \rangle = 0 \quad \text{and} \quad \langle \xi(t) \xi(s) \rangle = \delta(t-s) \quad . \tag{A.4}$$

Then, while neglecting the time dependence before the onset of exercise (i.e. we neglect the slow equilibration over hours), we can write the generalized Langevin equation

$$\frac{dy}{dt} = f(y,t) + g(y,t)\, \xi(t) \quad . \tag{A.5}$$

Defining $D(y) \equiv g^2$, the Fokker-Planck equation for $P(y,t)$ is

$$\frac{\partial P}{\partial t} = -\frac{\partial}{\partial y} [f\, P] + \frac{1}{2} \frac{\partial^2}{\partial y^2} [D(y)\, P] \quad . \tag{A.6}$$

The stationary density $P(y, \infty)$ is obtained when $\partial P/\partial t = 0$, that is when

$$\frac{\partial}{\partial y}\left[f\,P\right] = \frac{1}{2}\frac{\partial^2}{\partial y^2}\left[D(y)\,P\right] \quad . \tag{A.7}$$

We can integrating once and we know that the density goes to zero at $\pm\infty$, and so does its slope. In our specific case D does not depend of y and we can rearrange the equation in a suitable form to integrate again using separation of variables, such that

$$\begin{aligned}
\int \frac{dP}{P} &= \int \frac{2f(y)}{D} dy + C' \\
\ln P &= \frac{2}{D}\int f(y)\,dy + C' \\
\Rightarrow P &= P_o \exp\left[\frac{2}{D}\int f(y)\,dy\right]
\end{aligned}$$

where P_o is the normalization coefficient of the Gaussian. For our model, we can set $x(t) = 0$ without loss of generalization (e.g. if $x(t)$ is a constant, we can make a variable substitution $z(t) \equiv x - y(t)$). Then the drift term becomes $f = -\alpha\, y$, the diffusion term becomes $g = \sigma$ and we have $D = \sigma^2$. After substitution and integration over y, we obtain a stationary density that has a Gaussian form

$$P = P_o \exp\left[-\frac{\alpha}{\sigma^2} y^2\right] \qquad \text{with} \quad \text{var}(y) = \frac{\sigma^2}{2\,\alpha} \quad . \tag{A.8}$$

The stationary autocorrelation is then given by

$$A(t-s) = A_o \exp\left[-\alpha\,(t-s)\right] \qquad \text{where} \quad A_o = \text{var}(y) \quad . \tag{A.9}$$

To retrieve the parameters of interest, namely α and σ, fitting an exponential to the autocorrelation function yields the parameter α, and, after fitting a Gaussian to the stationary density of known variance $\sigma^2/2\alpha$, we can determine the parameter σ.

Appendix B

Modeling Physiological Response

As suggested in section 5.4.5 of Chapter 5, the driving term $x(t)$ can take any mathematical form, implying that our model (equation (5.6)) can be solve for arbitrary functions of $x(t)$:

$$y'(t) = \alpha\ [x(t) - y(t)] \quad . \tag{B.1}$$

For example, instead of fixing the metabolic heat production rate, the cycling resistance could be continuously adjusted such that $x(t)$ follows a sinusoidal function:

$$x(t) = A \sin(\omega t + \phi) + \gamma \quad . \tag{B.2}$$

Using the method of integrating factor to solve the differential equation (without noise), the model's entropy export response is given by

$$y(t) = \frac{\alpha\, A}{\alpha^2 + \omega^2}[\alpha \sin(\omega t + \phi) - \omega \cos(\omega t + \phi)] + [y_o + \beta - \gamma]e^{-\alpha t} + \gamma \tag{B.3}$$

where β is a constant given by

$$\beta = \frac{\alpha\, A}{\alpha^2 + \omega^2}(\omega \cos\phi - \alpha \sin\phi) \quad . \tag{B.4}$$

The figure B.1 shows the analytical and numerical solution to a sinusoidal driving term $x(t)$ if the system is in a steady-state (i.e. $y_o = 1 = \gamma - A$). The numerical solution was obtained using the Runge-Kutta method. This quick demonstration of the model's possible extension to arbitrary driving term highlights its connection to Linear Response Theory. Additionally, further investigations could consider modeling the fatigue build up in participants as they become increasingly exhausted from the physical exercise. One approach to model fatigue would be to add a time-dependence on the adaptation coefficient $\alpha \equiv \alpha(t)$ that monotonously decrease with time.

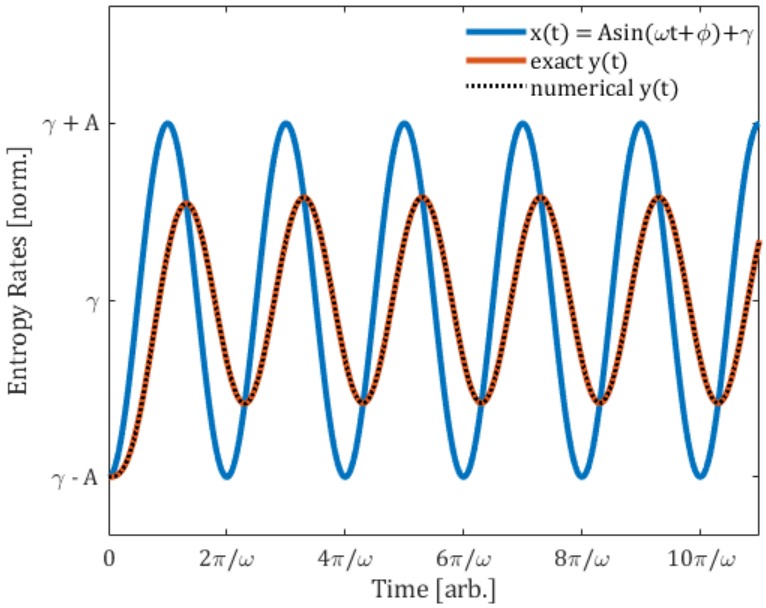

Figure B.1: Comparison between the analytical (red) and modeling (dashed black) results for a time-dependent driving term $x(t)$ (blue) in equation (B.1), where $x(t)$ has the form of a sinusoidal function.